Astrofisica Nucleare e Subnucleare

Gamma ray Bursts – III

BeppoSAX (1995 - 2002)

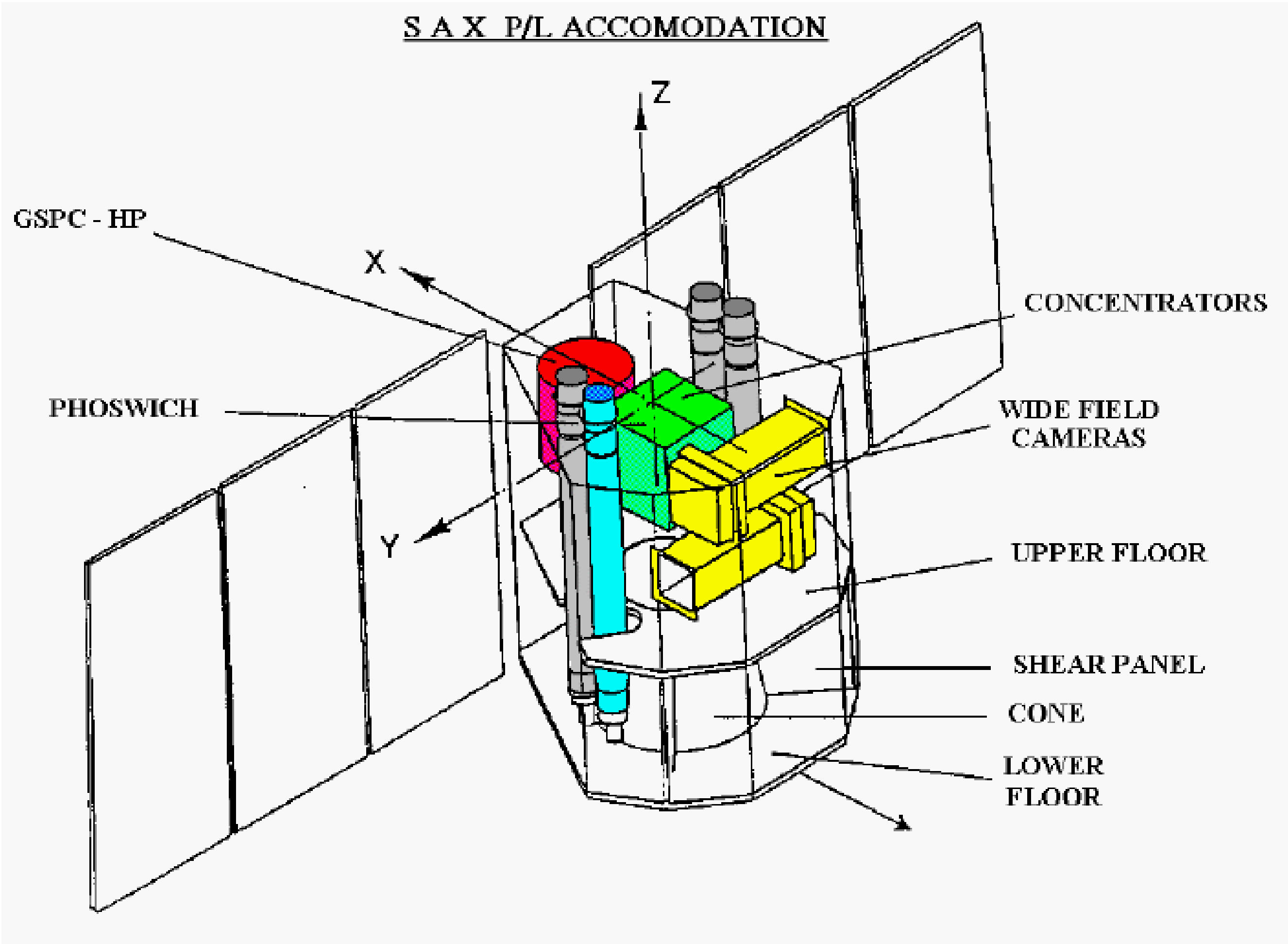

Coded Mask Imaging

The principle of the camera is straightforward: photons from a certain direction in the sky project the mask on the detector; this projection has the same coding as the mask pattern, but is shifted relative to the central position over a distance uniquely correspondent to the direction of the photons. The detector accumulates the sum of a number of shifted mask patterns.
Each shift encodes the position and its strength encodes the intensity of the sky at that position.

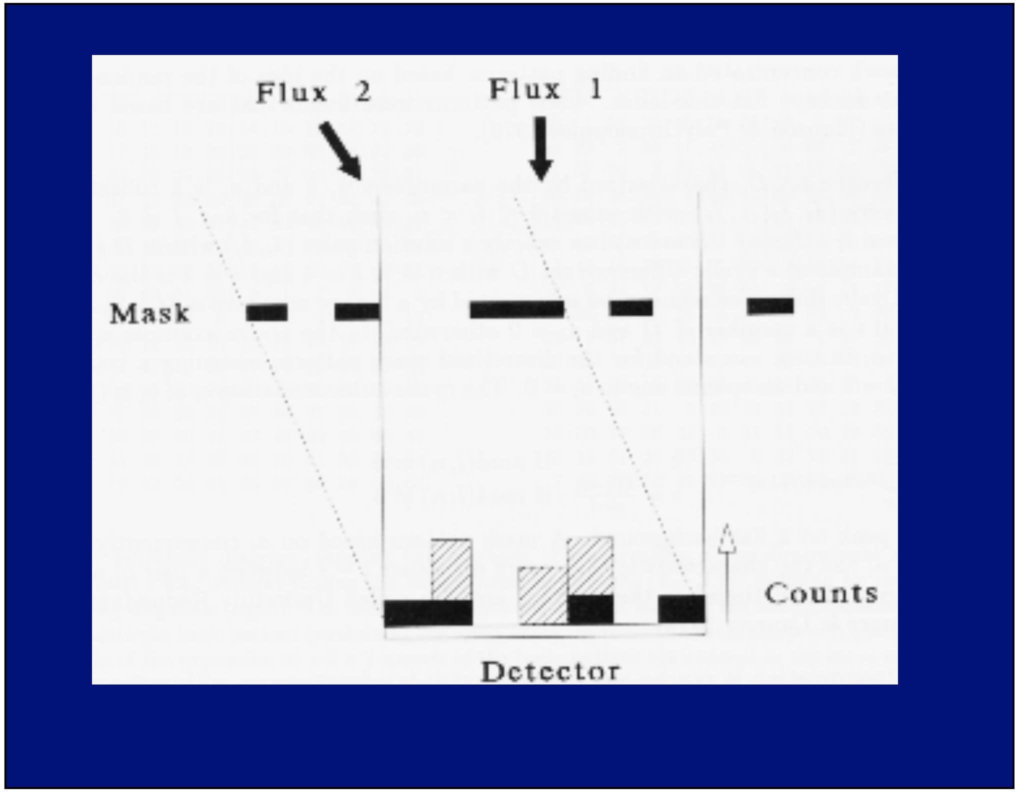

http://asd.gsfc.nasa.gov/archive/cai/coded_intr.html

Coded Mask Imaging

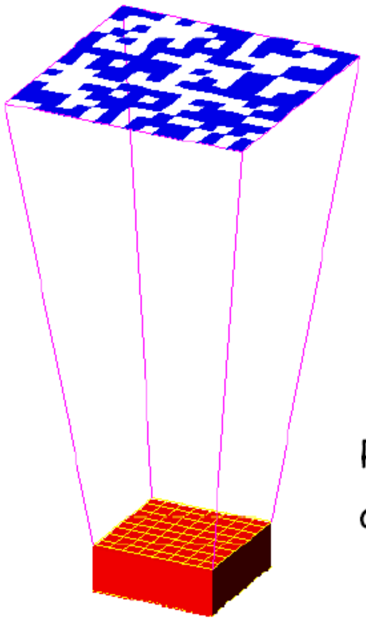

How to recover an image

Basic method :
' Correlation with the Mask Pattern '

Recorded pattern is Convolution of source distribution and the mask pattern, plus some background B

$$D = S \otimes M + B$$

Suppose we form an image as †

$$I = M \otimes D = M \otimes S \otimes M + M \otimes B$$
$$= M \otimes M \otimes S + M \otimes B$$
$$= ACF(M) \otimes S + M \otimes B$$

where ACF indicated the Autocorrellation function.
If ACF(M) were a Delta function and if $M \otimes B$ were zero we would have recovered S.

† coordinate reversals are ignored here

The GRB phenomenon

- in 1997, thanks to BeppoSAX observations, discovery of fading X-ray, optical, radio emission following the GRB

- photons received during the classical GRB phenomenon are then called "prompt emission" and the subsequent fading emission is called "afterglow emission"

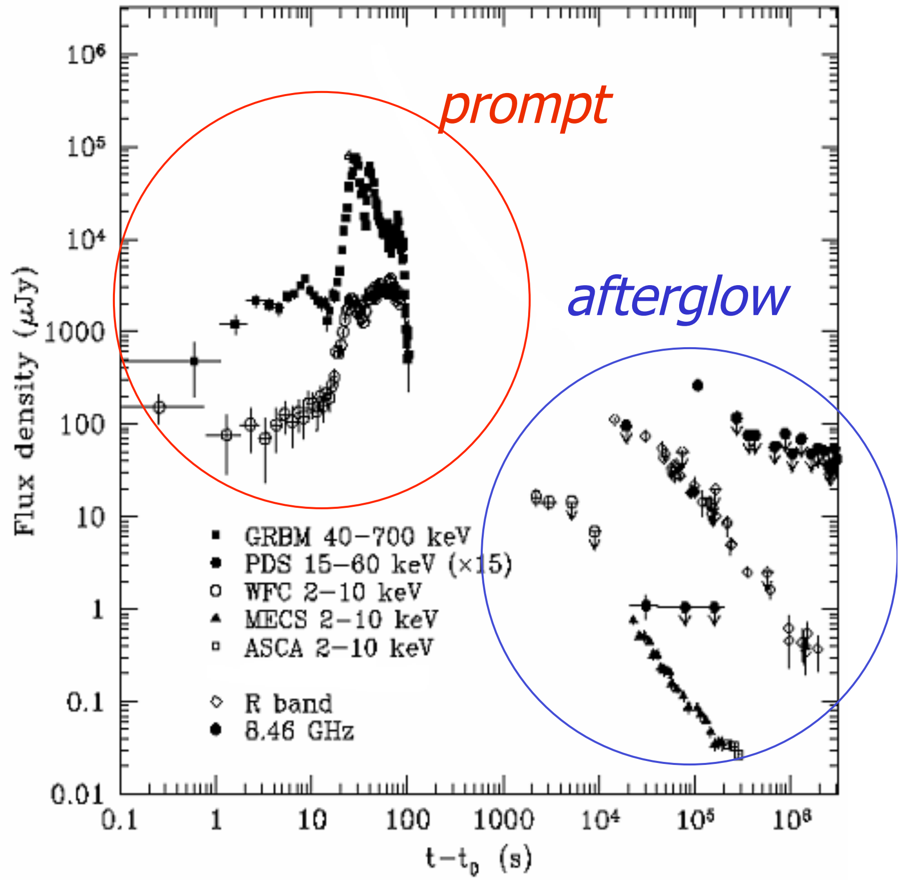

Adapted from Maiorano et al., A&A, 2005

The compactness problem

Light curve variability ~ 1 ms

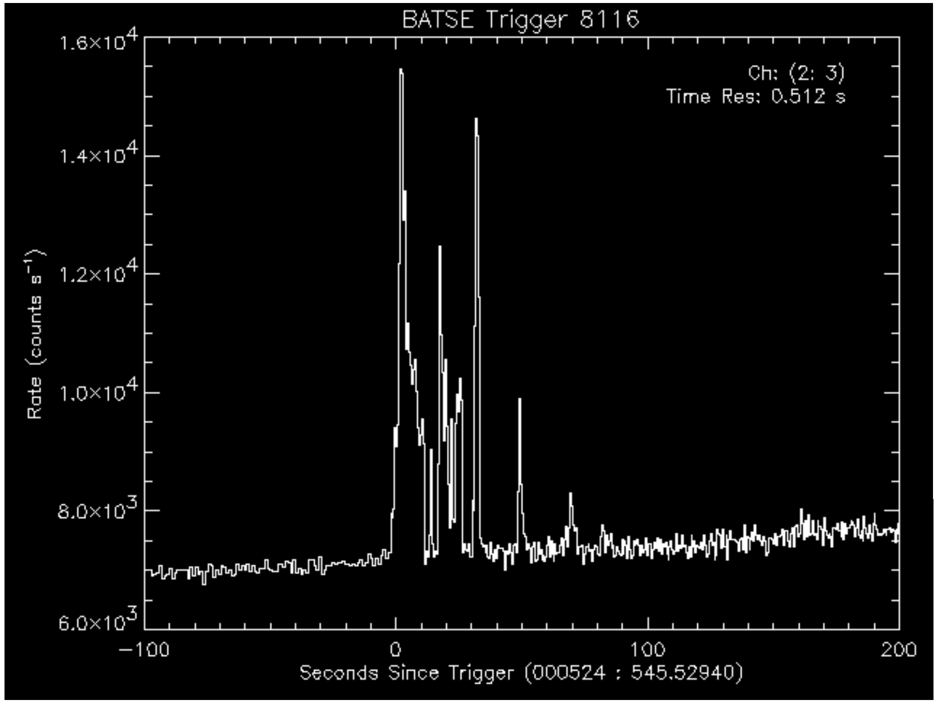

Briggs et al. (1999)

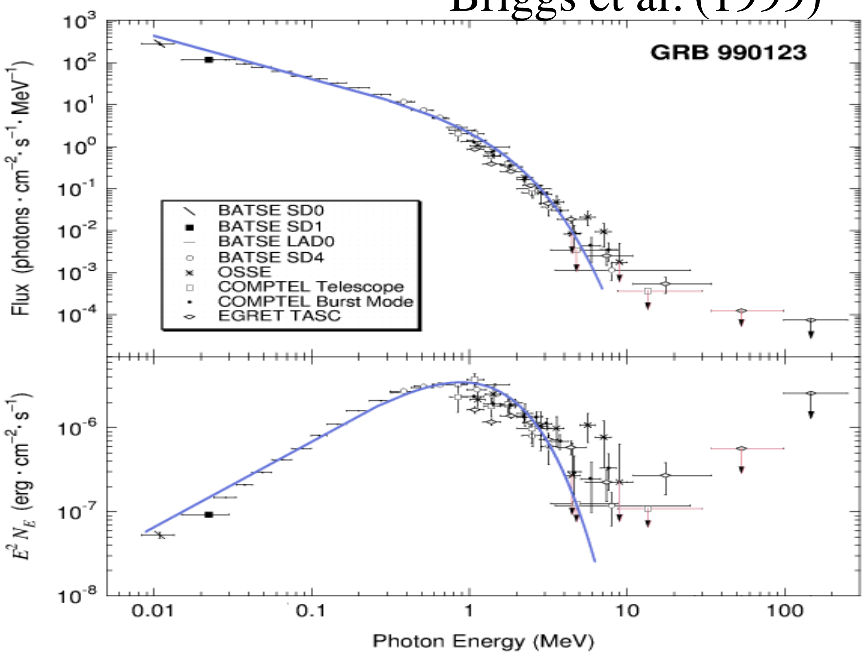

Non thermal spectra

- Fluence (γ): (0.1-10) x 10^{-6} erg/cm^2 ($\Omega/4\pi$)
- Total Energy: E ~ $10^{51} \div 10^{52}$ erg

The compactness problem

$$R_i < c\delta t \qquad \gamma\gamma \to e^+e^-$$

$$\boxed{\tau_{\gamma\gamma} = \frac{f_p \sigma_T F D_L^2}{R_i^2 m_e c^2} \approx 10^{17} f_p \left(\frac{F}{10^{-6} erg/cm^2}\right)\left(\frac{D_L}{3Gpc}\right)^2\left(\frac{\delta t}{1ms}\right)}$$

$$\tau_{\gamma\gamma} >> 1$$

Very High Optical Depth to pair production

Size

Pair fraction

$$\Gamma = \frac{1}{\sqrt{1-\beta^2}} \qquad R_i < \Gamma^2 c\delta t \quad f_p \to f_p \Gamma^{-2\alpha}$$

$$\boxed{\tau_{\gamma\gamma} = \frac{f_p \sigma_T F D_L^2}{R_i^2 m_e c^2} \approx \frac{10^{17}}{\Gamma^{4+2\alpha}} f_p \left(\frac{F}{10^{-6} erg/cm^2}\right)\left(\frac{D_L}{3Gpc}\right)^2\left(\frac{\delta t}{1ms}\right)}$$

$$\Gamma \approx 10^2 \div 10^3$$

Piran (1999)

Relativistic motion of the emitting region

The Fireball model

- Relativistic motion of the emitting region
- Shock mechanism converts the kinetic energy of the shells into radiation.
- Baryon Loading problem

External Shock
- Synchrotron & SSC
- High conversion efficiency
- Not easy to justify the rapid variability

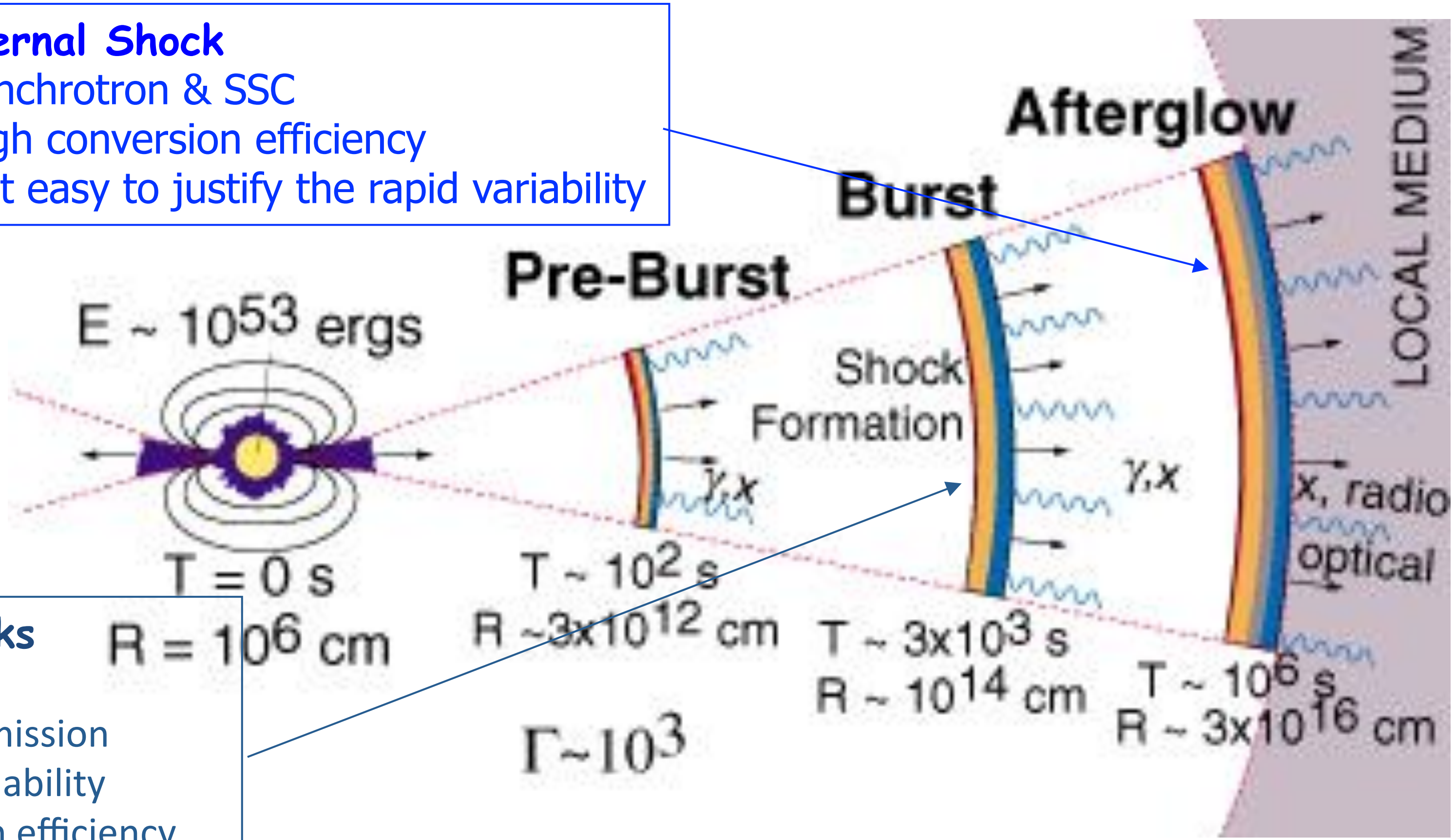

Internal Shocks
- Source activity
- Synchrotron Emission
- Rapid time Variability
- Low conversion efficiency

Afterglow Observations

Harrison et al (1999)

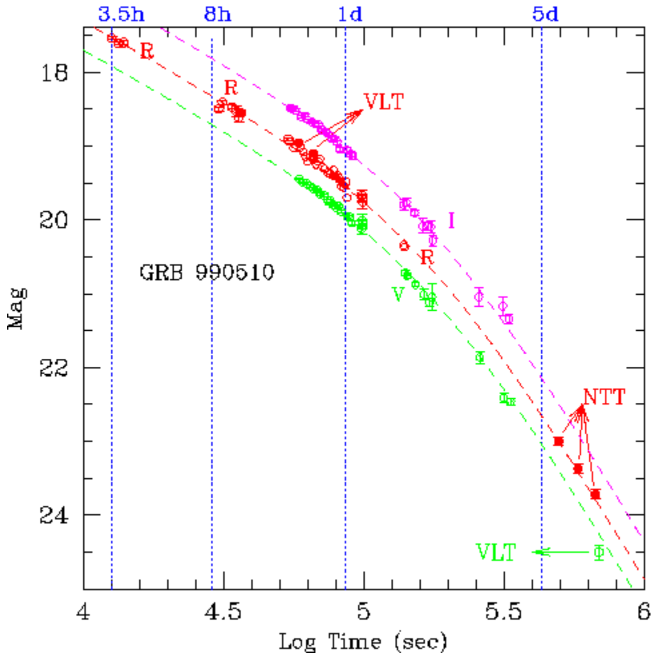

Achromatic Break

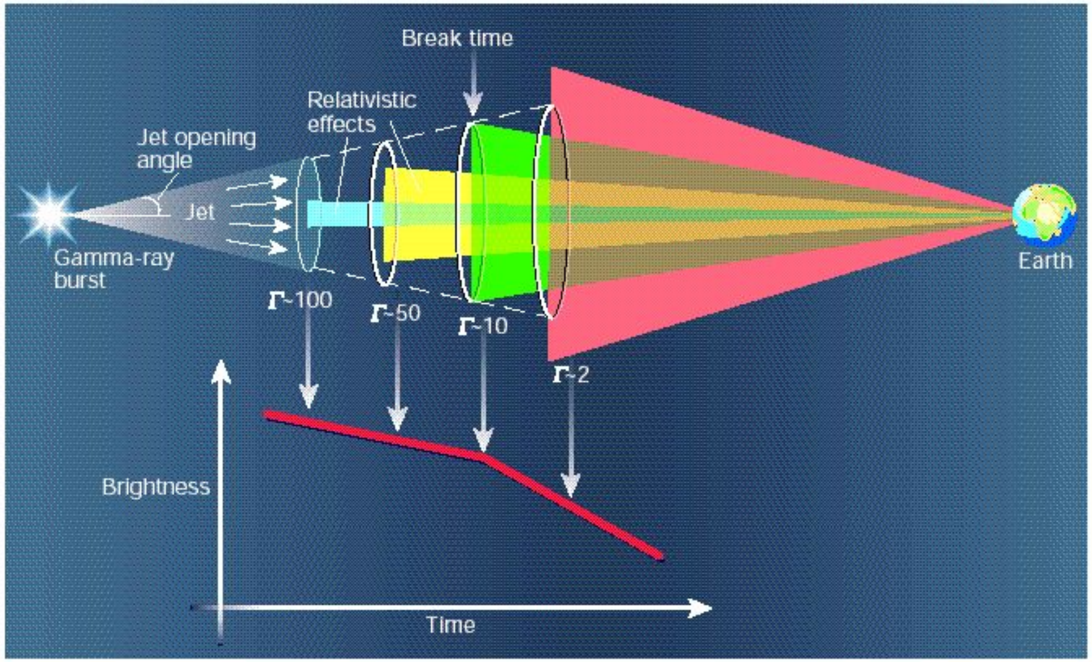

Woosley (2001)

Jet breaks

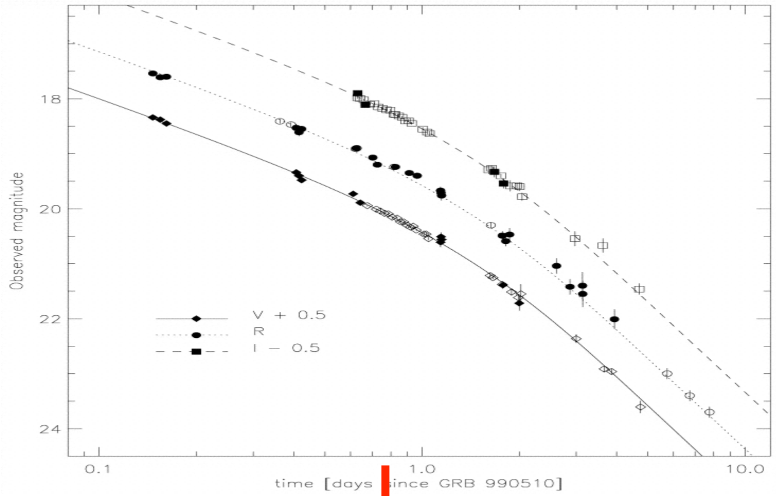

➢ breaks in the afterglow decay light curves -> collimation ?

$$\theta = 0.09 \left(\frac{t_{jet,d}}{1+z}\right)^{3/8} \left(\frac{n\,\eta_\gamma}{E_{\gamma,iso,52}}\right)^{1/8}$$

$$E_\gamma = (1-\cos\theta) E_{\gamma,iso}.$$

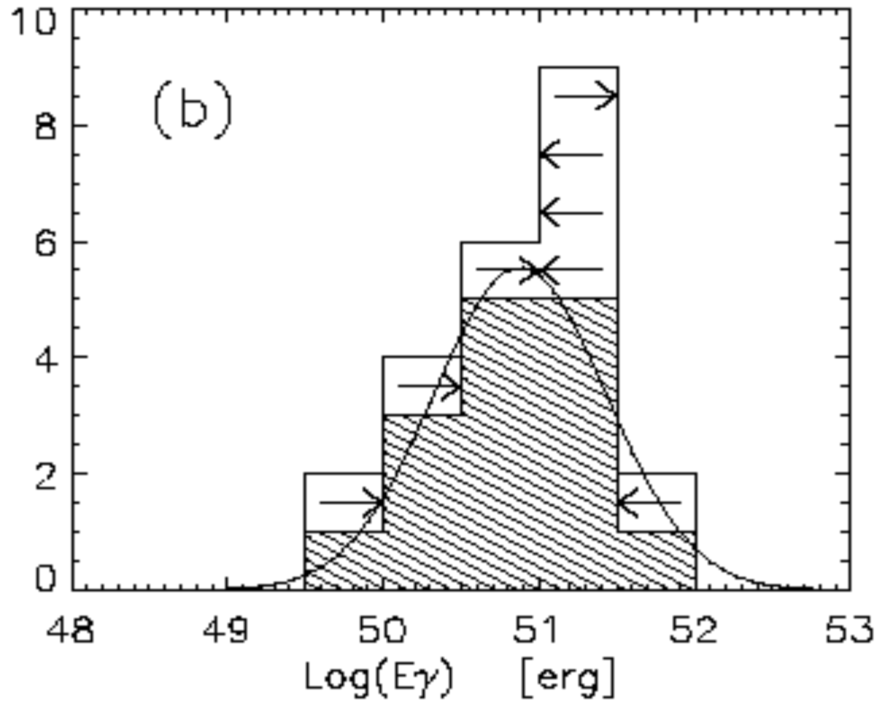

GRB for Cosmology

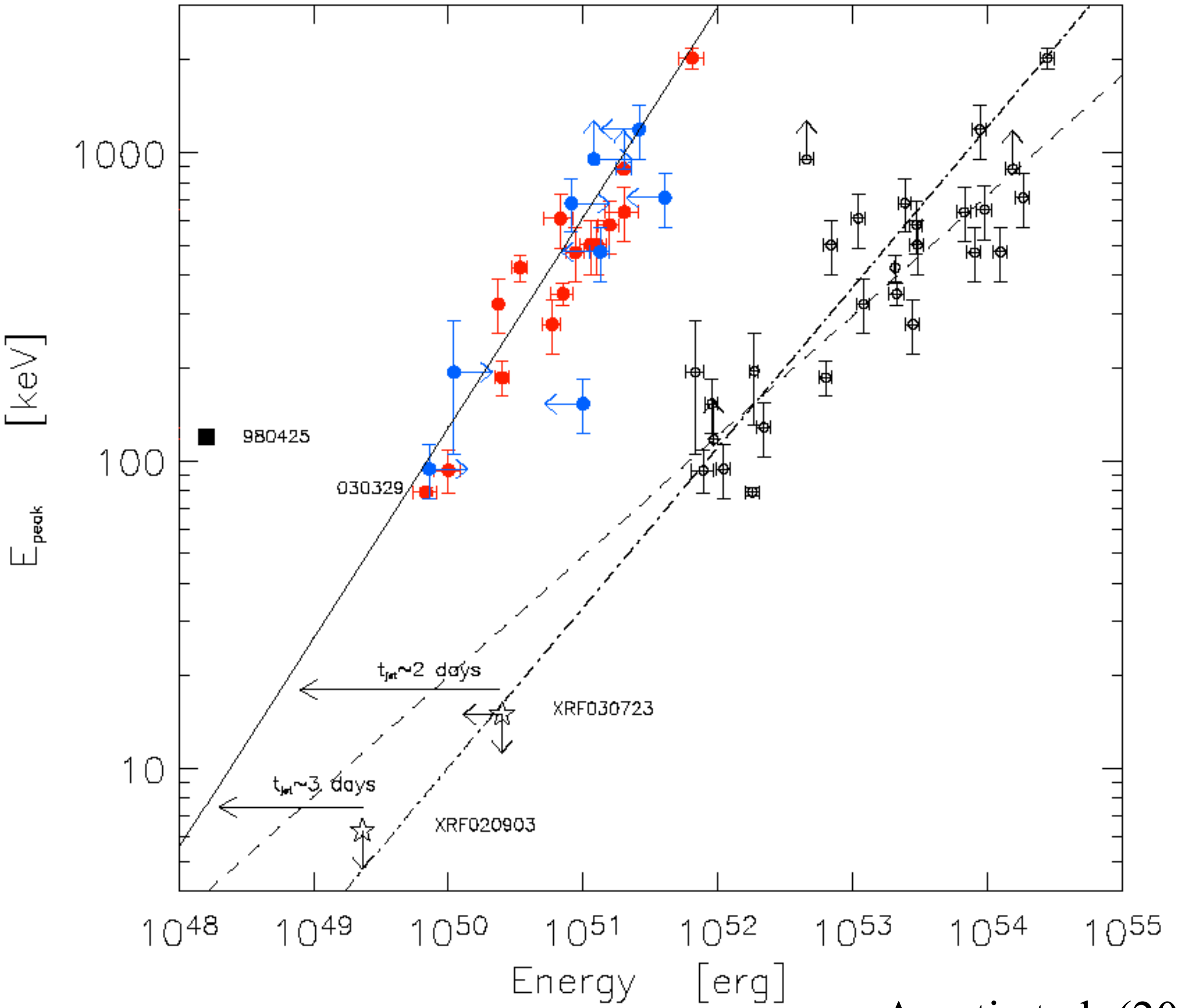

Amati et al. (2002)
Ghirlanda et al. (2004)

SN Ia Cosmology

SNe Ia as a "standard candle"

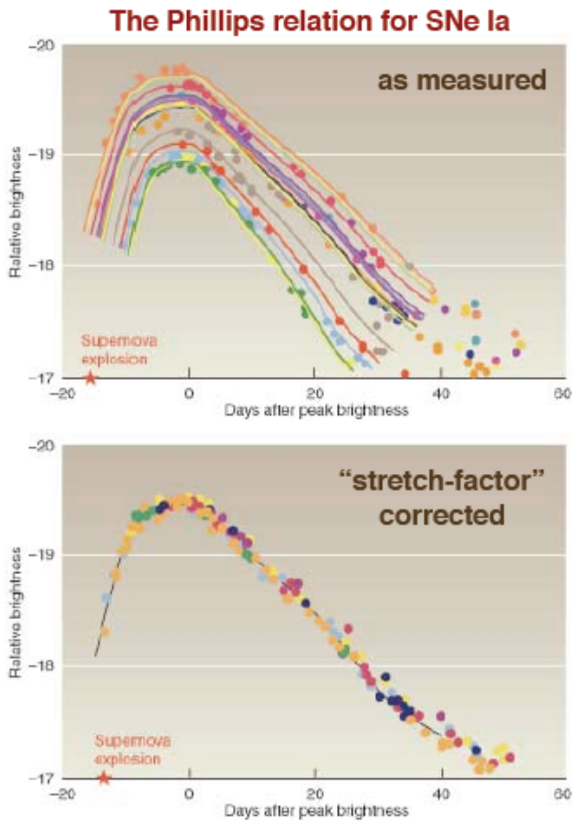

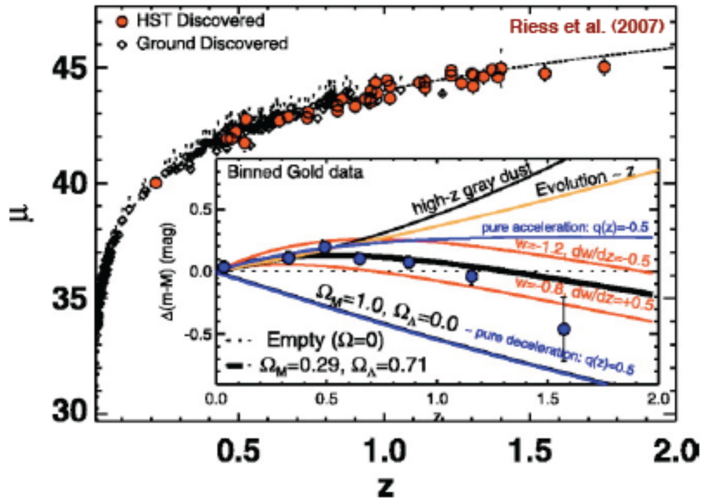

Can we apply GRBs as a standardized candle?

GRB for Cosmology

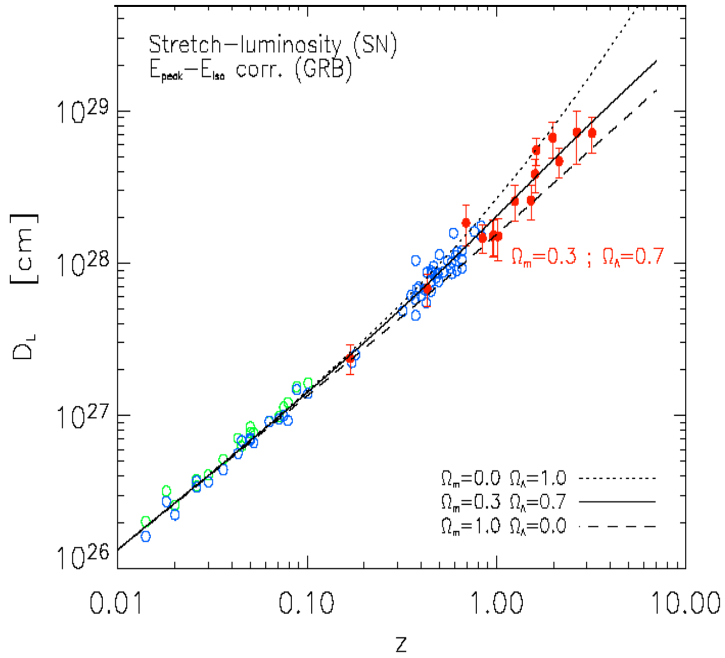

Ghirlanda et al. (2004)

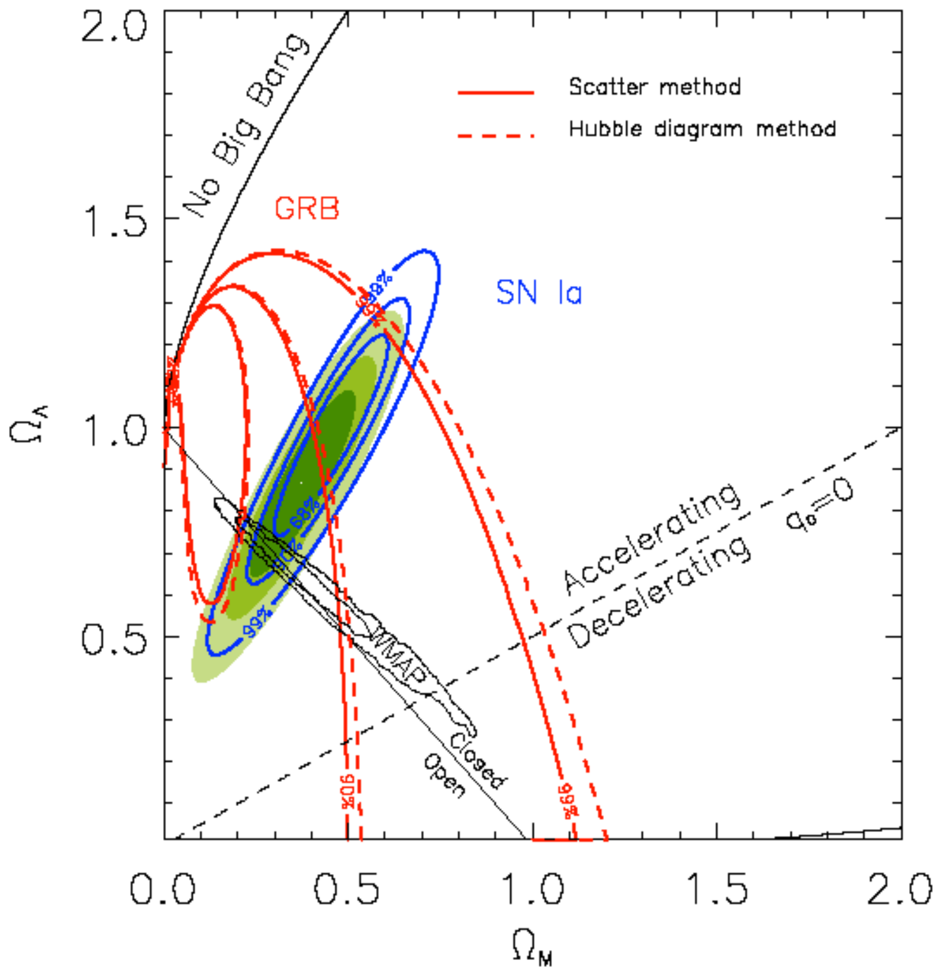

❑ **Method** (e.g., Ghirlanda et al, Firmani et al., Dai et al., Zhang et al.):

$$E_{p,i} = E_{p,obs} \times (1 + z)\ ,\ t_{b,i} = t_b / /1 + z)$$

$$E_{\gamma,iso} = \frac{4\pi D_l^2}{(1+z)} \int_{1/1+z}^{10^4/1+z} E\,N(E)\,dE \quad \text{erg} \longrightarrow D_l = D_l(z\,,\, H_0,\, \Omega_M,\, \Omega_\Lambda, \ldots)$$

➤ fit the correlation and construct an Hubble diagram for each set of cosmological parameters -> derive c.l. contours based on chi-square

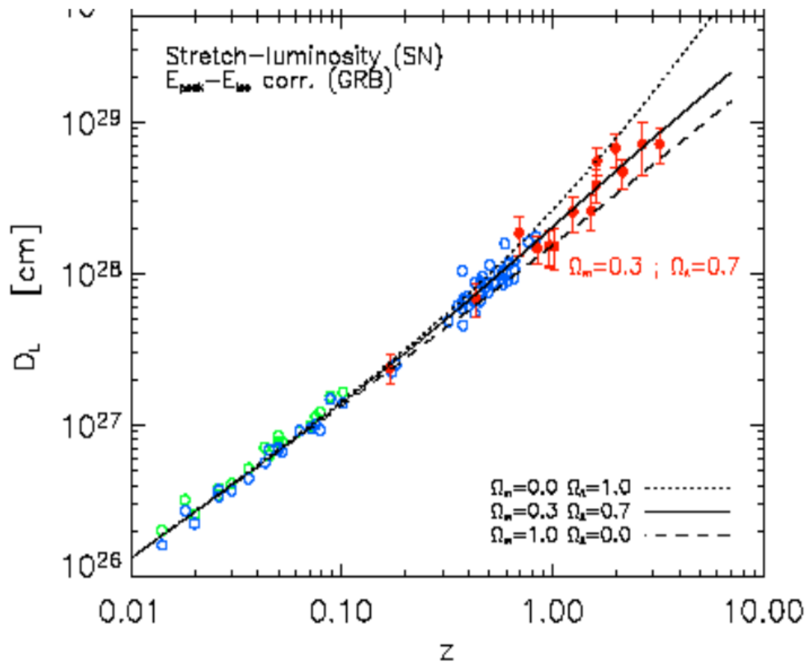

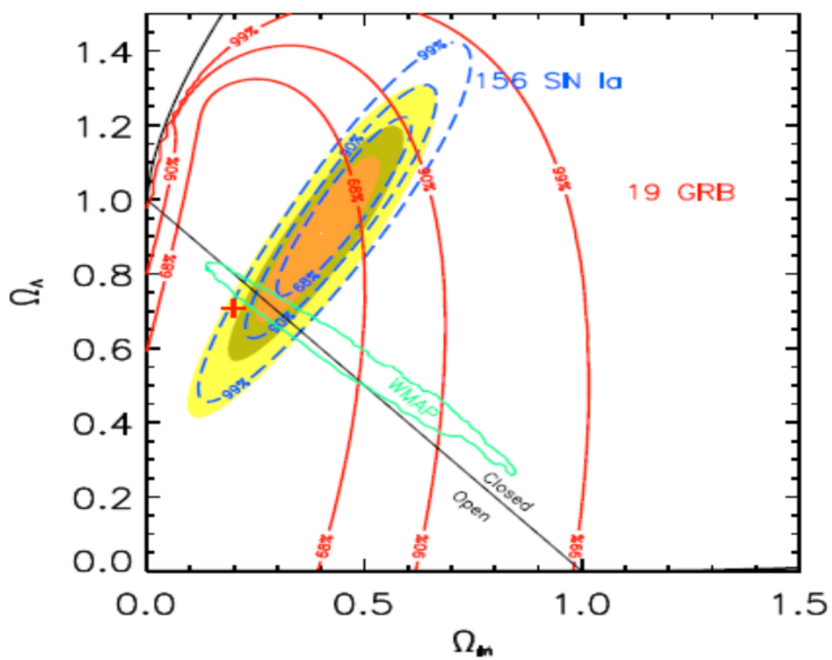

❑ results obtainable with 150 GRBs with estimates of z, $E_{p,i}$ and tb

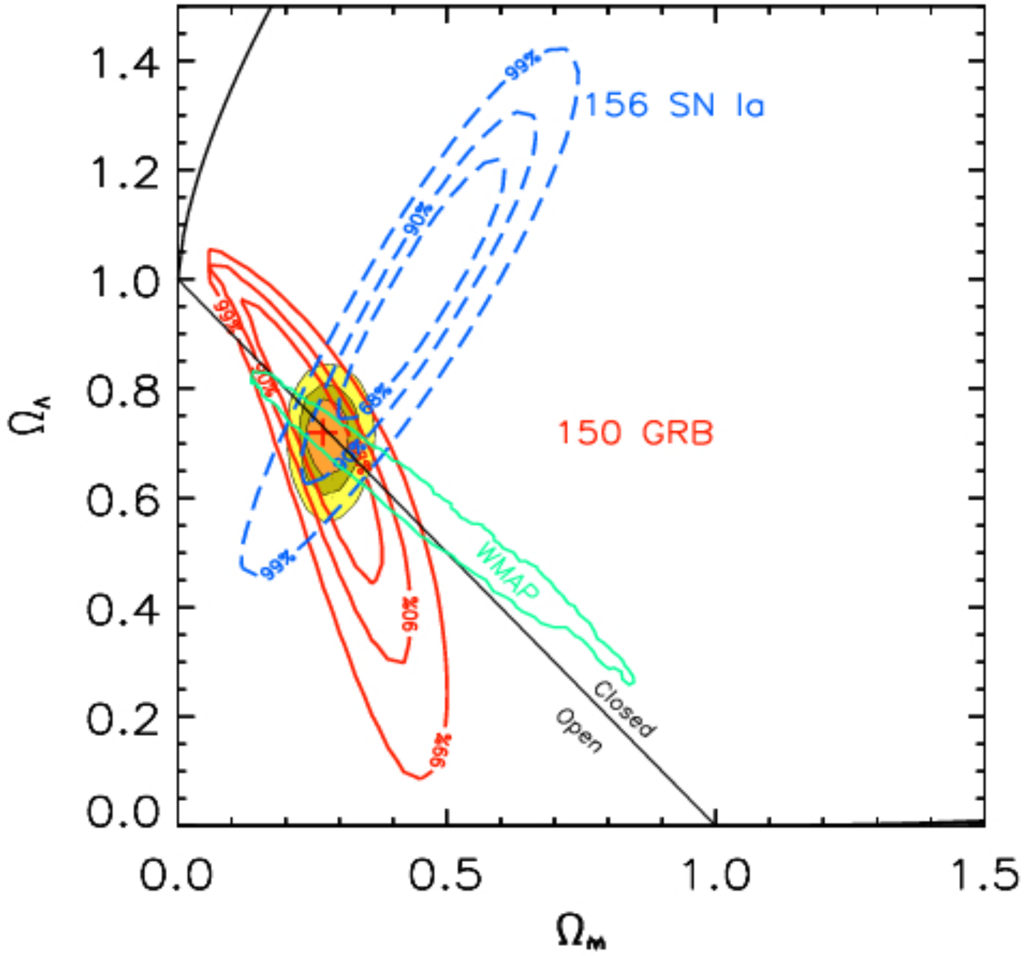

Ghirlanda et al. 2006 A&A

Ghirlanda et al. 2006 JOP Review, GRB Special Issue

Caveats

GRBs as a standard candle?

Caveats:

- lack of a low-z calibration sample
- $E_{peak} \in$ [10 keV, 1MeV], not always well constrained
- Θ_{jet} is model dependent

For a homogeneous circumburst medium (Sari et al. 1999)

$$\theta_{\rm jet} = 0.161 \left(\frac{t_{\rm jet,d}}{1+z}\right)^{3/8} \left(\frac{n\,\eta_\gamma}{E_{\rm iso,52}}\right)^{1/8}$$

For a wind profile from massive stars (Nava et al. 2006)

$$n(r) = A/r^2$$

$$\theta_{\rm jet} = 0.206 \left(\frac{t_{\rm jet,d}}{1+z}\right)^{1/4} \left(\frac{A_*\,\eta_\gamma}{E_{\rm iso,52}}\right)^{1/4}$$

$$A = \dot{M}_{\rm w}/(4\pi v_{\rm w}) = 5\times 10^{11}\, A_*\ {\rm g\,cm^{-1}}$$

- uncertain jet break time and CBM density

The Ghirlanda E_p - E_γ relation (2004)

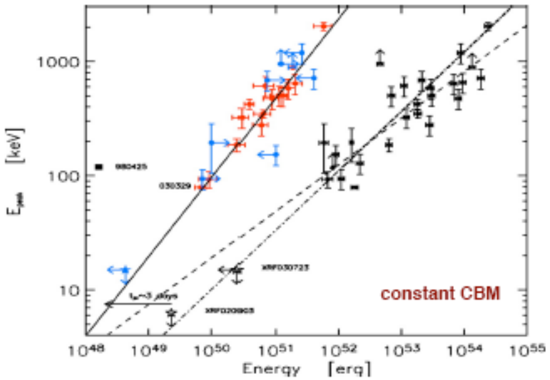

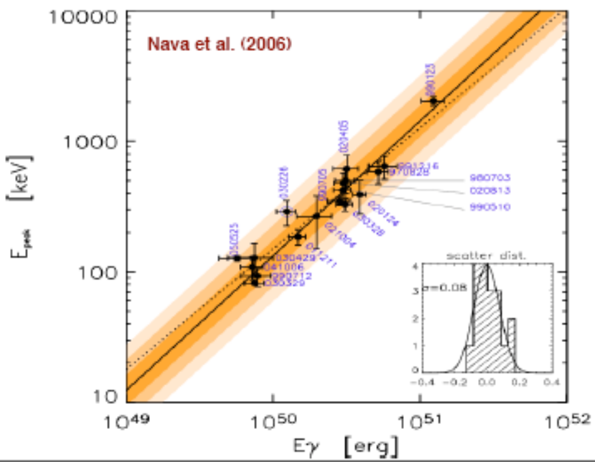

Luminosity distance

Distance measures in cosmology

David W. Hogg

Institute for Advanced Study, 1 Einstein Drive, Princeton NJ 08540
hogg@ias.edu

2000 December

1 Introduction

In cosmology (or to be more specific, *cosmography*, the measurement of the Universe) there are many ways to specify the distance between two points, because in the expanding Universe, the distances between comoving objects are constantly changing, and Earth-bound observers look back in time as they look out in distance. The unifying aspect is that all distance measures somehow measure the separation between events on radial null trajectories, ie, trajectories of photons which terminate at the observer.

In this note, formulae for many different cosmological distance measures are provided. I treat the concept of "distance measure" very liberally, so, for instance, the lookback time and comoving volume are both considered distance measures. The bibliography of source material can be consulted for many of the derivations; this is merely a "cheat sheet." Minimal *C* routines (KR) which compute all of these distance measures are available from the author upon request. Comments and corrections are highly appreciated, as are acknowledgments or citation in research that makes use of this summary or the associated code.

2 Cosmographic parameters

The *Hubble constant* H_0 is the constant of proportionality between recession speed v and distance d in the expanding Universe;

$$v = H_0\, d \tag{1}$$

The subscripted "0" refers to the present epoch because in general H changes with time.

The Luminosity Distance

$$\Omega_{\rm M} + \Omega_\Lambda + \Omega_k = 1$$

$$z \equiv \frac{\nu_{\rm e}}{\nu_{\rm o}} - 1 = \frac{\lambda_{\rm o}}{\lambda_{\rm e}} - 1$$

$$E(z) \equiv \sqrt{\Omega_{\rm M}\,(1+z)^3 + \Omega_k\,(1+z)^2 + \Omega_\Lambda}$$

$$H_0 = 100\,h\ \mathrm{km\,s^{-1}\,Mpc^{-1}} \qquad D_{\rm H} \equiv \frac{c}{H_0} \qquad D_{\rm C} = D_{\rm H} \int_0^z \frac{dz'}{E(z')}$$

$$D_{\rm M} = \begin{cases} D_{\rm H}\,\frac{1}{\sqrt{\Omega_k}}\,\sinh\left[\sqrt{\Omega_k}\,D_{\rm C}/D_{\rm H}\right] & \text{for } \Omega_k > 0 \\ D_{\rm C} & \text{for } \Omega_k = 0 \\ D_{\rm H}\,\frac{1}{\sqrt{|\Omega_k|}}\,\sin\left[\sqrt{|\Omega_k|}\,D_{\rm C}/D_{\rm H}\right] & \text{for } \Omega_k < 0 \end{cases}$$

$$D_{\rm L} = (1+z)\,D_{\rm M}$$

astro-ph/9905116v4

Luminosity distance and redshift

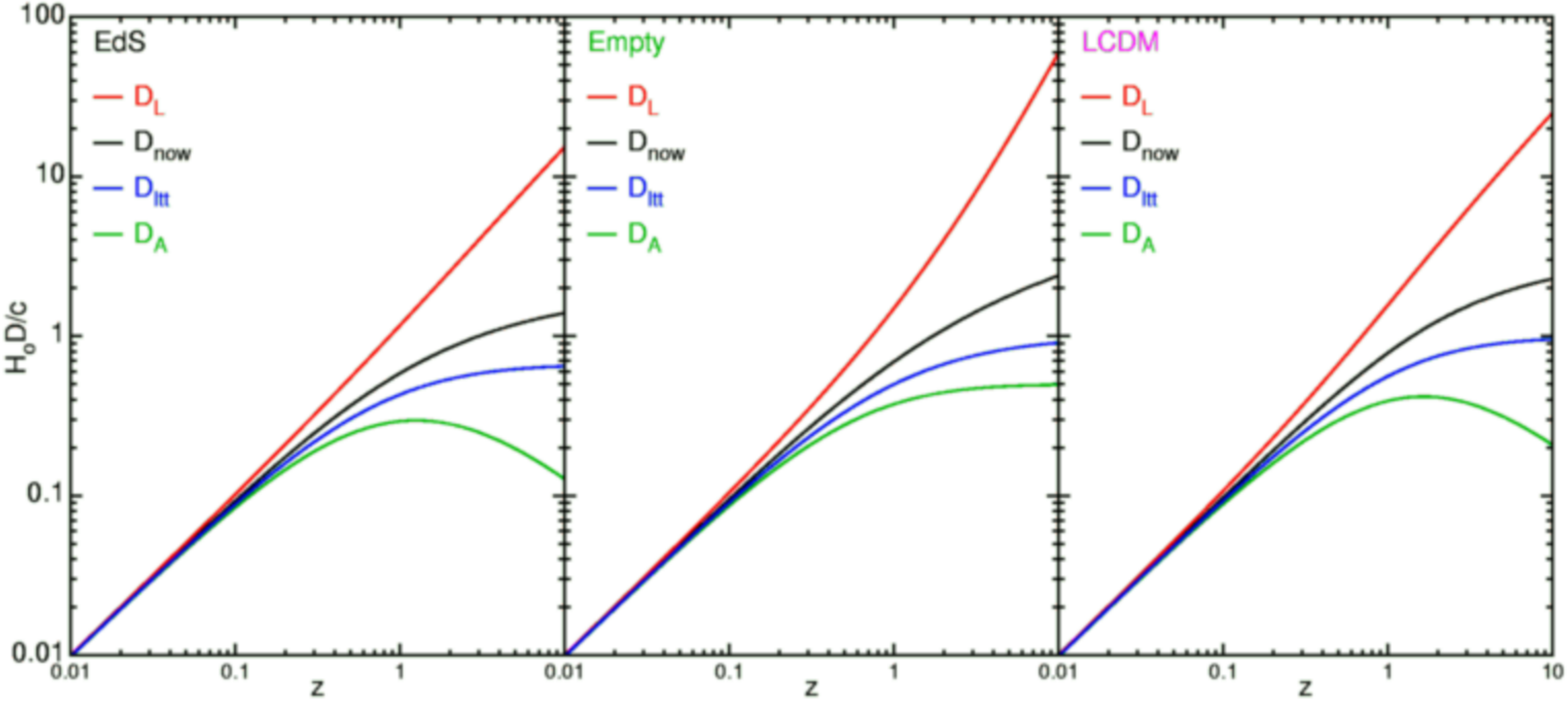

Swift Instruments

Instruments

- Burst Alert Telescope (BAT)
  - New CdZnTe detectors
  - Most sensitive gamma-ray imager ever
- X-Ray Telescope (XRT)
  - Arcsecond GRB positions
  - CCD spectroscopy
- UV/Optical Telescope (UVOT)
  - Sub-arcsec positions
  - Grism spectroscopy
  - 24th mag sensitivity (1000 sec)
  - Finding chart for other observers

Spacecraft

- Autonomous re-pointing, 20 - 75 s
- Onboard and ground triggers

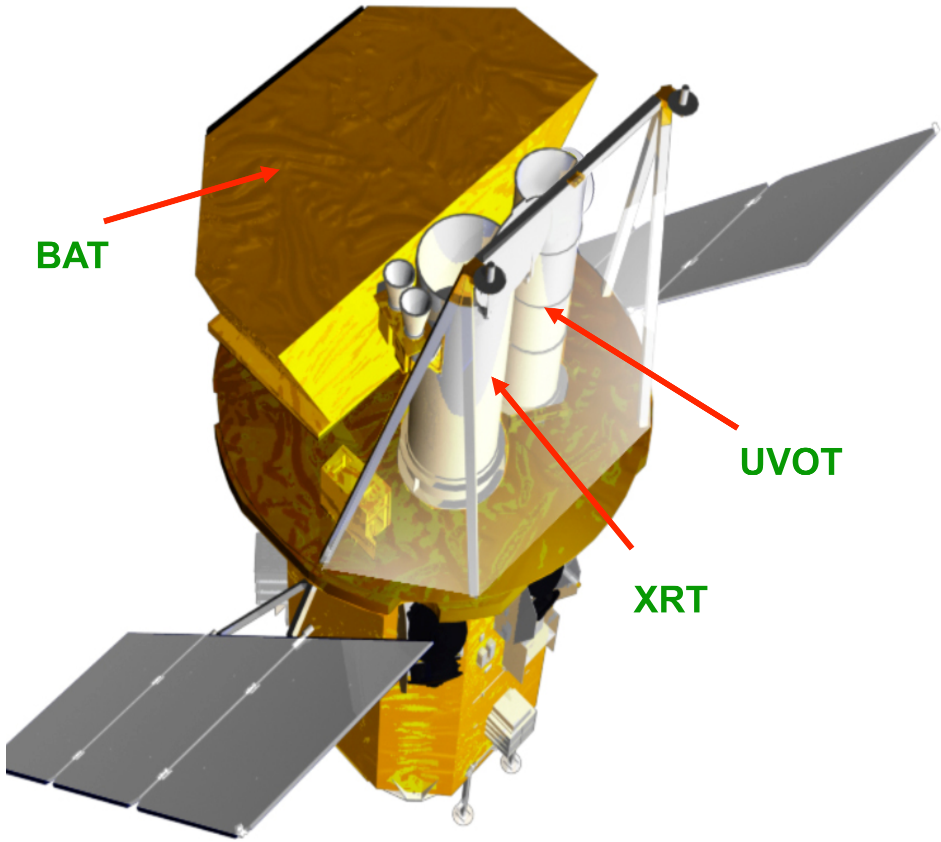

Swift

Details

- **BAT** (15-350 keV). Large (2 sr) field of view – detects bursts with arc min accuracy. And tells observers immediately.
- *Swift* automatically determines if it can view the GRB, and if so, slews to it.
- **XRT** (0.3-10 keV) and **UVOT** (~1000-6000 Å) begin observing typically within 100 s of the trigger.
- XRT can automatically detect afterglows, and downlinks limited data immediately. ~90% of BAT GRBs have promptly detected XRT afterglows.

SWIFT

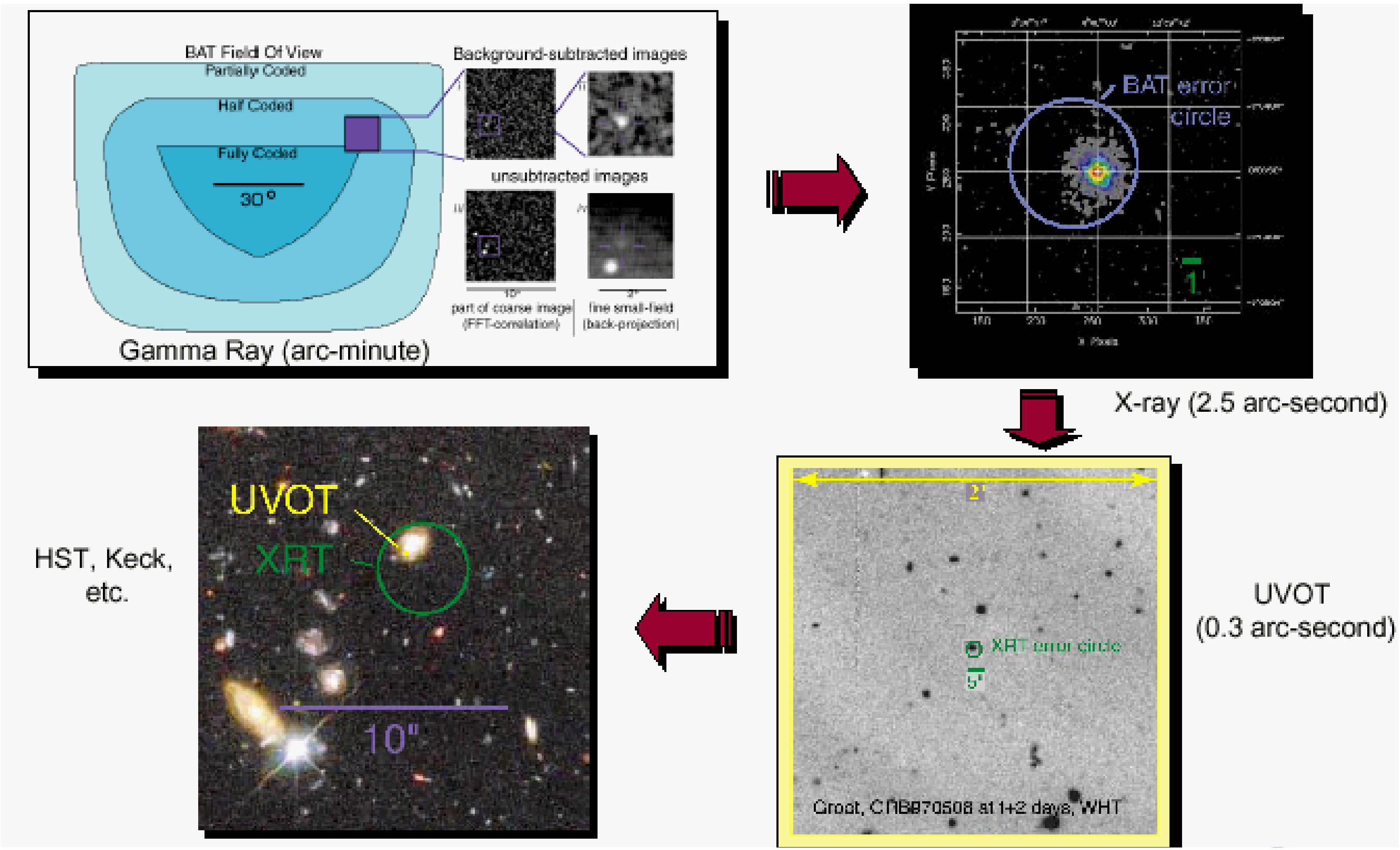
BAT Field Of View
Partially Coded
Half Coded
Fully Coded
30°
Background-subtracted images
unsubtracted images
part of coarse image (FFT-correlation)
fine small-field (back-projection)
Gamma Ray (arc-minute)
BAT error circle
X-ray (2.5 arc-second)
2'
XRT error circle
5"
Groot, GRB970508 at 1+2 days, WHT
UVOT (0.3 arc-second)
UVOT
XRT
10"
HST, Keck, etc.

Exercise #3

- Check and navigate into Swift web sites

SWIFT

https://swift.gsfc.nasa.gov/

SWIFT

https://www.swift.ac.uk/index.php

U.S. site
Italian site
U.K. site

UNIVERSITY OF LEICESTER

School of Physics & Astronomy

Home | About | Support | Data Access | Data Analysis | GRB Products | Publications | Links

site map | Search: ?

The Neil Gehrels Swift Observatory

As of 3rd March, Swift has resumed normal science operations, with both ToO and GRB response re-enabled. High urgency ToOs can again be submitted. (GCN 31668)

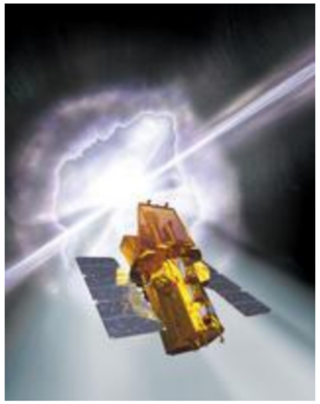

Picture courtesy of Spectrum Astro

Welcome to the UK Swift Science Data Centre.

The NASA-led Swift satellite discovers Gamma-Ray Bursts (GRBs) and measures their X-ray and optical afterglows to arc-second accuracy within a minute or two, continuing to make spectral observations until they fade from view days, weeks or even months later. Swift has been finding around 90 new bursts a year since launch in November 2004. It has provided the most complete study of GRBs so far, finding the most distant objects in the Universe and rapidly advancing science in this area. Swift is a rapid-response multi-wavelength facility which is ideal for observations of transient and variable sources; it has a Guest Investigator programme and a flexible Target of Opportunity programme which is well used.

On this site you can find out more about the mission and GRBs, as well as obtaining data from the on-board instruments and building X-ray products.

One of our team is tweeting about life as a Swift scientist - follow him on Twitter!

Latest Swift Detected GRBs

GRB 220310C
GRB 220310A
GRB 220306B
GRB 220305A
GRB 220302A

Quick Links

Swift in the news
Training Opportunities
GRB and Swift Conferences
Targets of Opportunity
Guest Investigator Program
Build XRT products

Helpdesk

Questions about Swift? Try our guide to Swift or the guide to data processing and analysis. If these don't solve your problem, please feel free to e-mail us at swifthelp@le.ac.uk.

List of acronyms and abbreviations

We are located in the Department of Physics & Astronomy , at the University of Leicester (directions).

SWIFT

https://swift.asdc.asi.it/

Space Science Data Center

Home | About SSDC | News and Communication | Quick Look | Missions | Multimission Archive | Catalogs | Tools | Links | Bibliographic services | Helpdesk | Privacy

Swift Home | About Swift | ASI HQ Swift Home | Swift Data Archive | Swift pointings | Swift Catalogs | Swift Quicklook Data | Swift Data Analysis | Swift Helpdesk | GCN | ToO Request Form | Malindi ground station | Gallery

The Swift Gamma-Ray Burst Mission

ASI Swift Scientific Page (Italian)

Swift is a MIDEX Gamma Ray Burst mission led by NASA with participation of Italy and the UK. The Swift data are available to the scientific community through data centers in the USA, Italy and the UK.

Italy contributes to the mission providing:

- **The XRT X-ray mirror**
- **The Malindi ground station**
- **XRT data reduction and analysis software**

The ASI Science Data Center (ASDC) contributes to the mission providing:

- **Swift Data Archive Mirror**
- **On-line XRT & UVOT data analysis**
- **Swift Quick Look Data (XRT & UVOT Interactive Quick Look)**
- **XRT Burst Support (XBS) and Burst Advocate (BA) activity**

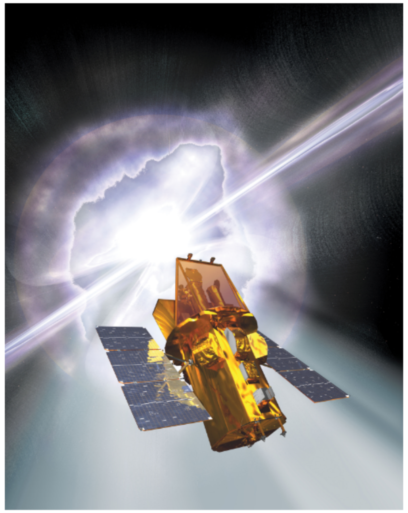

An artist rendering of the Swift satellite catching a Gamma-ray Burst

Discoveries in the *Swift* era

① X-ray afterglow of short GRBs

② Prompt optical-IR emission and very early optical afterglows

③ X-ray flares from GRB

④ Early steep decay of X-ray afterglows

Swift data

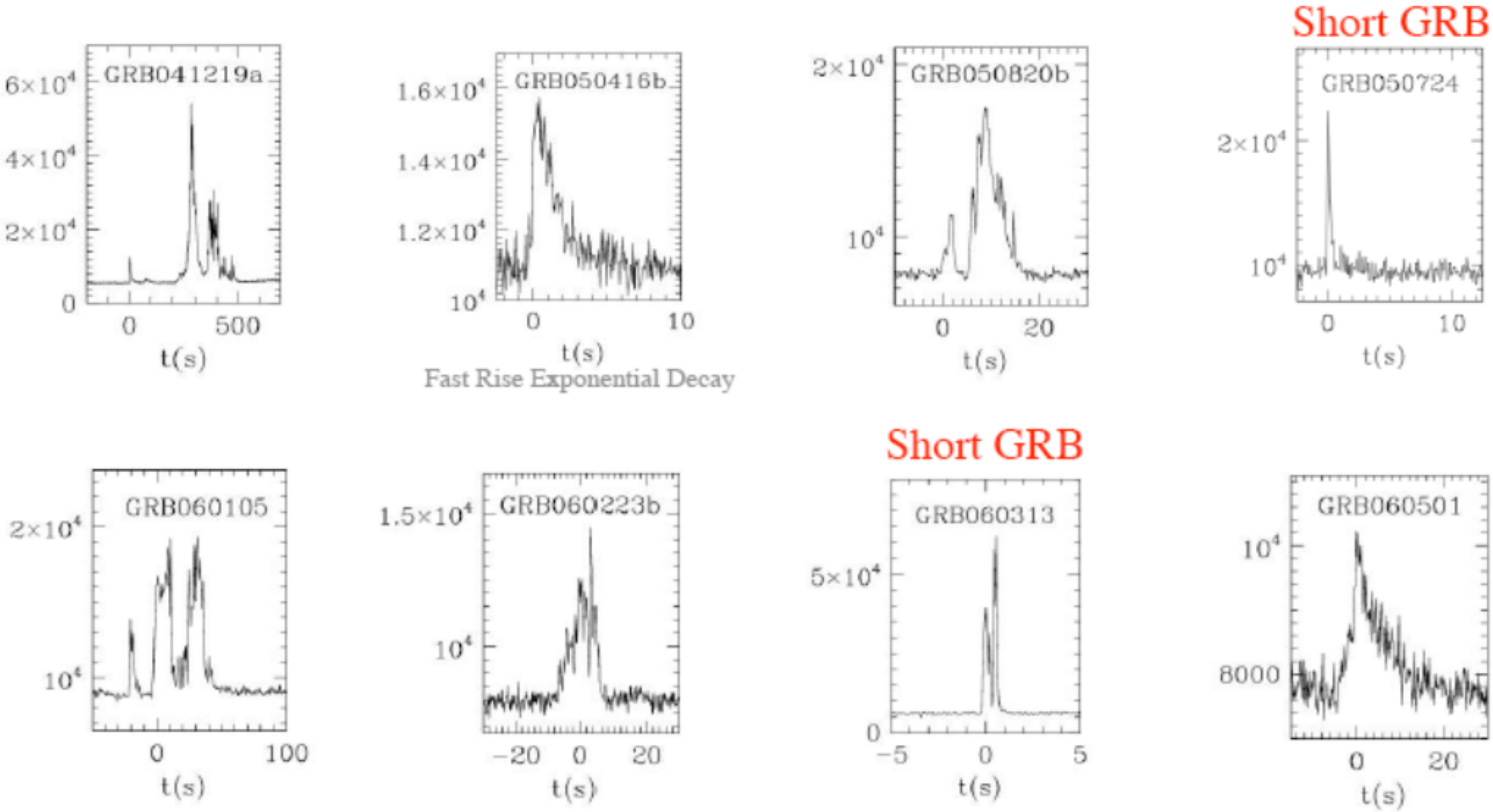
Short GRB
GRB041219a
GRB050416b
GRB050820b
GRB050724
Fast Rise Exponential Decay
t(s)
Short GRB
GRB060105
GRB060223b
GRB060313
GRB060501

Questions for *Swift*

- Do short GRBs have afterglows, and hence can we locate them more precisely?
- Can we pin down the progenitors?
- Are there new subclasses of GRBs?
- Can we find high-redshift bursts and study the early universe?

Swift discoveries

Short GRBs.

- GRB 050509B was a short GRB discovered by *Swift*, with an X-ray afterglow reported 2:29 after the trigger.

- Outskirts of an elliptical galaxy.
- Later sGRBs had optical afterglows too.
- Subsequently found in all galaxy types.

VLT image
Hjorth et al.

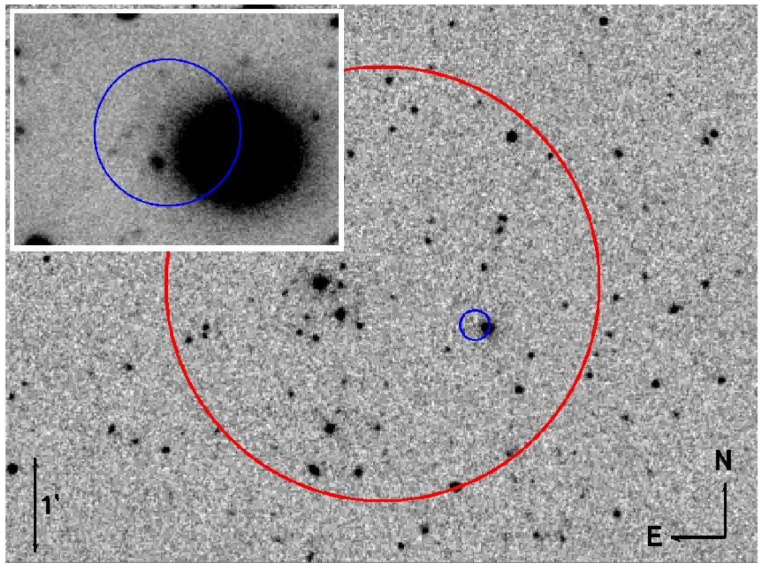

Swift discoveries

Progenitors

- Short GRBs found in all types of galaxy – old population (compact merger/magnetar)
- Long GRBs always found in star forming galaxies and regions – deaths of massive stars.

Swift discoveries

Short GRB with extended emission

- Blurred the distinction between “short” and “long” bursts, and made it more detector-dependent.

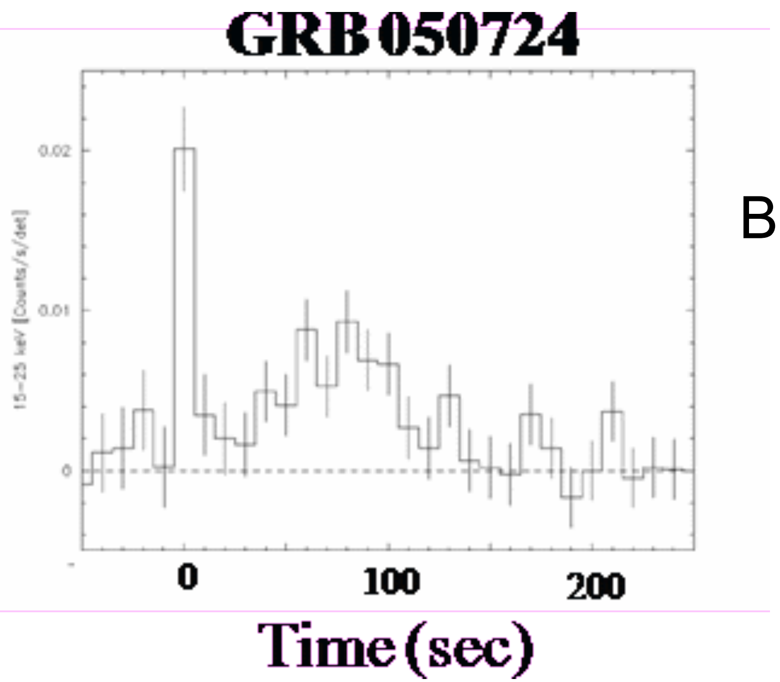

Barthelmy et al. 2005

Swift discoveries

Long GRBs with no SNe

- GRB 060614 and GRB 060505 were nearby, apparently long GRBs, with no related supernova, down to deep limits.
- The GRB taxonomy is clearly more complex than previously thought.
- Maybe a new, progenitor-based classification is needed?

Ultra Long GRBs

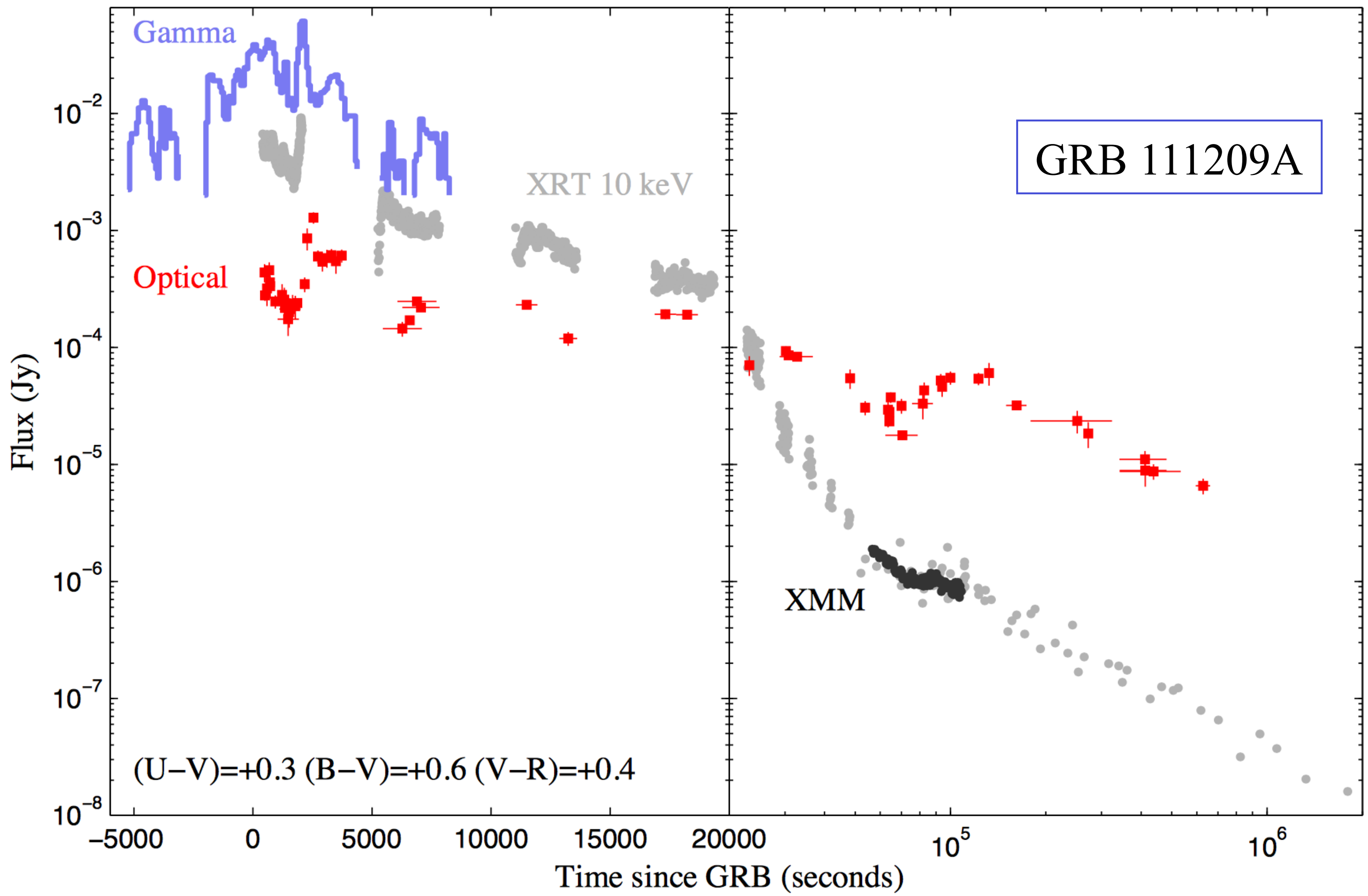

Swift discoveries

High redshift bursts

- 17 GRBs observed by *Swift* have *z*>3.5
- 10 have *z*>4, and 5 have *z* > 5 – a large, rapidly growing population of distant objects.
- GRB 050904 was at z=6.29 (Cusumano et al. 2007)
- GRB 080913 was at z=6.7, and was a fainter-than-normal burst! (Greiner et al. 2009)
- GRB 090423 was at z=8.26 !!!!
- GRB 090429B was at z=9.2 !!!!!!

High redshift GRB

High-Redshift GRBs

z	GRB	Optical Brightness
9.4	090429B	K = 19 @ 3 hrs
8.2	090423	K = 20 @ 20 min
6.7	080813	K = 19 @ 10 min
6.29	050904	J = 18 @ 3 hrs
5.6	060927	I = 16 @ 2 min
5.3	050814	K = 18 @ 23 hrs
5.11	060522	R = 21 @ 1.5 hrs

Metallicity

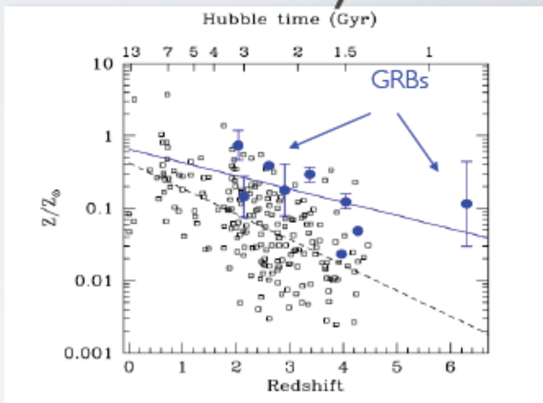

Savaglio 2006

Star Formation Rate

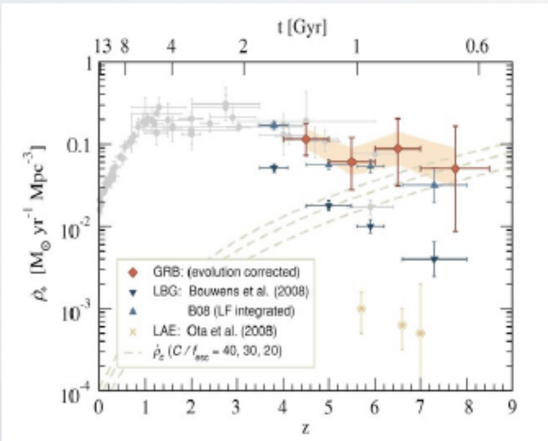

Kistler et al. 2009;
Robertson & Ellis 2011

Fermi/Swift GRB Conference 2012, Munich, May 7-11, 2012

High z - searches

High-z Universe: searching for the best probe

Galaxies

Pros

- ★ Multiband data are available (some)
- ★ Refurbished HST
- ★ Different technique (LBG/Lyα emission)
- ★ Do not “disappear”

Cons

- ★ Small region of the sky (11 arcmin^2)
- ★ Required several hours of observations
- ★ Very faint objects
- ★ Galaxy templates are complex
- ★ Difficult determination of Age/dust/SFR

Gamma-ray Bursts

Pros

- ★ Very bright
- ★ Happens everywhere
- ★ Can be followed quickly from space and ground (now at least)
- ★ **Have a very simple spectrum** (synchrotron, simple power-law)
- ★ Allow better investigation of τ_{HI}

Cons

- ★ Rare (few “good ones”)
- ★ Fade fast, ~minute position identification (space mission)
- ★ Require multiband observations

Swift discoveries

Where are the jet breaks?

- Strong, achromatic light curve steepening was expected in most/all GRBs – it's now exciting if we think we've got one!
- They could be hidden (Curran et al. 2008), or we're not considering enough possibilities (Racusin et al. 2009)
- Perhaps the jets are structured/complex, so breaks are not achromatic? (e.g. Oates et al. 2007, de Pasquale et al. 2008).

Afterglows in the Swift era …

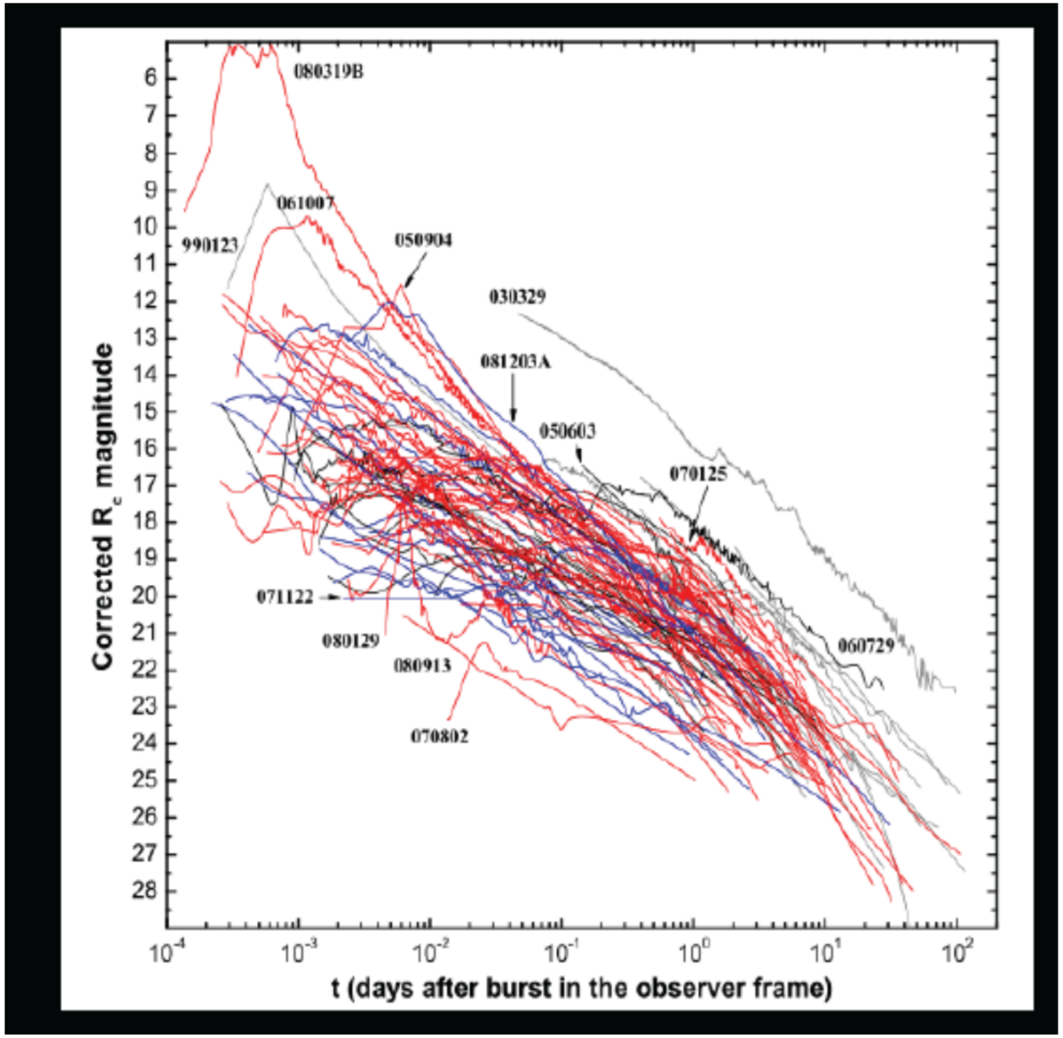

Afterglows in the Swift era

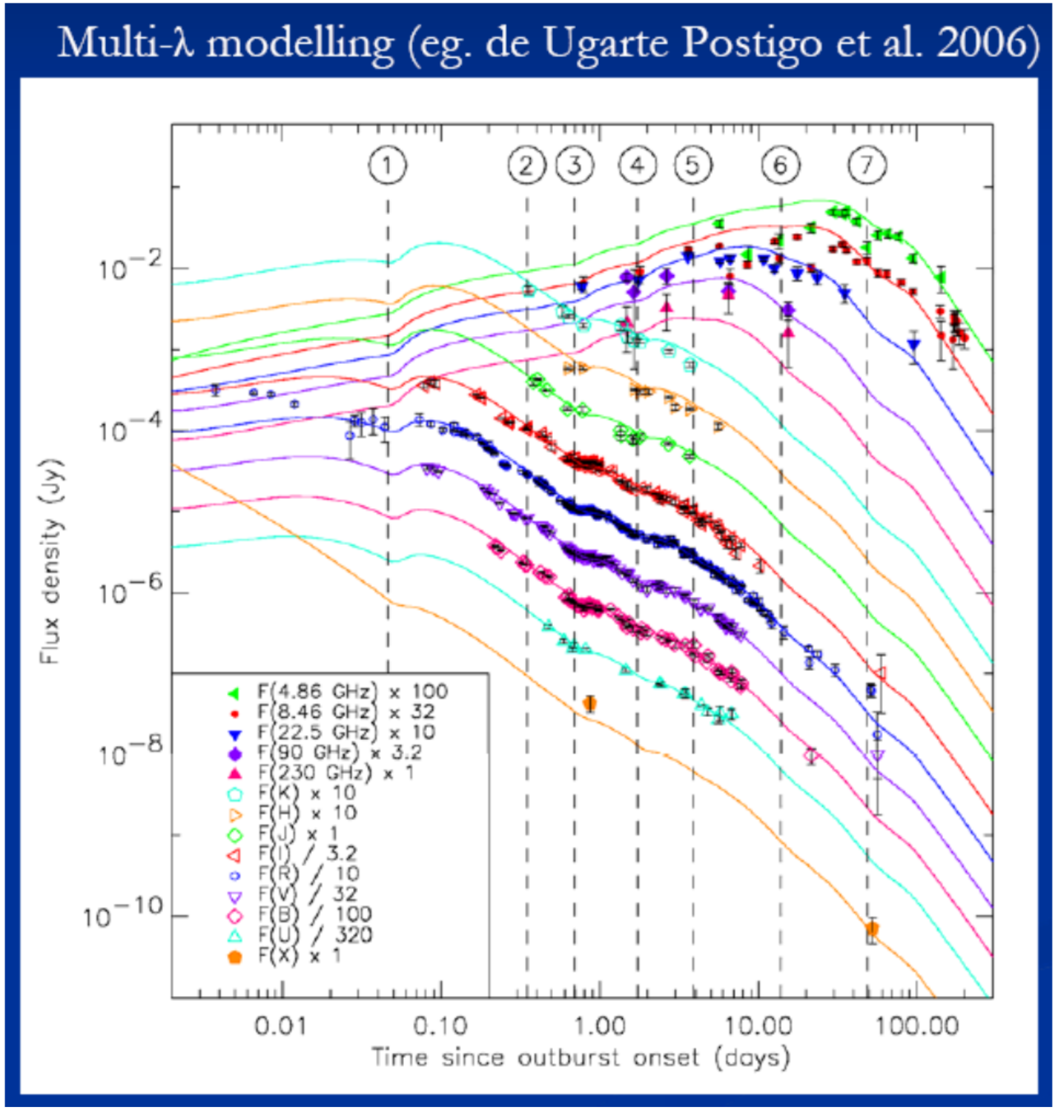

Swift discoveries

GRB 080319B

- Very bright – reached m_v=5.3

Movie from Pi of the sky.

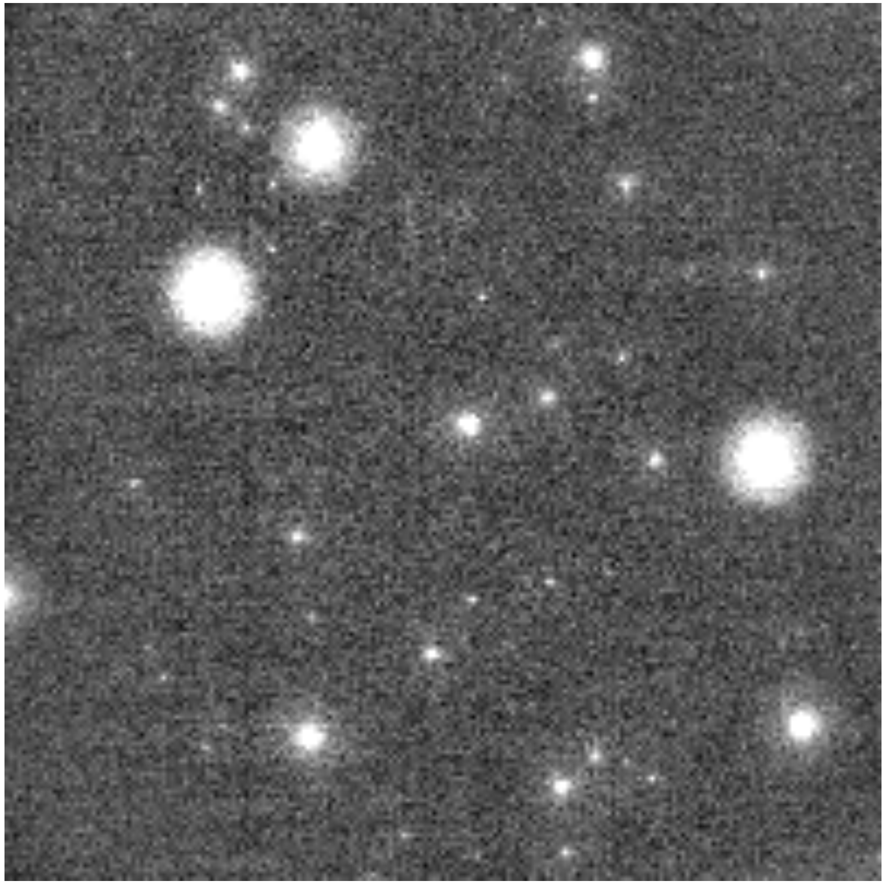

Swift discoveries

GRB 080319B

- Very bright – reached m_v=5.3
- z=0.9
- If it were at the Galactic centre, it would appear as bright as the Sun!
- Bright in X-rays and Gamma-rays, but nothing like as extraordinary as in the optical.
- Implies a complex jet structure (Racusin et al. 2008, Nature).

080319B

First "naked-eye" Burst GRB 080319B

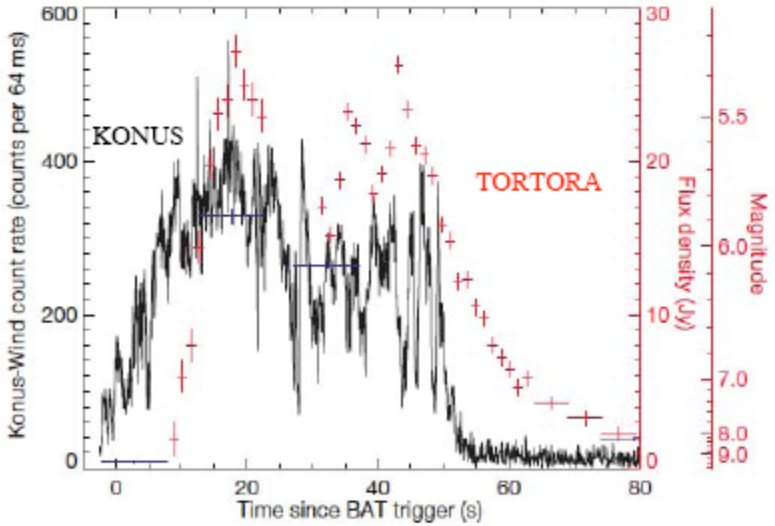

Racusin et al. 2008

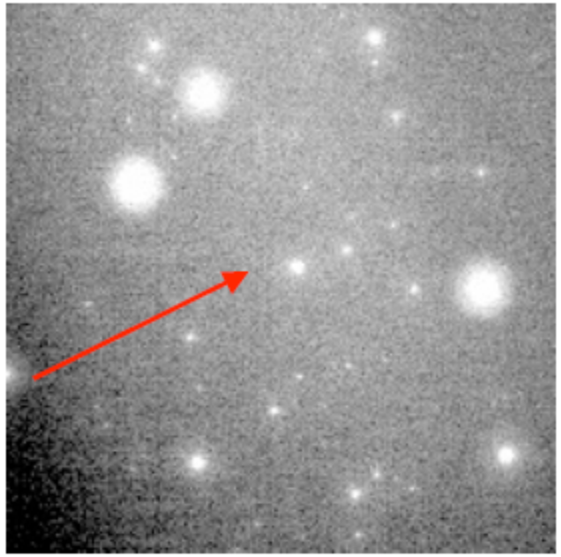

Pi-of-the-Sky

T90 = 50s   z = 0.94

Prompt optical observations:
- Pi-of-the-Sky (Chile) pre-burst
- RAPTOR (New Mexico)
- REM/TORTORA (Chile)

Peak brightness of 5.6 magnitudes!!

080319B

Even corrected for distance, brightest optical burst

In our Galaxy, such a burst would be brighter than the sun!

GRBs much more luminous than most energetic quasars & SNe

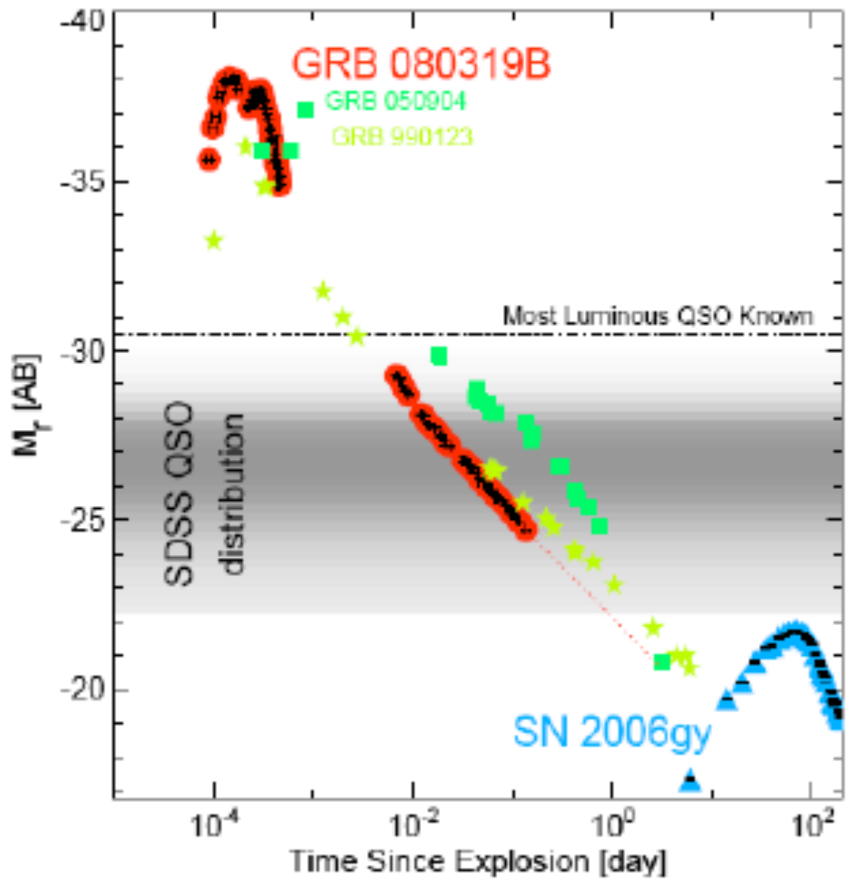

Bloom et al. 2008

Swift discoveries

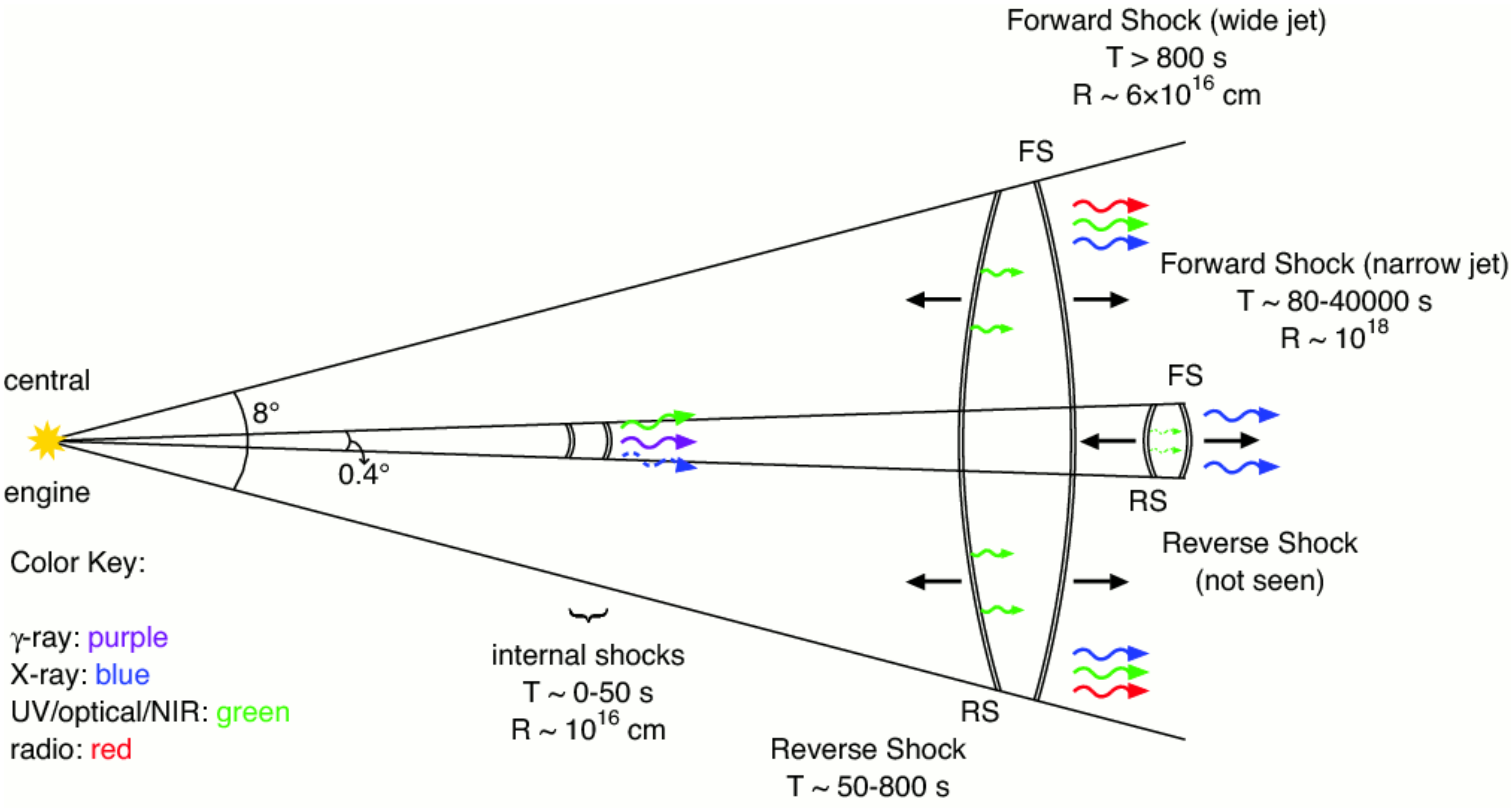

Summary

- *Swift* has helped to answer some questions:
  - Localised short GRBs
  - Supported collapsar and compact merger progenitor models.
- Asked a load of new questions!
  - What are the subtypes?
  - How do we get X-ray afterglows? And flares?
  - What is the jet structure?

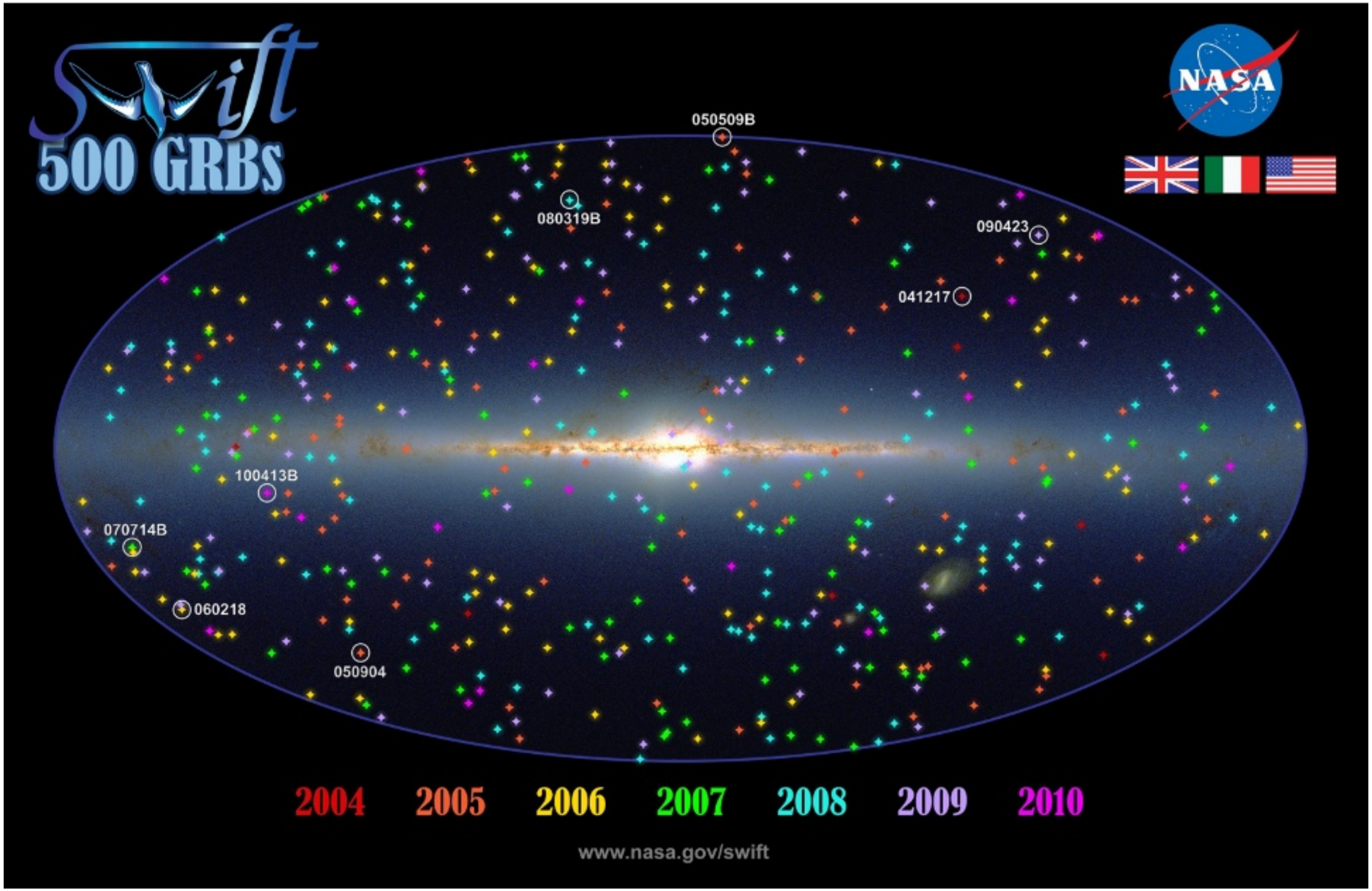
Swift
500 GRBs
NASA
050509B
080319B
090423
041217
100413B
070714B
060218
050904
2004
2005
2006
2007
2008
2009
2010
www.nasa.gov/swift

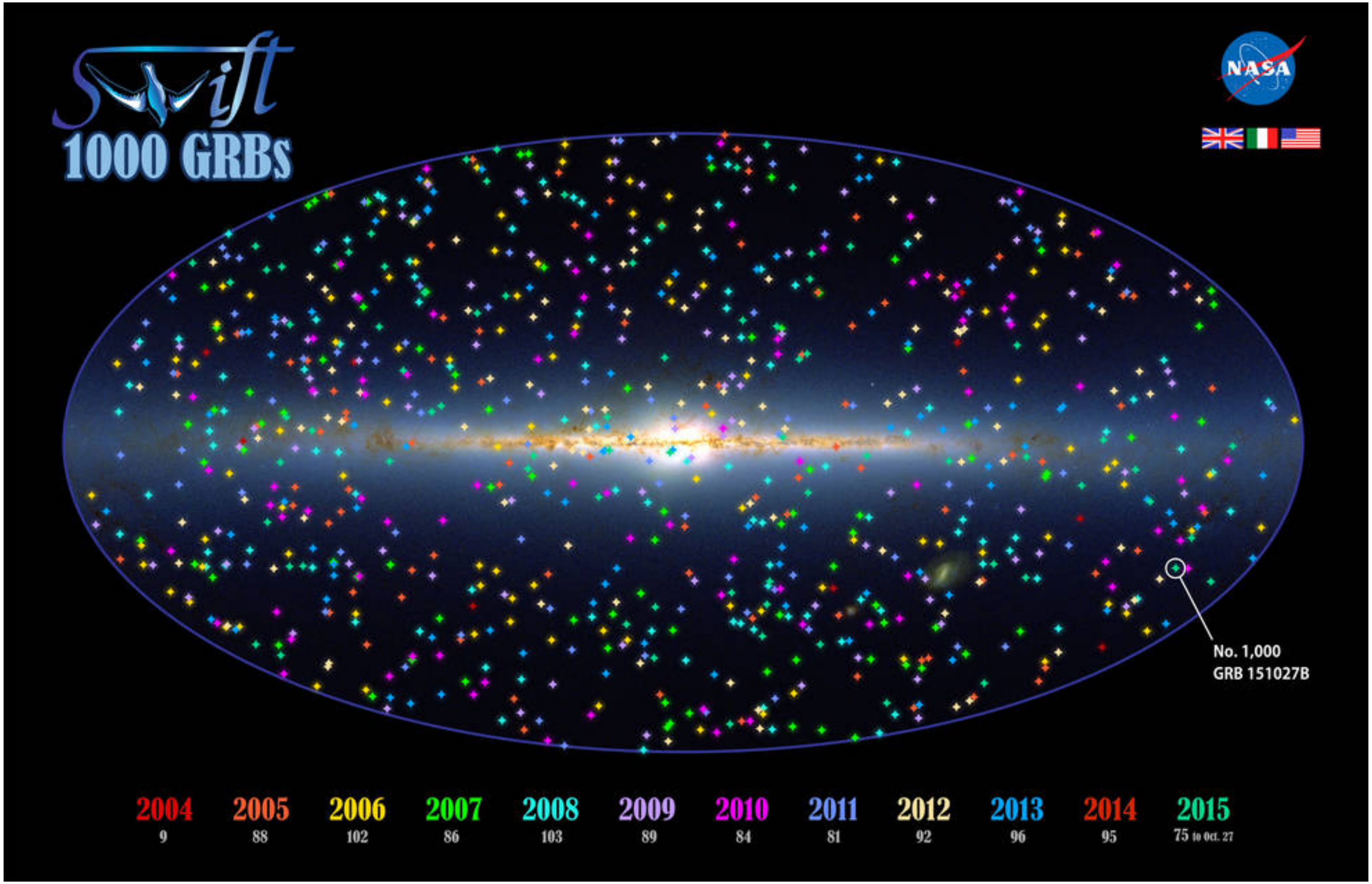

Swift
1000 GRBs
NASA
No. 1,000
GRB 151027B
2004
9
2005
88
2006
102
2007
86
2008
103
2009
89
2010
84
2011
81
2012
92
2013
96
2014
95
2015
75 to Oct. 27

Astrofisica Nucleare e Subnucleare

Solid State Detectors

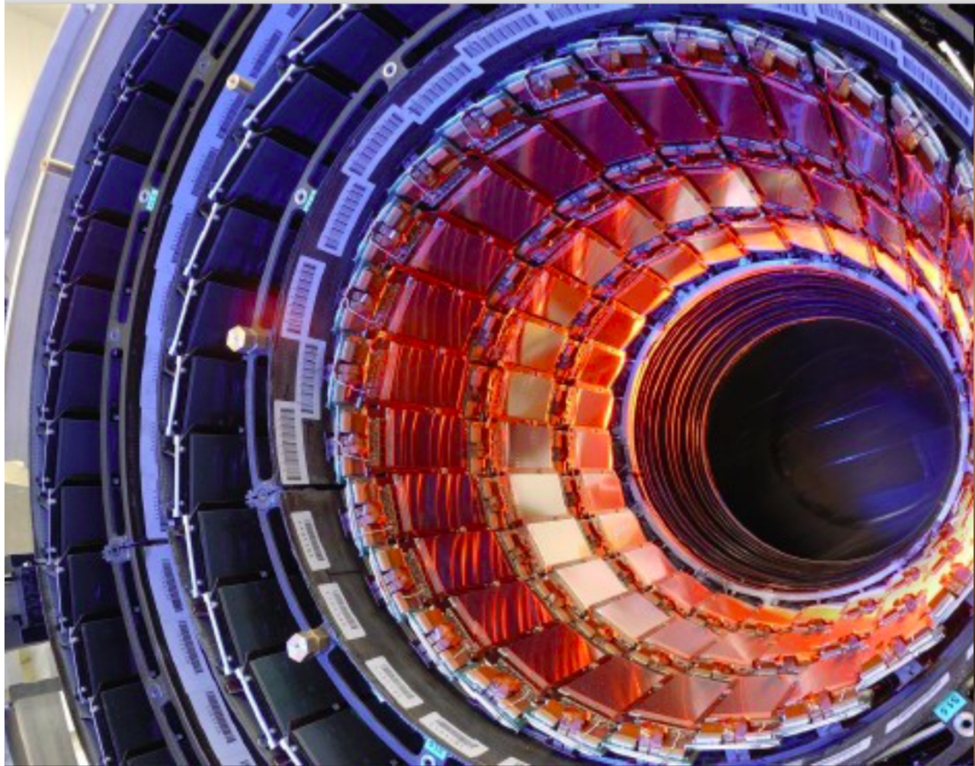


Detectors for Particle Physics

Semiconductor Detectors

D. Bortoletto

Solid State Detector

- A solid state detector is an ionization chamber
  - Ionizing radiation creates electron/hole pairs
  - Charge carriers move in applied E field
  - Motion induces a current in an external circuit, which can be amplified and sensed.

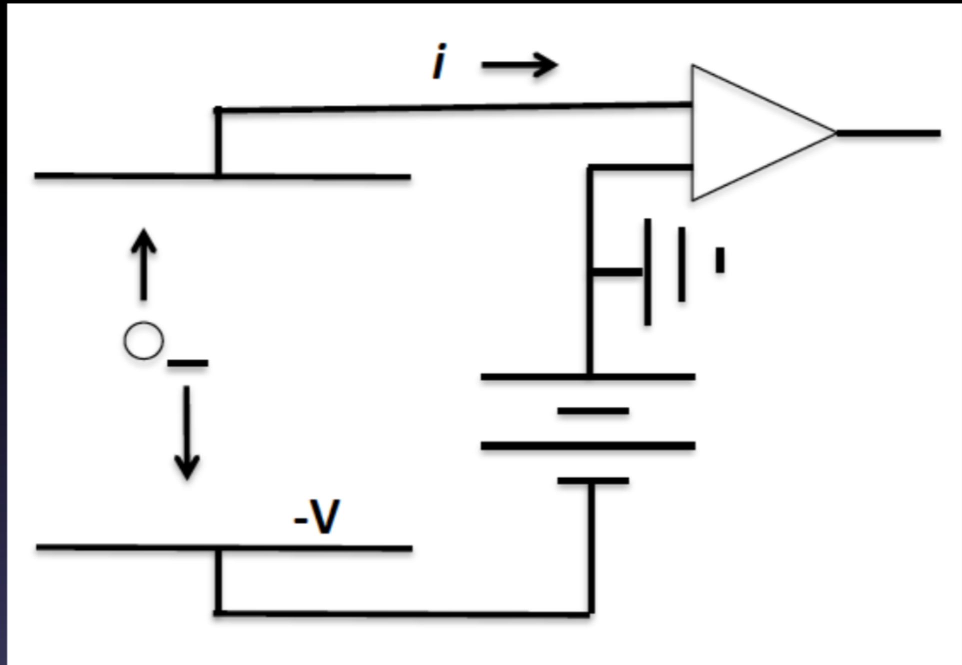

	Gas	Solid
Density	Low	High
Atomic number (Z)	Low	Moderate (Z=14)
Ionization Energy (ε_I)	Moderate ($\approx$ 30 eV)	Low ($\approx$3.6 eV)
Signal Speed	Moderate (10ns-10μs)	Fast (<20 ns)

Comparison solid state versus gas

Ionization chamber medium could be gas, liquid, or solid

- **Gas ⇒ electron and ion pairs; Semiconductor ⇒electron and hole pairs**

	Gas	Solid
Density	Low	High
Atomic number (Z)	Low	Moderate (Z=14)
Ionization Energy (ε_I)	Moderate (≈ 30 eV)	Low (≈3.6 eV)
Signal Speed	Moderate (10ns-10μs)	Fast (<20 ns)

Solid State Detectors

- Energy (E) to create e-h pairs 10 times smaller than gas ionization ⇒ increase charge⇒ good E resolution

$$\frac{\Delta E}{E} \propto \frac{1}{\sqrt{N}} \propto \frac{1}{\sqrt{E/\varepsilon_I}} \propto \sqrt{\varepsilon_I}$$

- Greater density:
  - Reduced range of secondary electrons ⇒ excellent spatial resolution
  - Average E_{loss} ≈390eV/ μm ≈108 e-h/ μm (charge collected is a function of thickness d. Up-to-now no multiplication)
- To minimize multiple scattering d is small
  - 300 μm ≈32,000 e-h pairs ➔ good S/N

Solid State Detectors

Gas Detectors

In gaseous detectors, a charged particle is liberating electrons from the atoms, which are freely bouncing between the gas atoms.

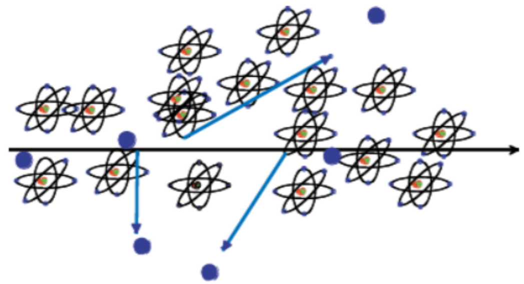

An applied electric field makes the electrons and ions move, which induces signals on the metal readout electrodes.

For individual gas atoms, the electron energy levels are discrete.

Solid State Detectors

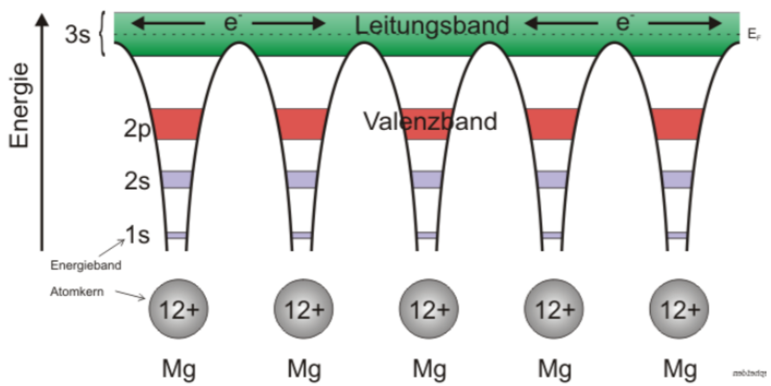

In solids (crystals), the electron energy levels are in 'bands'.

Inner shell electrons, in the lower energy bands, are closely bound to the individual atoms and always stay with 'their' atoms.

In a crystal there are however energy bands that are still bound states of the crystal, but they belong to the entire crystal. Electrons in these bands and the holes in the lower band can freely move around the crystal, if an electric field is applied.

Solid State Detectors

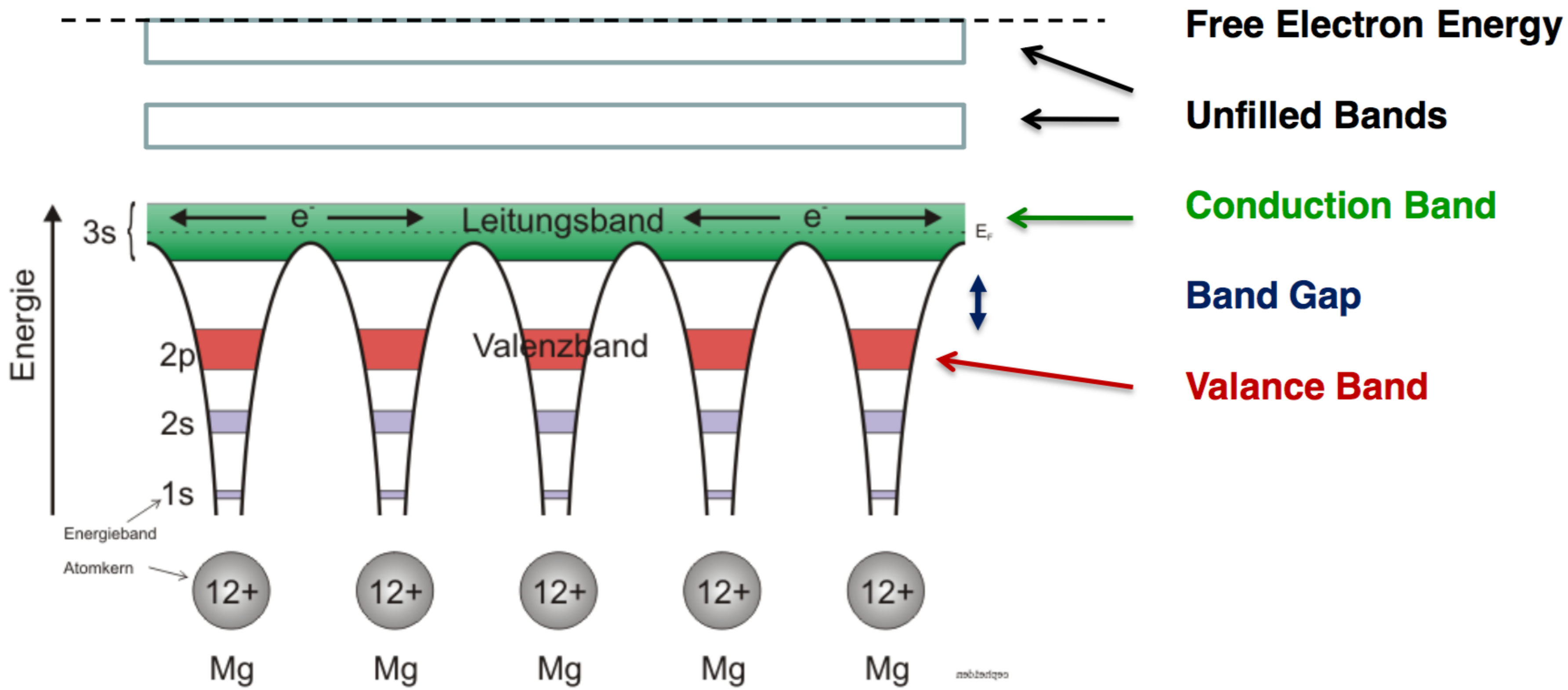

Conductor, Insulator, Semiconductor

In case the conduction band is filled the crystal is a conductor.

In case the conduction band is empty and 'far away' from the valence band, the crystal is an insulator.

In case the conduction band is empty but the distance to the valence band is small, the crystal is a semiconductor.

Solid State Detectors

Band Gap, e-h pair Energy

The energy gap between the last filled band – the valence band – and the conduction band is called band gap E_g.

The band gap of Diamond/Silicon/Germanium is 5.5, 1.12, 0.66 eV.

The average energy to produce an electron/hole pair for Diamond/Silicon/Germanium is 13, 3.6, 2.9eV.

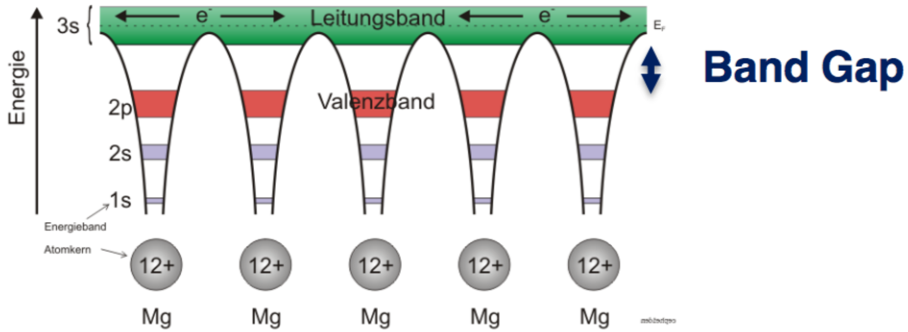

Temperature, Charged Particle Detection

In case an electron in the valence band gains energy by some process, it can be excited into the conduction band and a hole in the valence band is left behind.

Such a process can be the passage of a charged particle, but also thermal excitation → probability is proportional Exp($-E_g/kT$).

The number of electrons in the conduction band is therefore increasing with temperature i.e. the conductivity of a semiconductor increases with temperature.

Solid State Detectors

Primary 'ionization':

The average energy to produce an electron/hole pair is:
Diamond (13eV), Silicon (3.6eV), Germanium (2.9eV)

Comparing to gas detectors, the density of a solid is about a factor 1000 larger than that of a gas and the energy to produce and electron/hole pair e.g. for Si is a factor 7 smaller than the energy to produce an electron-ion pair in Argon.

Solid State vs. Gas Detector:

The number of primary charges in a Si detector is therefore about 10^4 times larger than the one in gas → while gas detectors need internal charge amplification, solid state detectors don't need internal amplification.

While in gaseous detectors, the velocity of electrons and ions differs by a factor 1000, the velocity of electrons and holes in many semiconductor detectors is quite similar → very short signals.

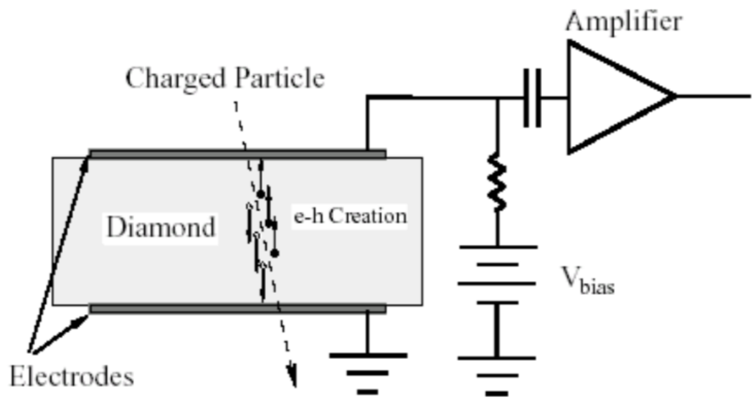

Diamond → A solid state ionization chamber

Semiconductor

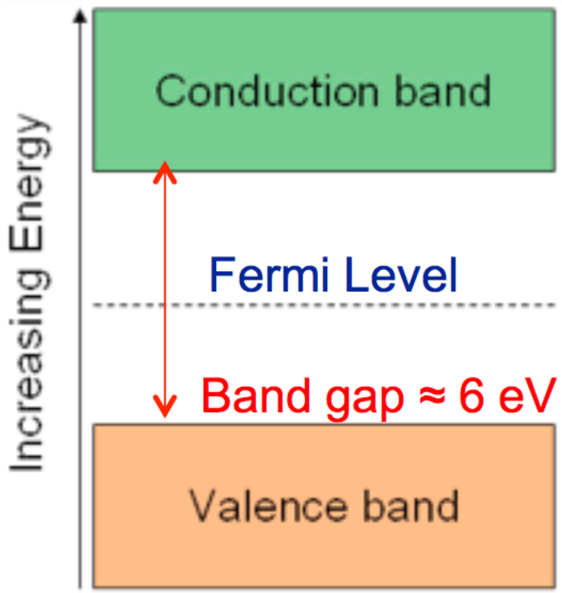

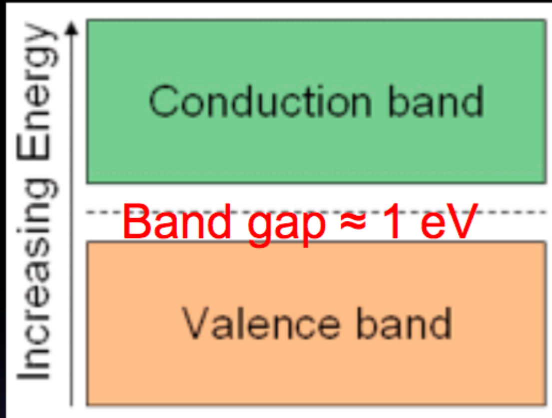

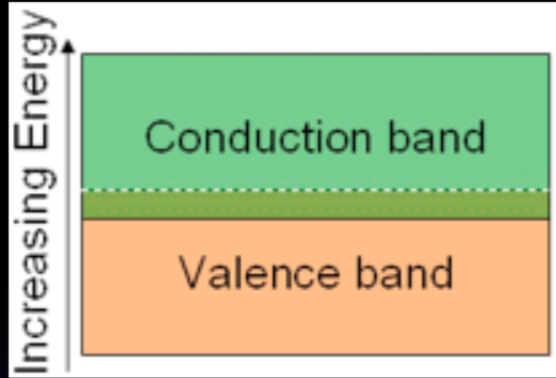

- Fermi level
  - Maximum electron energy at T = 0 K

- Semiconductor: at room temperature electrons can already occupy the conduction band and may recombine with holes.
- Thermal equilibrium is reached between excitation and recombination when the charge carrier concentration $n_e = n_h = n_i$= intrinsic carrier concentration≈1.5×10^{10} cm^{-3}

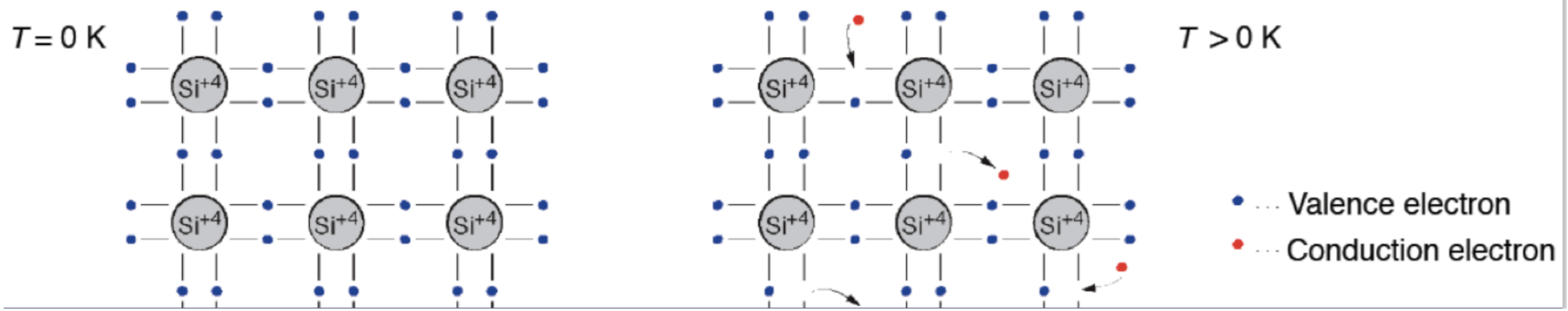

Doped semiconductors

DONOR (N)

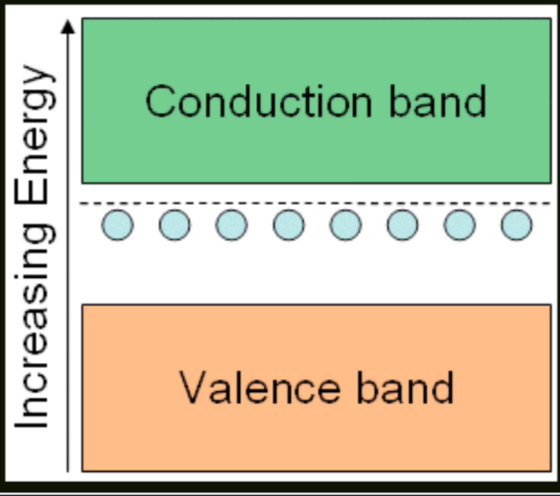

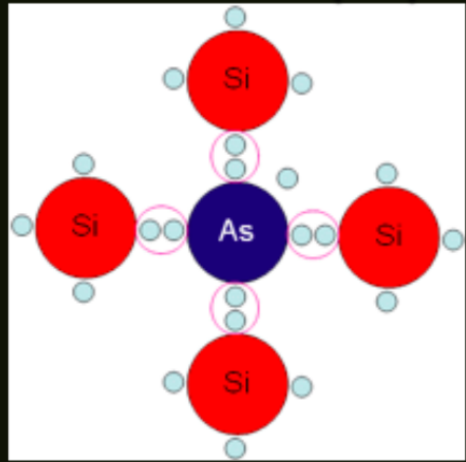

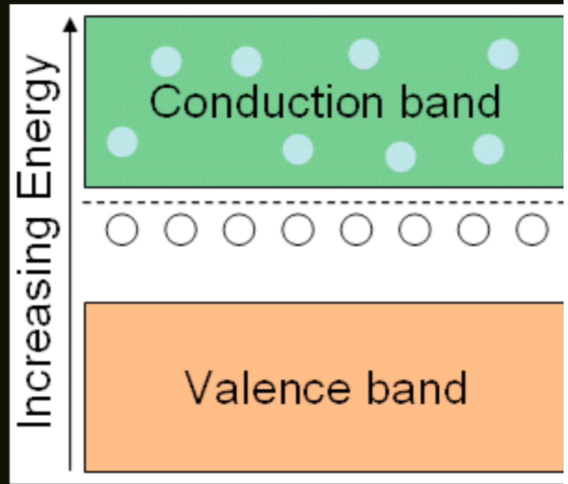

ACCEPTOR (P)

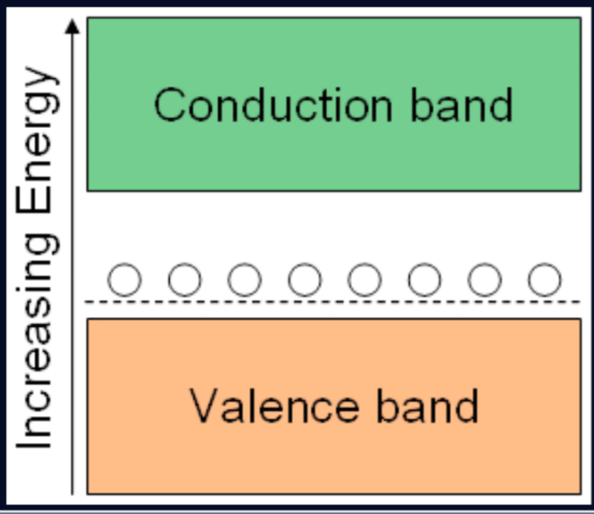

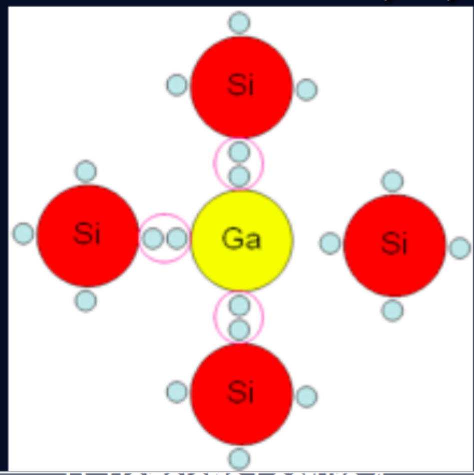

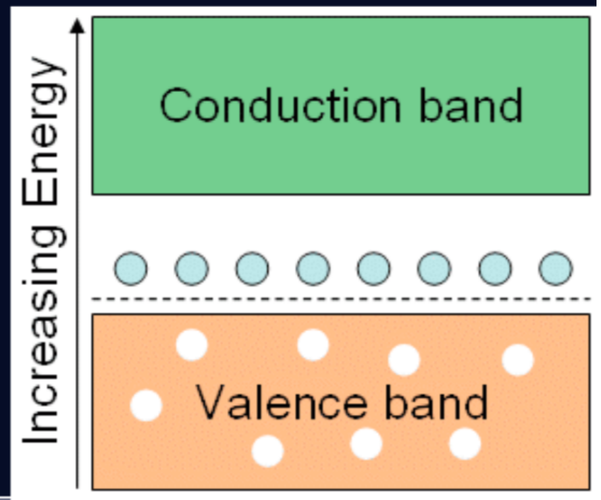

Doping of Silicon

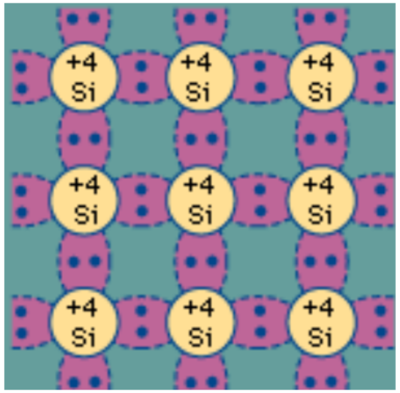

doping

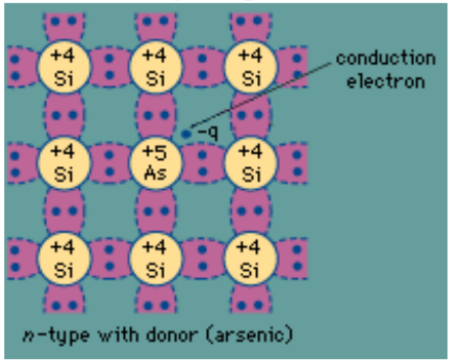

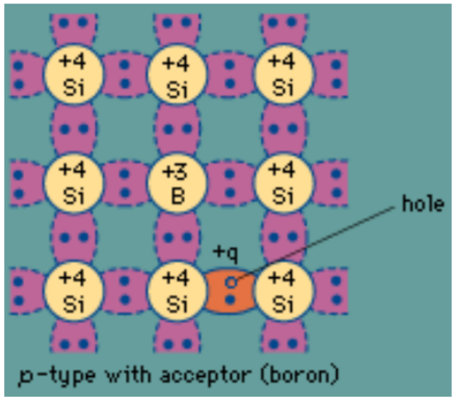

In a silicon crystal at a given temperature the number of electrons in the conduction band is equal to the number of holes in the valence band.

Doping Silicon with Arsen (+5) it becomes and n-type conductor (more electrons than holes).

Doping Silicon with Boron (+3) it becomes a p-type conductor (more holes than electrons).

Bringing p and n in contact makes a diode.

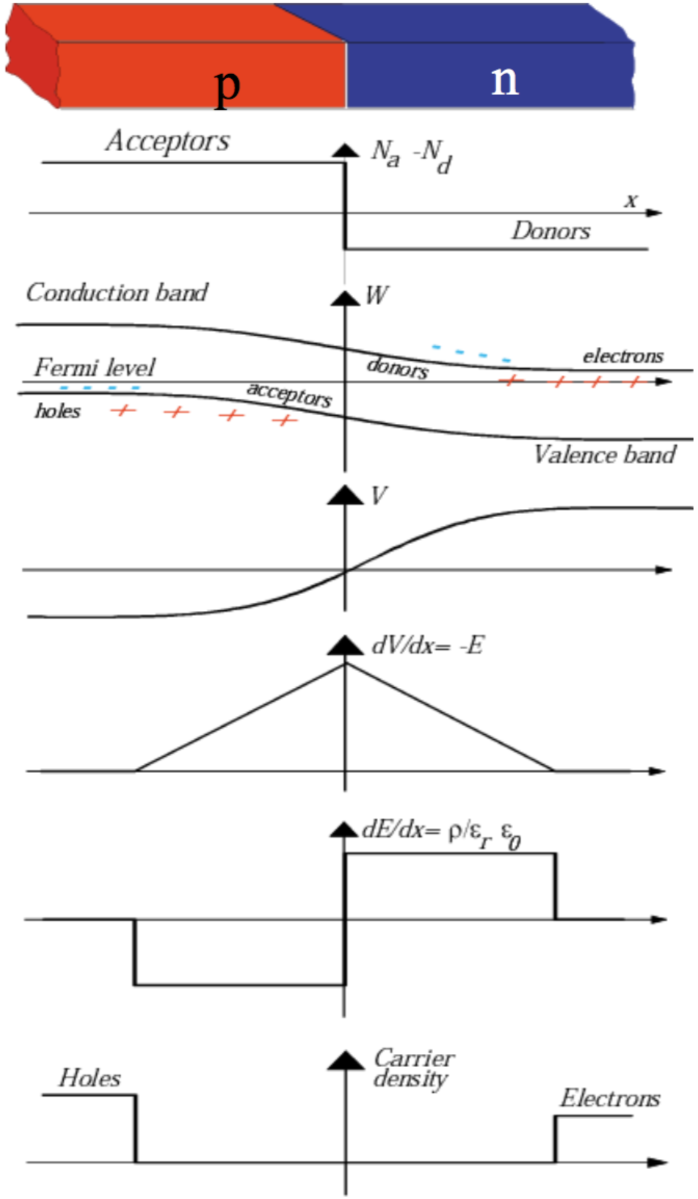

PN Junction

- PN junction without external voltage
  - Free charges move until the chemical potential is balanced by an electrical potential called the built-in potential

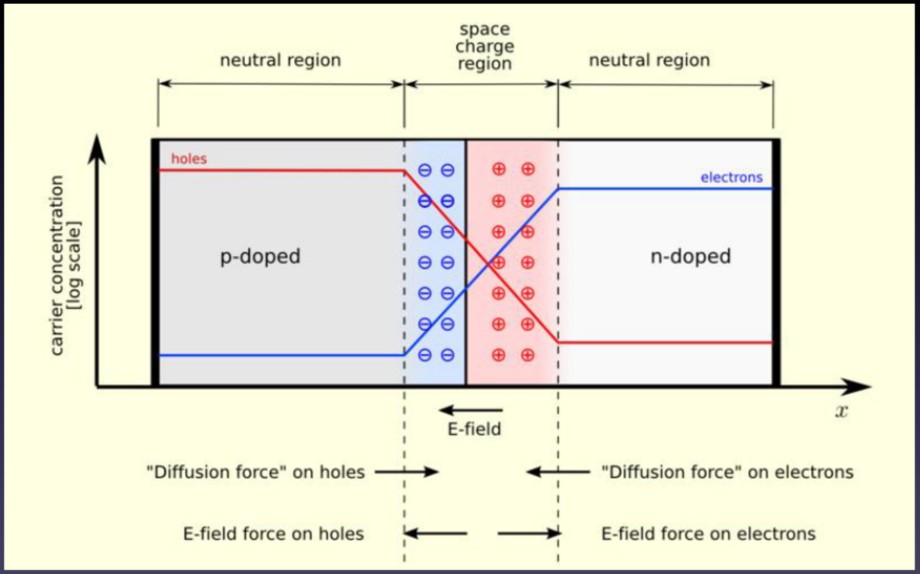

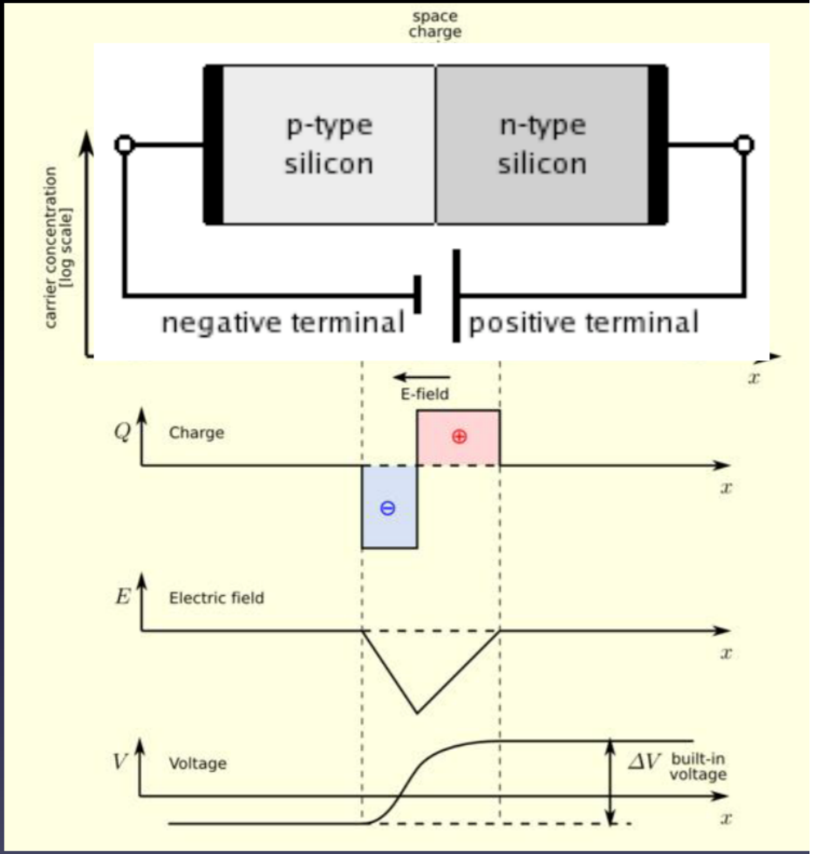

- The space charge (depletion) region can be made bigger by applying a reverse bias voltage

Si-Diode used as a Particle Detector !

At the p-n junction the charges are depleted and a zone free of charge carriers is established.

By applying a voltage, the depletion zone can be extended to the entire diode → highly insulating layer.

An ionizing particle produces free charge carriers in the diode, which drift in the electric field and induce an electrical signal on the metal electrodes.

As silicon is the most commonly used material in the electronics industry, it has one big advantage with respect to other materials, namely highly developed technology.

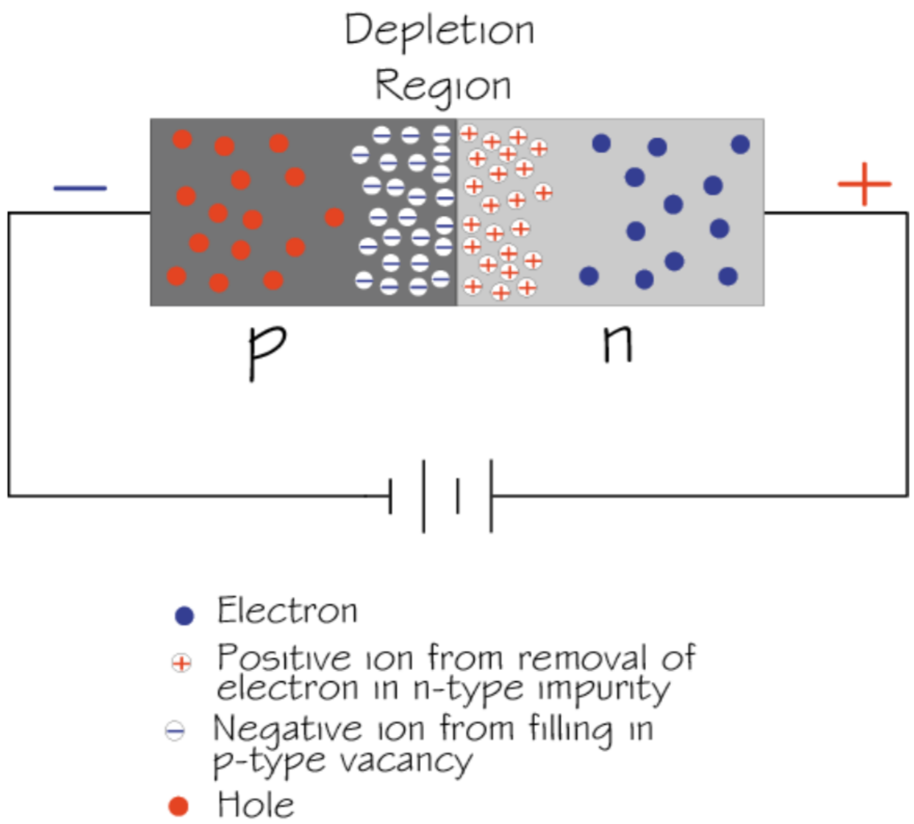

Under-Depleted Silicon Detector

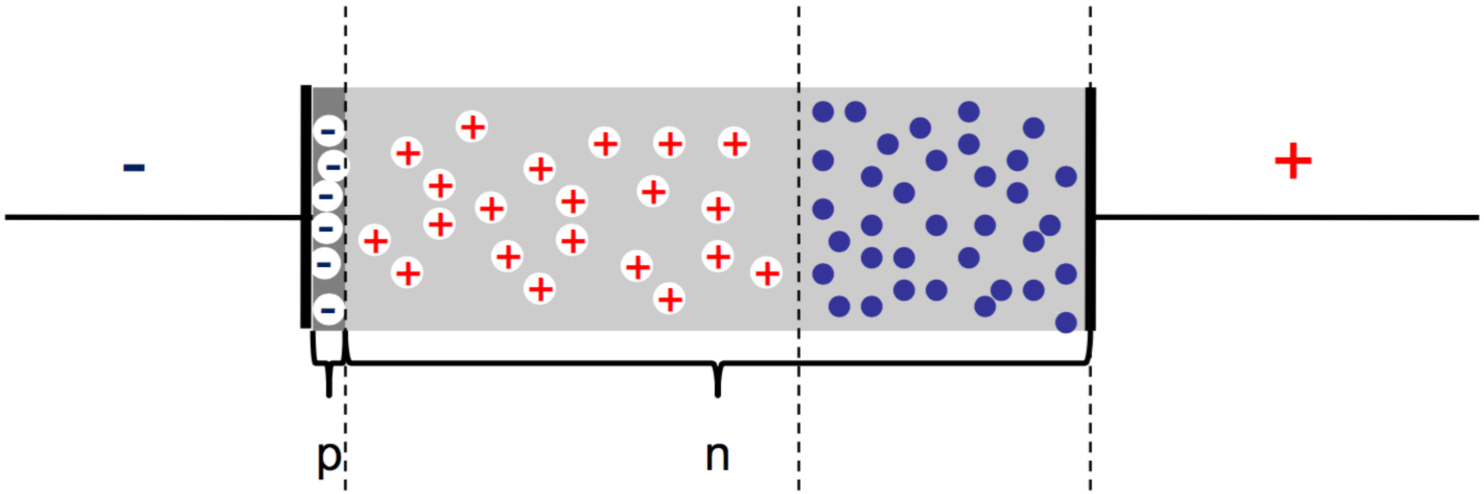

Zone without free charge carriers positively charged. Sensitive Detector Volume.

Zone with free electrons. Conductive. Insensitive to particles.

Fully-Depleted Silicon Detector

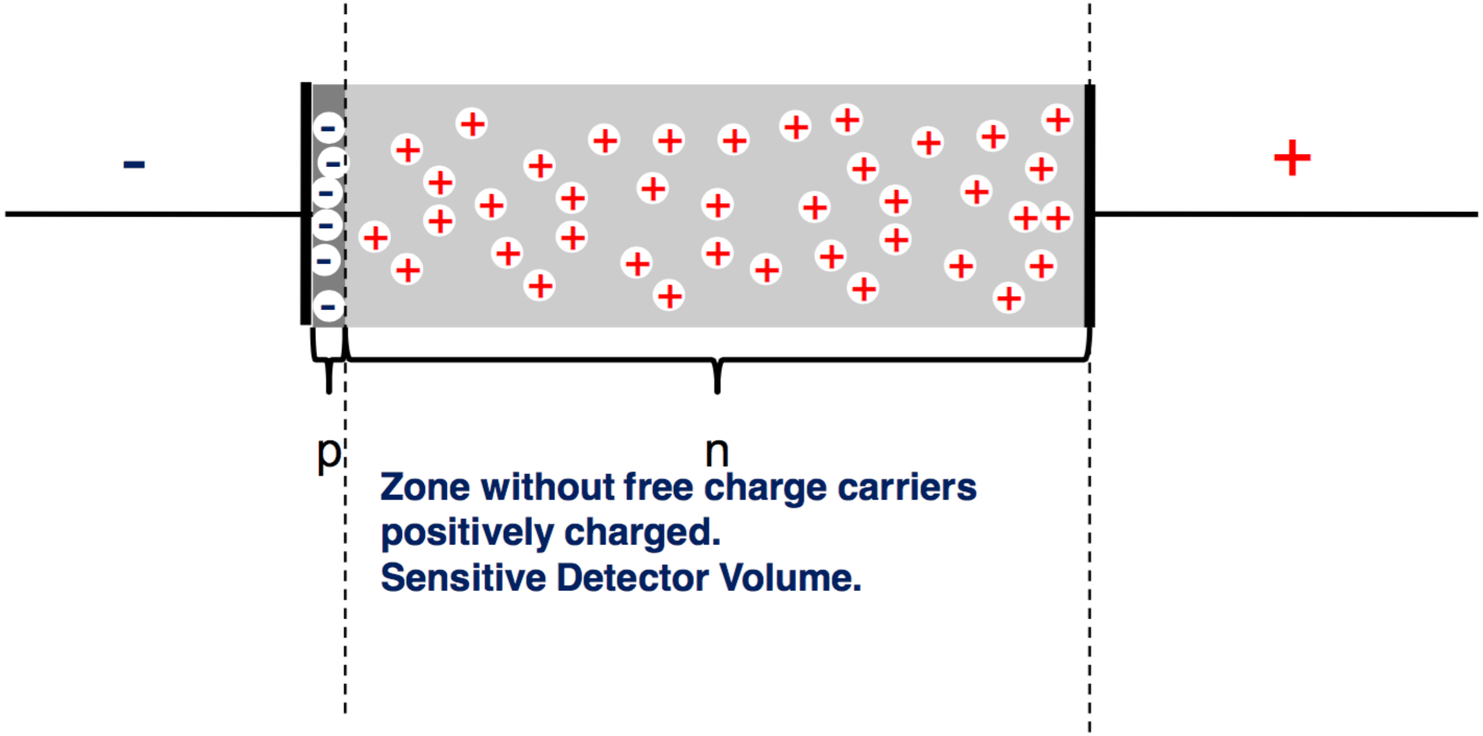

Zone without free charge carriers positively charged.
Sensitive Detector Volume.

Silicon Detector

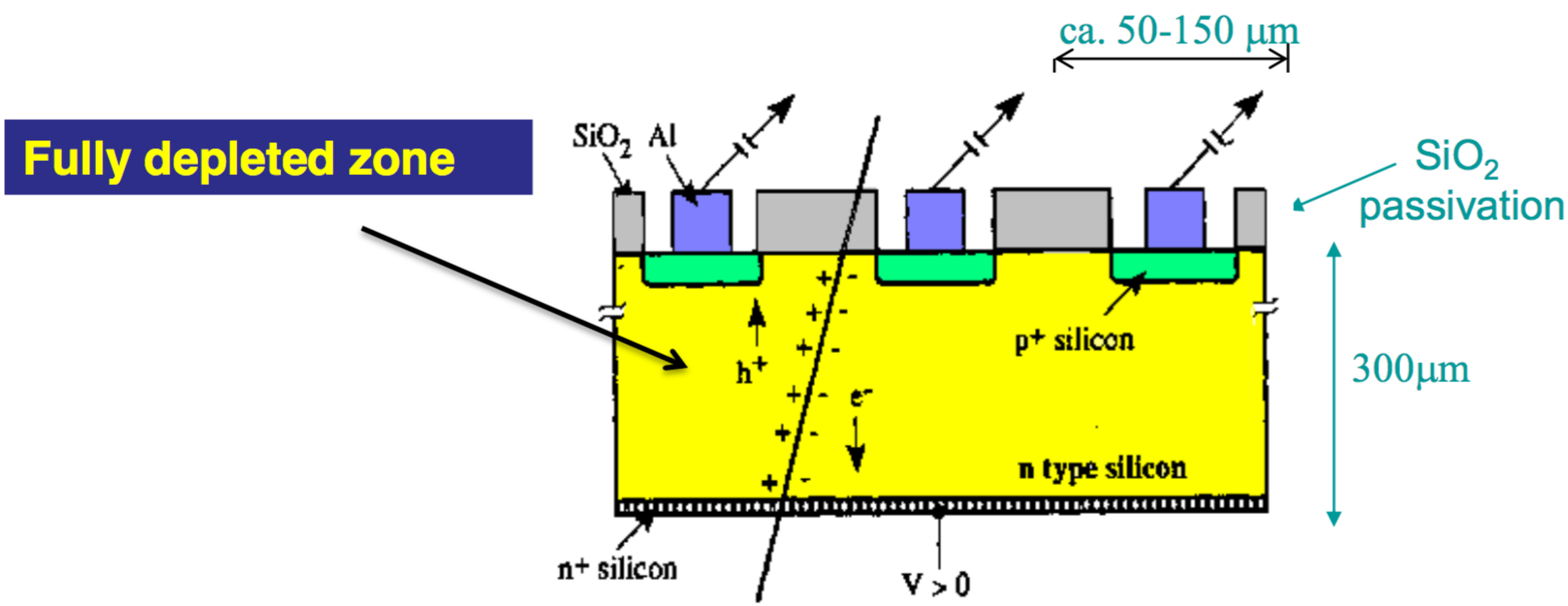

N (e-h) = 11 000/100μm

Position Resolution down to ~ 5μm !

Silicon Strip Detectors (SSD)

- By segmenting the implant we can reconstruct the position of the traversing particle in one dimension
- DC-coupled strip detector – simplest position sensitive Silicon detector
- Standard configuration:
  - Strips p implants
  - Substrate n doped (~2-10 kΩcm) and ~300μm thick
  - $V_{dep} < 200$ V
  - Backside Phosphorous implant to establish ohmic contact and to prevent early breakdown
- Highest field close to the collecting electrodes (junction side) where most of the signal is induced

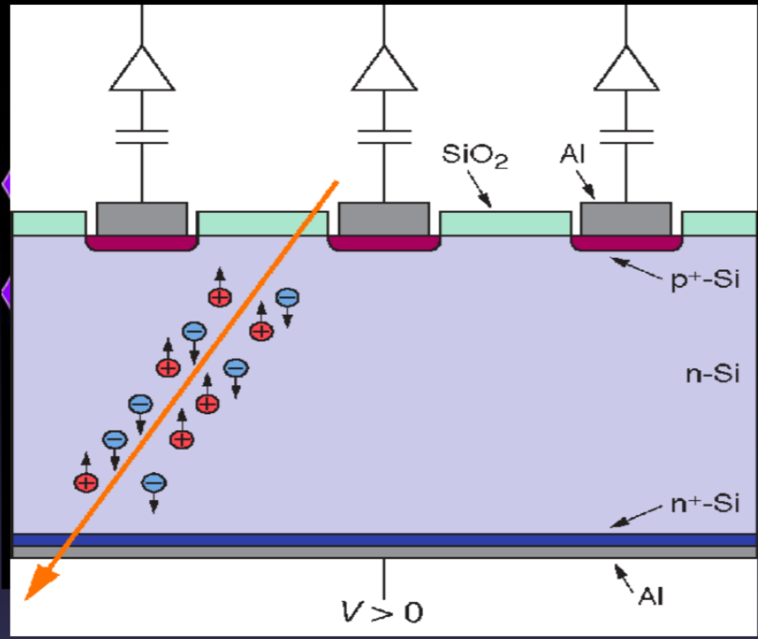

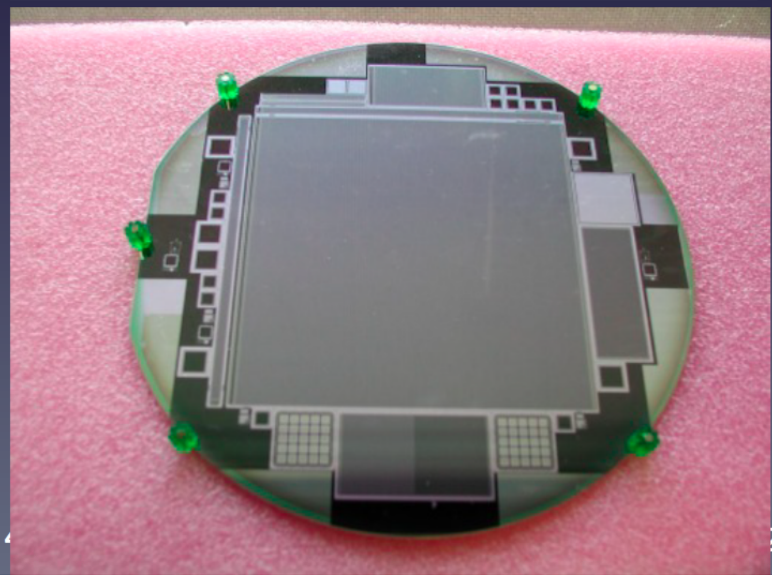

Double Sided Silicon Detectors

- **Advantages:**
  - More elegant for measuring 2 coordinates than using stereo modules
  - Saves material
- **Disadvantages:**
  - Needs special strip insulation of n-side (p-stop, p-spray techniques)
  - Complicated manufacturing and handling procedures
- Expensive
- Ghost hits possible

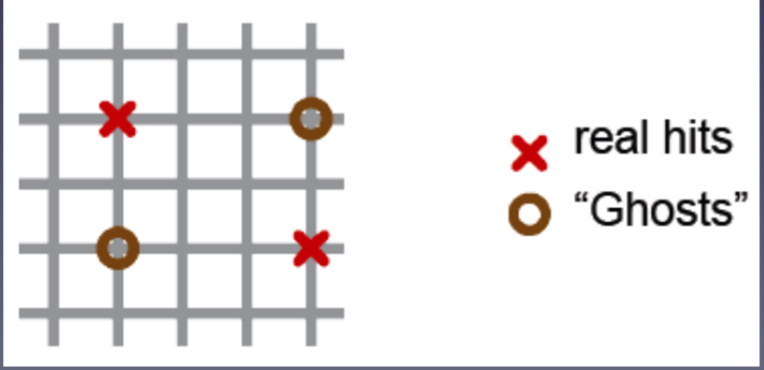

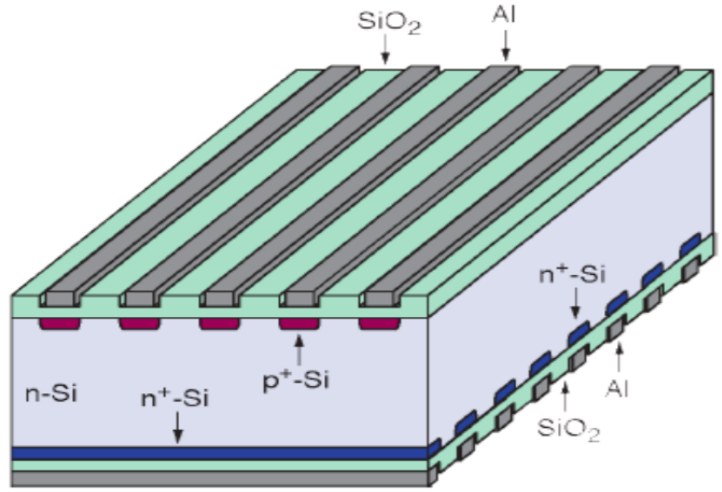

Scheme of a double sided strip detector (biasing structures not shown)

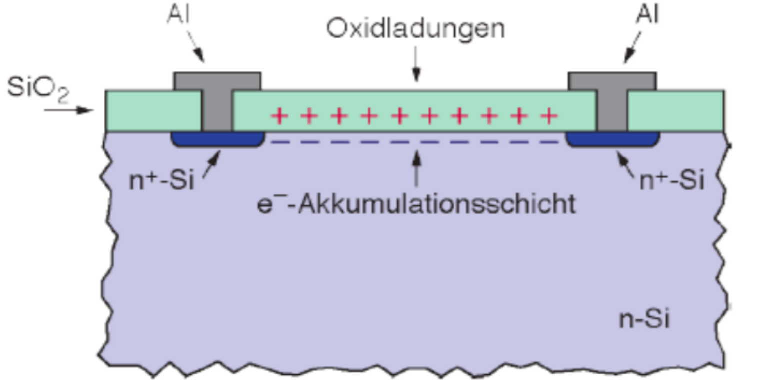

Positive oxide charges cause electron accumulation layer.

Silicon Detector

Every electrode is connected to an amplifier →
Highly integrated readout electronics.

Two dimensional readout is possible.

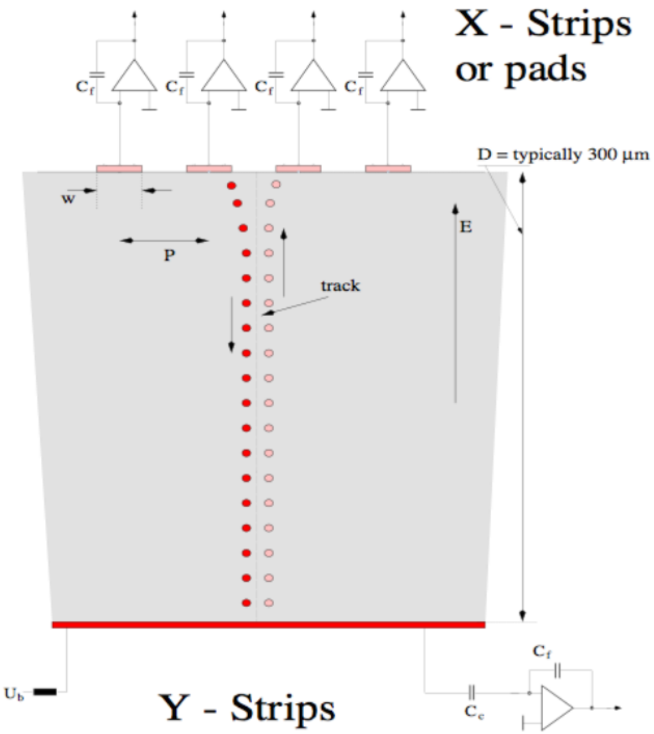

CMS Outer Barrel Module

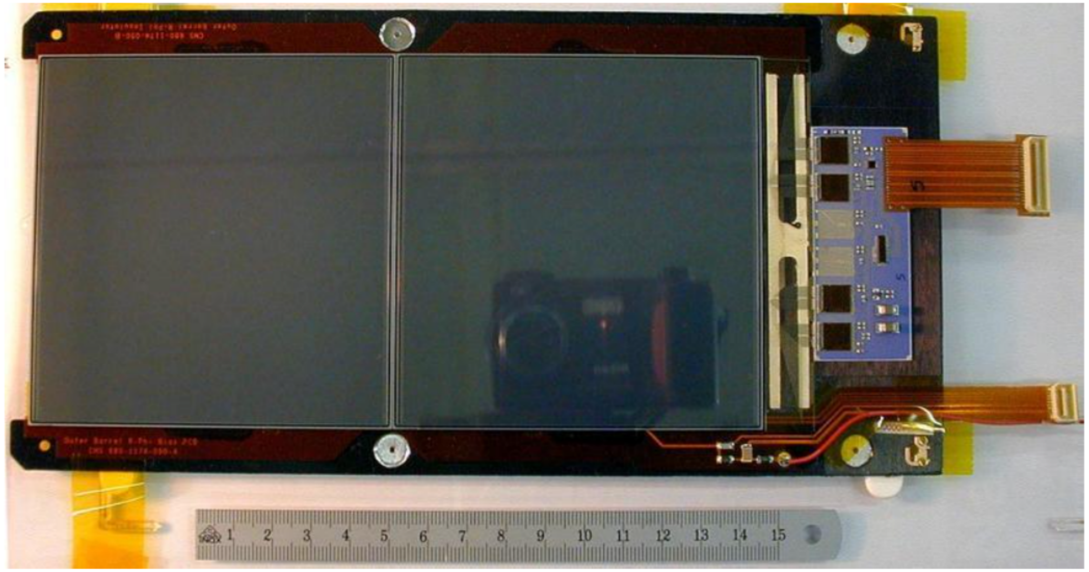

Silicon Drift Detector (like gas TPC !)

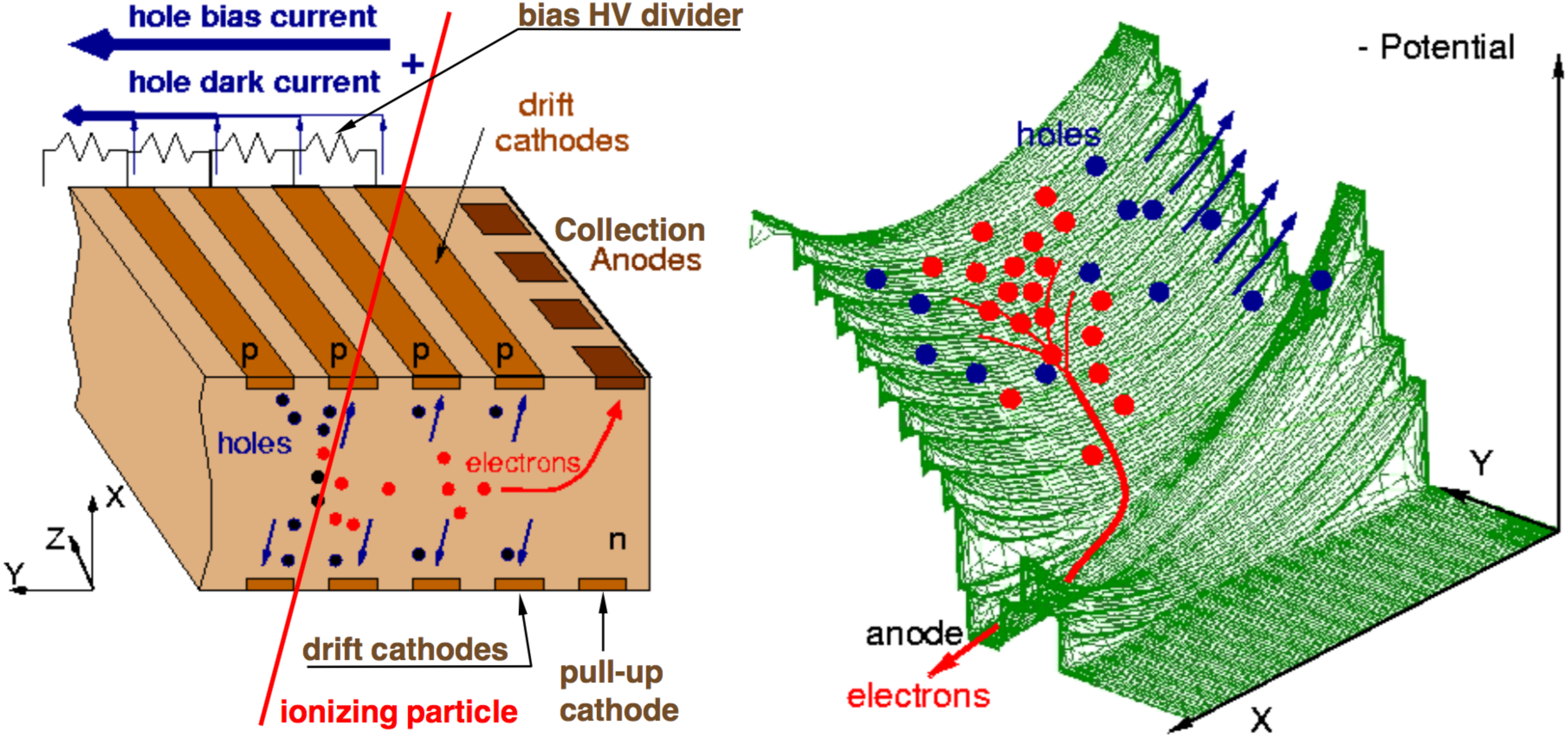

Astrofisica Nucleare e Subnucleare

"X-ray" Astrophysics

Detector Project

GLAST Project

For SWG discussion , Huntsville, 2002.9.13

Definition of Terms

- **Effective Area:**

  A_{eff}

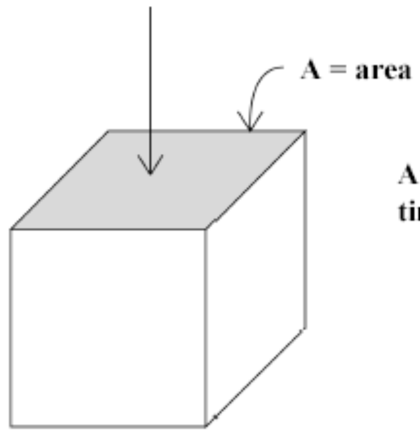

Area at normal incidence times detection efficiency.

- **Energy Resolution:**

  E_R

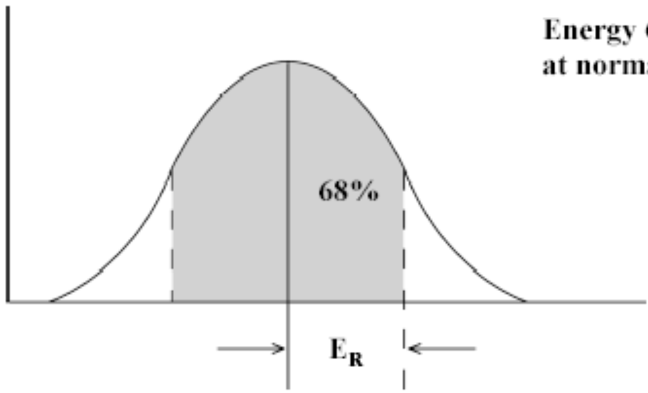

Energy 68% spread at normal incidence.

Detector Project

Definition of Terms

- **Angular Resolution:**

  Θ_R

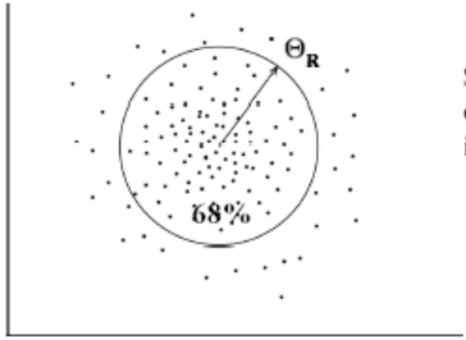

Space angle for 68% containment at normal incidence.

- **Field of View:**

  FOV

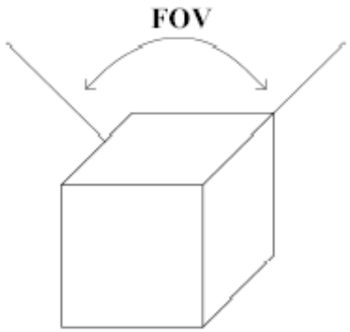

Integral effective area over solid angle divided by peak effective area.

- **Sensitivity:**

Flux of weakest source that can be detected at 5 sigma significance.

Nobel prize 2002 – R.Giacconi

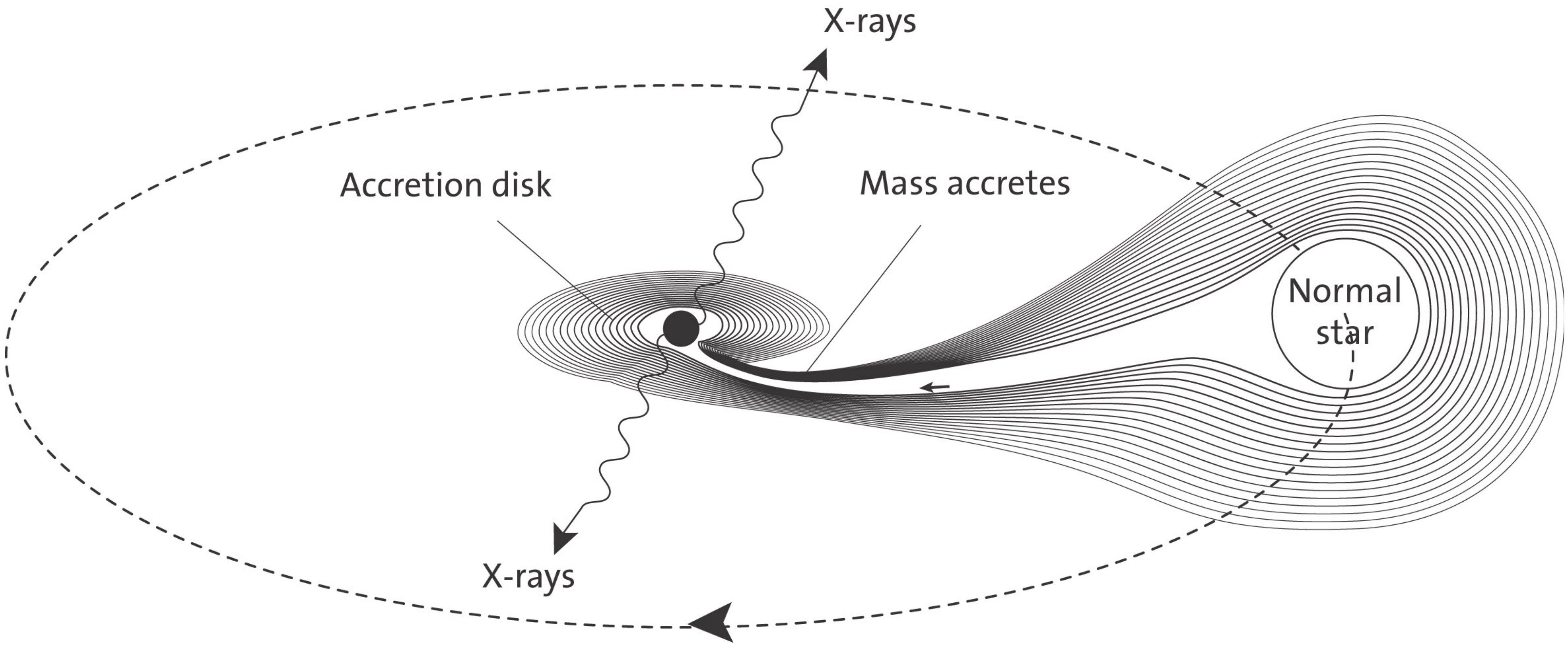

“ … for pioneering contributions to astrophysics,
which have led to the discovery of cosmic X-ray sources”

Scanning with Slat Collimators

- Imaging the sky with non-imaging X-ray instruments as a goal
- Linear scanning means position is determined in one direction
- At least a second scanning, preferentially in the direction perpendicular to the previous one
- First all-sky survey in X-rays by Uhuru (1970-72): 2 prop. counters with metal collimators (0.5°×5°, 5°×5° FWHM)

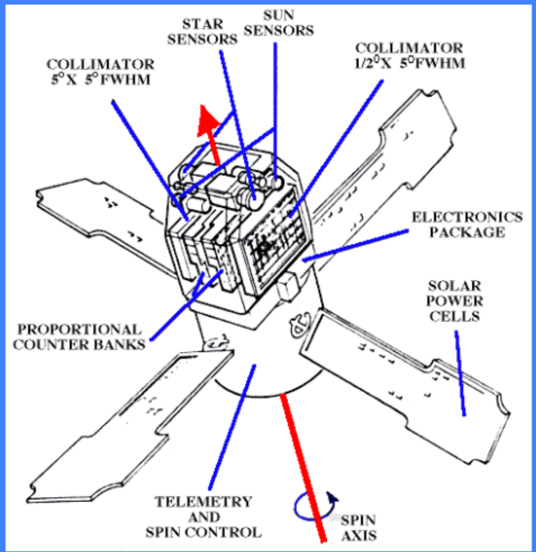

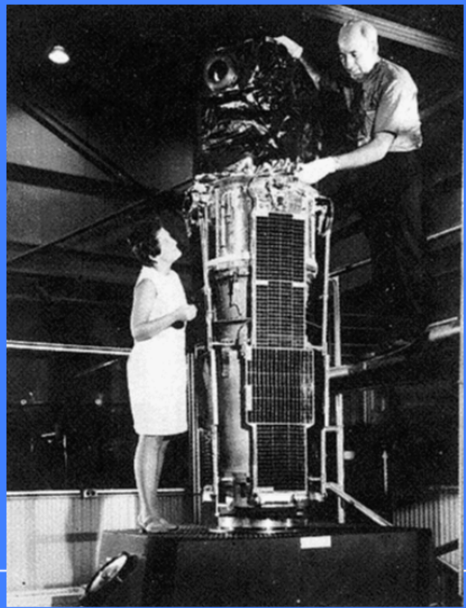

Scanning Grid Collimators

- Two or more plane ("grid" of absorbing rods) collimators to improve angular resolution

- Higher resolution with three or more grids (e.g., 4 in HEAO-1 A-3 experiment)

- Two-dimensional measurements need scans in two or more directions

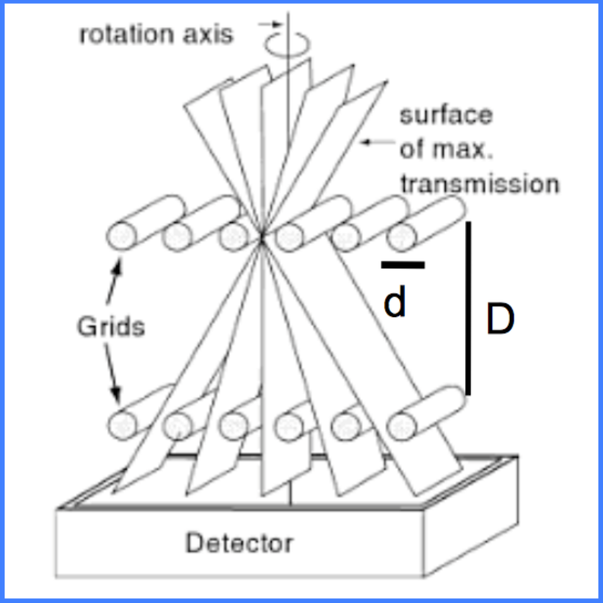

Double-grid collimator
Transmission Function of triangular shape
Angular resolution: d/D

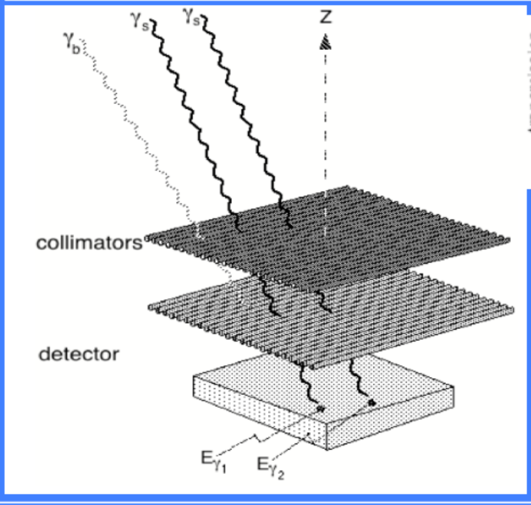

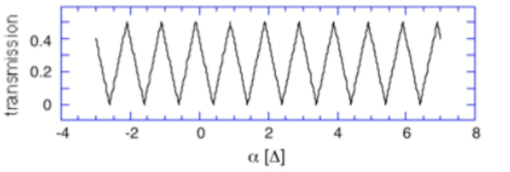

Modulation curve

Sensibilità - 1

- Sensibilità = flusso minimo rivelabile
  - Emissione nel continuo: fotoni cm^{-2} s^{-1} keV^{-1}
  - Emissione di righe: fotoni cm^{-2} s^{-1}
- C_S = Tasso di conteggi di sorgente
- C_{Bkg} = Tasso di conteggi di fondo

assumendo una statistica poissoniana

$$SNR = n_\sigma = \frac{C_S}{\sqrt{C_S + C_{Bkg}}}$$

In realta' quello che si misura e' (S+B)-B in un dato intervallo di tempo

$$S = (S+B) - B \longrightarrow \sigma_S^2 = \sigma_{S+B}^2 + \sigma_B^2 =$$

$$= (\sqrt{(S+B)})^2 + (\sqrt{B})^2 = S + B + B = S + 2B$$

$$SNR = S/\sigma_S = S/\sqrt{(S+2B)}$$

Sensibilità – 2 – “basic” dependencies

$S = \varepsilon\ A\ T\ \Delta E\ F_{src}$

$B = A\ T\ \Delta E\ F_{bkg}$

ε=efficienza di rivelazione fotoni della sorgente
A=area efficace
T=tempo di esposizione
ΔE=banda energetica
F_{src}=flusso della sorgente
F_{bkg}=fondo strumentale

$B \ll \varepsilon\ F_{src}$

$$SNR = \frac{S}{\sqrt{S+2B}} \approx \sqrt{S} \propto \sqrt{F_{src} T}$$

the source dominates the signal

$B \gg \varepsilon\ F_{src}$

$$SNR = \frac{S}{\sqrt{S+2B}} \approx S/\sqrt{2B} \propto \sqrt{T}\left(F_{src}/\sqrt{2F_{bkg}}\right)$$

Backg-dominated obsn.

$$\mathrm{SNR} = n_\sigma \approx \frac{\varepsilon\cdot \mathrm{A}\cdot \mathrm{T}\cdot \Delta\mathrm{E}\cdot \mathrm{F}}{\sqrt{\mathrm{A}\cdot \mathrm{T}\cdot \Delta\mathrm{E}\cdot \mathrm{B}}} \rightarrow F_{Min} = \frac{n_\sigma}{\varepsilon}\sqrt{\frac{B}{\mathrm{A}\cdot \mathrm{T}\cdot \Delta\mathrm{E}}}$$

to give an idea of the main dependencies of the limiting flux (sensitivity)

In the “real world”, the background is not only instrumental but also cosmic

S=source flux density [counts/m^2 s]
A=area of the detector
Ω=solid angle subtended by the beam of the telescope on the sky
B_1=instrumental (particle) background [counts/s]
B_2=cosmic background (XRB) [phot/m^2 s ster]
T=exposure time
SOURCE=S×A×T (photons related to the source)
BACKGROUND=B_1×T + B_2×A×Ω×T (photons related to the backgrounds)

$$N = \sqrt{(B_1 + B_2 A\Omega) \times T}$$

$$S/N = \frac{SAT}{\sqrt{(B_1 + B_2 A\Omega) \times T}} = \frac{SA^{1/2}T^{1/2}}{\sqrt{\left(\frac{B_1}{A}\right) + \Omega B_2}}$$

$$S/N = 5 \Rightarrow S_{\min} = 5\sqrt{\frac{B_1/A + \Omega B_2}{AT}}$$

Focalizzazione vs collimazione

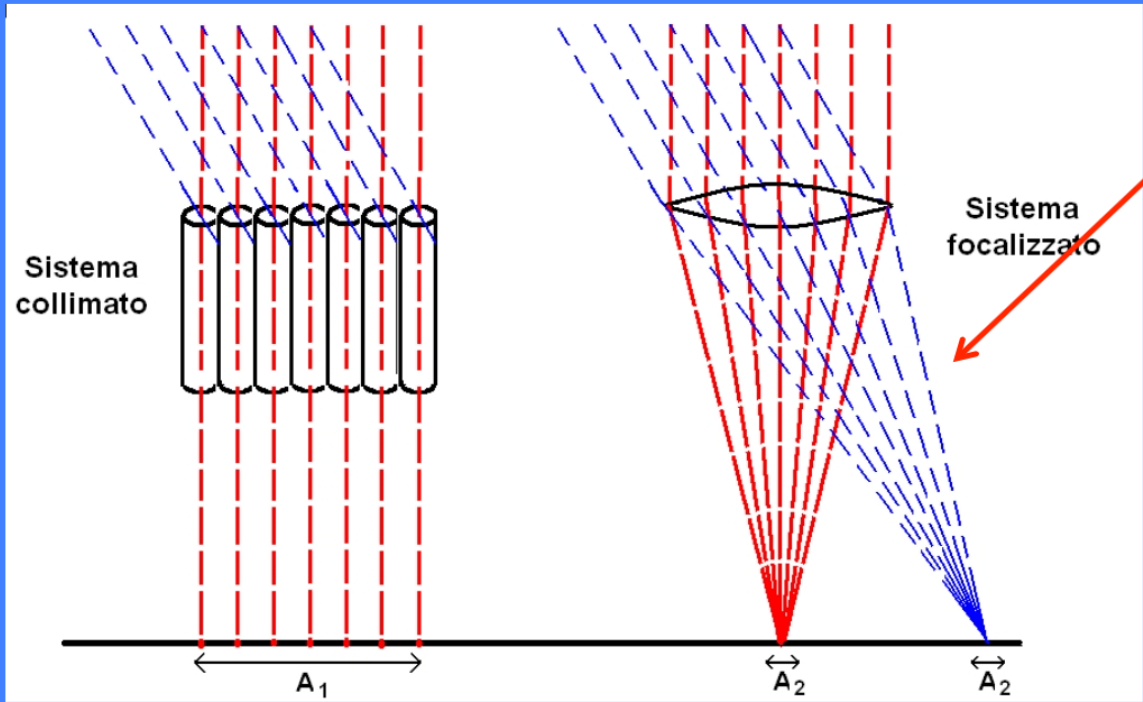

Proper imaging of X-rays below 20-40 keV

$$F_{\min} \approx n_\sigma \frac{\sqrt{2B}}{\sqrt{A_{\det} T_{\text{int}} \Delta E}}$$

A_d= PSF projected on the focal plane

$$F_{\min} \approx n_\sigma \frac{\sqrt{B A_d}}{A_{eff} \sqrt{T_{\text{int}} \Delta E}}$$

Sistema collimato: limita la regione di cielo da cui puo' provenire un segnale, (quindi limita il background), non incrementandone la "densita"

Sistema focalizzato: fa corrispondere ad ogni sorgente un punto nel piano focale, e "concentra" il segnale, producendo un'immagine

$$C_B = B\, A_d\, \Delta E\, \Delta t$$

Background counts from a collimated telescope with detector area A_d, sensitive over the band ΔE, in a time interval Δt

$$\sigma(C_B) = C_B^{1/2}$$

The counts obey the Poisson statistics

$$C_S = S_E\, A_d\, \Delta E\, \Delta t\, \eta_E$$

Source counts collected from a source with flux S_E in the same conditions (QE=η_E)

$$C_{\text{meas}} = (C_S + C_B) - C_B$$

Measured counts (backg-subtracted)

$$\sigma^2(C_{\text{meas}}) = 2\sigma^2(C_B)$$

Background dominates fluctuations

$$S/N = n_\sigma = \frac{C_S}{\sqrt{2C_B}} = \frac{S_E\, A_d\, \Delta E\, \Delta t\, \eta_E}{\sqrt{2B\, A_d\, \Delta E\, \Delta t}}$$

$$S_{E,\min} = \frac{n_\sigma}{\eta_E} \frac{\sqrt{2B}}{\sqrt{A_d\, \Delta t\, \Delta E}}$$

X-Ray Mirrors

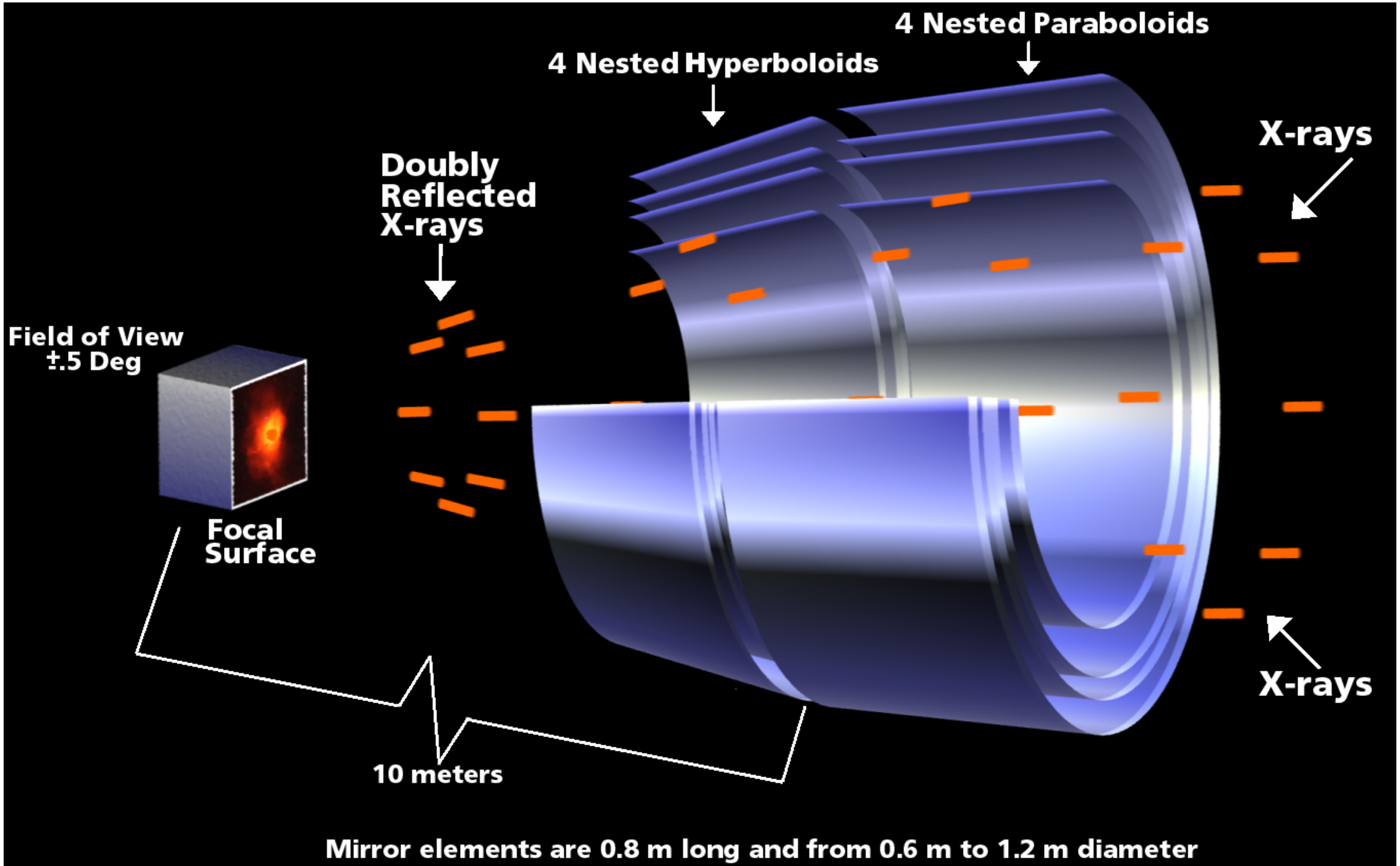

Why do we use X-ray optics

- To achieve the best 2-dim angular resolution

  - To distringuish nearby sources or different regions of the same source
  - To perform morphological studies

- As a collector to “gather” weak fluxes (case of limited photon statistics)

- As a concentrator, so that the image photons may interact in a small region of the detector, thus limiting the influence of the background

- To serve with high spectral resolution dispersive spectrometers such as transmission or reflection gratings

- To simultaneously measure both the source(s) of interest and the contaminating background in other (source-free) regions of the detector

X-ray optical constants

- X-rays are hard to refract or reflect: the refractive index of all materials in X-rays is very close to 1 and only slightly less than 1 ➔ X-rays are above the characteristic energy of bonded e- in atoms
- complex index of refraction of the reflector to describe the interaction X-rays /matter (see, for a review, Aschembach et al. 1985, Rep. Prog. Phys. 48, 579)

$$n=1-\delta+i\beta$$

where δ describes the phase change and β accounts for the absorption

δ and β depend on the wavelength

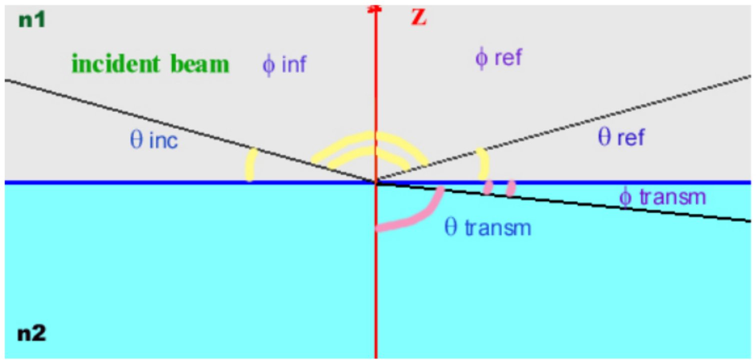

- the amplitute of reflection is described by the Fresnel's equations

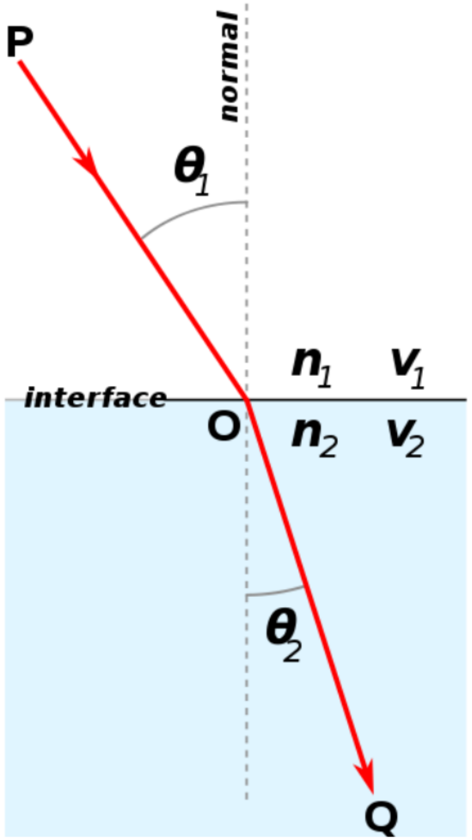

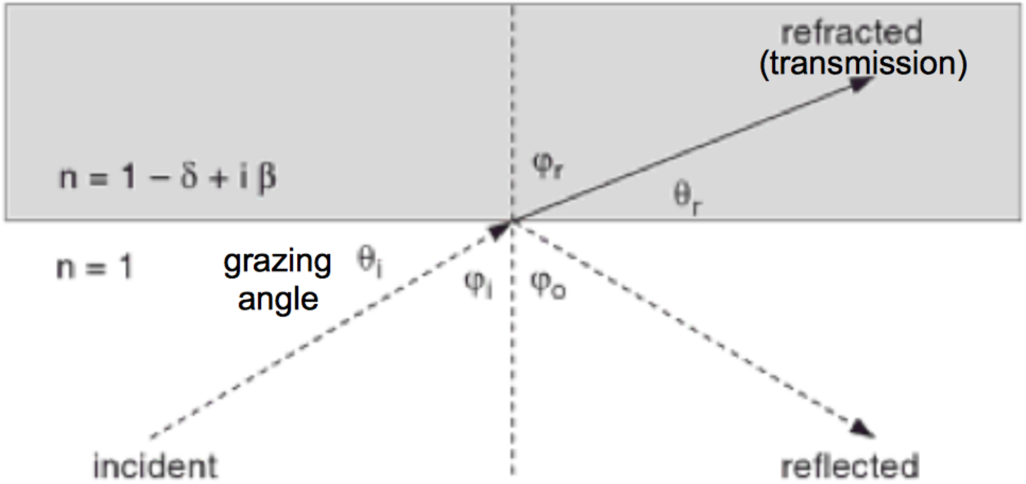

Snell's Law of Refraction:
relationship between the angles of incidence and refraction in a medium

$$\boxed{n_1 \sin\theta_1 = n_2 \sin\theta_2}$$

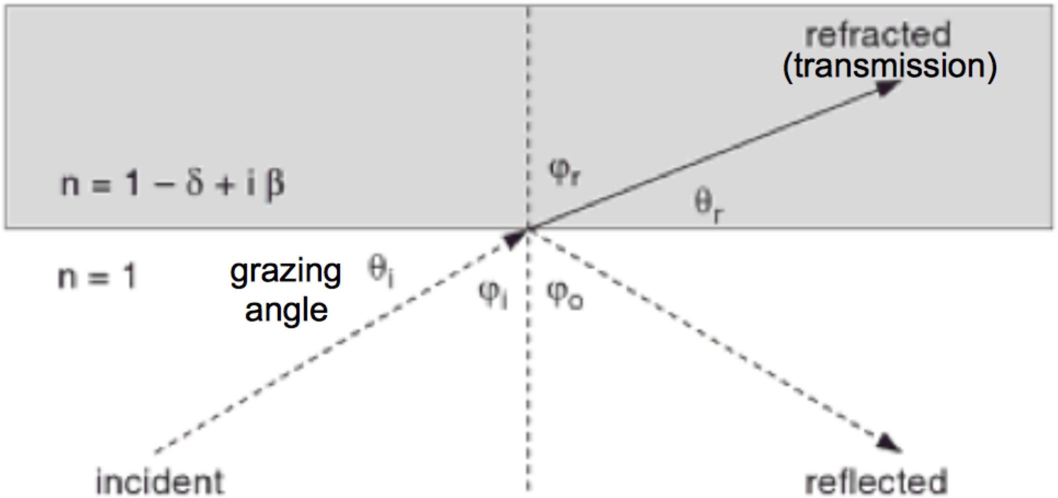

$$n_1 = 1,\ n_2 = (1-\delta) \ \rightarrow \ \sin\phi_i = (1-\delta)\sin\phi_r$$

$$\vartheta = (\pi/2) - \phi$$

$$\cos(90-\phi_i) = \cos\vartheta_i = (1-\delta)\cos(90-\phi_r) = (1-\delta)\cos\vartheta_r$$

$$\Rightarrow \cos\vartheta_i = \cos\vartheta_r(1-\delta)$$

Total reflection if no real solution for ϑ_r
$\delta>0$, $\cos\theta_r \leq 1$ ➔ There is a **critical angle θ_c** below which refraction is impossible and total external reflection occurs (grazing angle, $\theta_i=\theta_c$)

Extreme case for low θr values

$$\boxed{1 = \cos\vartheta_r = \cos\vartheta_c/(1-\delta) \rightarrow \cos\vartheta_c = 1-\delta}$$

Total X-ray reflection at grazing incidence

- Real part of n slightly less than unity for matter at X-rays, =1 in vacuum (total external reflection); $\delta << 1$

- Snell's law ($n1 \cos\theta_1 = n2 \cos\theta_2$) to find a critical angle for total reflection

- (Total) external reflection in vacuum for angles < critical angle: $\boxed{\cos\theta_{crit} = 1-\delta}$

- X-ray partially reflected also for $\theta > \theta_{crit}$; also, some absorption in the material

- $\boxed{\cos(\theta_{crit}) = 1 - \theta^2_{crit}/2 = 1-\delta \xrightarrow{\text{low angles}} \theta_{crit} = \sqrt{2\delta}}$

- Far from fluorescent edges: $\boxed{\delta \approx \dfrac{N_0 Z r_e \rho \lambda^2}{2\pi A}}$

where N_0=Avogadro's number
Z=atomic number
r_e=electron radius
ρ=density
λ=wavelength of the incoming photon
A=atomic weight

Critical angle:

- Inversely dependent on energy
- Higher Z materials reflect higher energies, for a fixed grazing angle
- Higher Z materials have a larger critical angle at any energy

- For heavy elements, $Z/A \approx 0.5$, and if $\delta \ll 1$:

$$\boxed{\theta_{crit} \approx \sqrt{2\delta} \approx 5.6\lambda\sqrt{\rho}}$$

where λ[Å] and ρ[g/cm^3], and θ[arcmin]

$$\boxed{\theta_{crit} \propto \sqrt{\rho}/E}$$

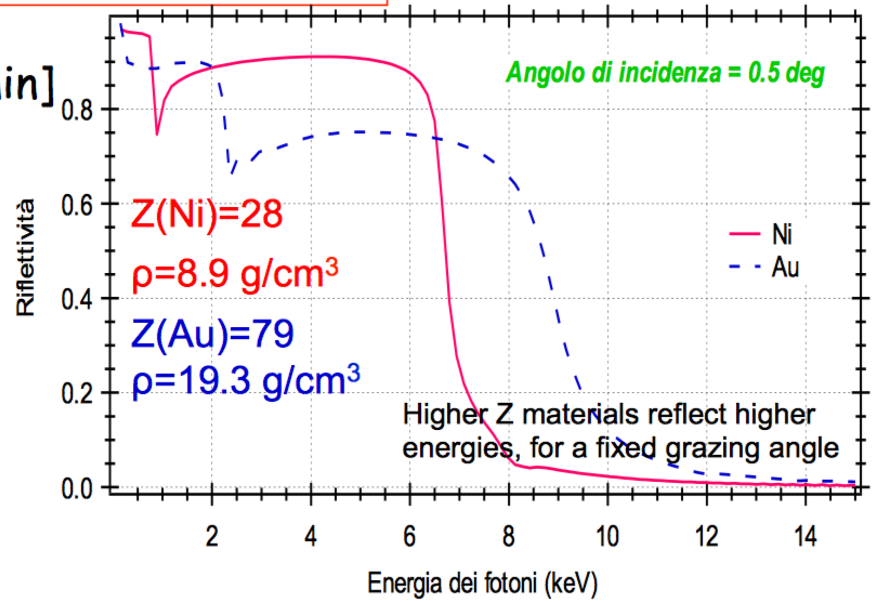

- Some reflectivity is lost due to scattering related to the presence of micro-roughness at the surface

- Use of heavy materials (but attention at the absorption edges…)

X-ray mirrors with parabolic profile

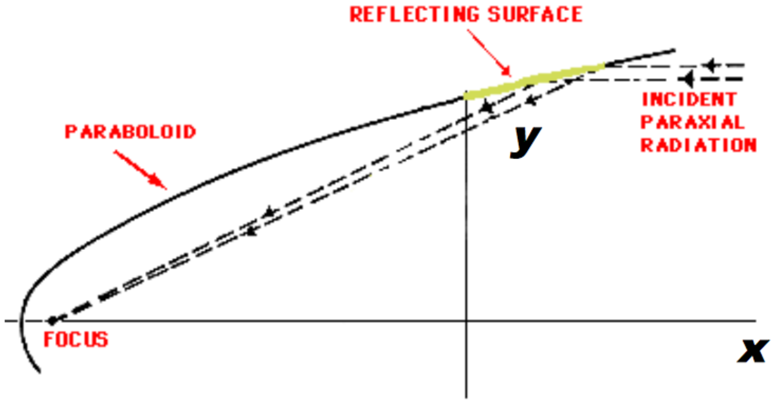

- perfect on-axis focusing
- off-axis images <u>strongly</u> affected by coma

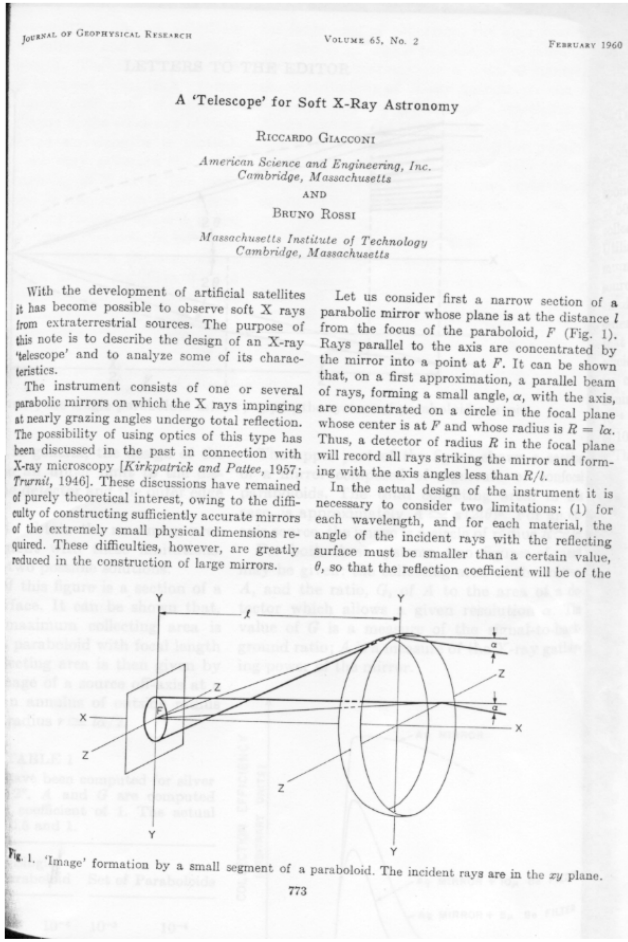
JOURNAL OF GEOPHYSICAL RESEARCH VOLUME 65, NO. 2 FEBRUARY 1960

A 'Telescope' for Soft X-Ray Astronomy

RICCARDO GIACCONI

American Science and Engineering, Inc.
Cambridge, Massachusetts

AND

BRUNO ROSSI

Massachusetts Institute of Technology
Cambridge, Massachusetts

With the development of artificial satellites it has become possible to observe soft X rays from extraterrestrial sources. The purpose of this note is to describe the design of an X-ray 'telescope' and to analyze some of its characteristics.

The instrument consists of one or several parabolic mirrors on which the X rays impinging at nearly grazing angles undergo total reflection. The possibility of using optics of this type has been discussed in the past in connection with X-ray microscopy [*Kirkpatrick and Pattee*, 1957; *Trurnit*, 1946]. These discussions have remained of purely theoretical interest, owing to the difficulty of constructing sufficiently accurate mirrors of the extremely small physical dimensions required. These difficulties, however, are greatly reduced in the construction of large mirrors.

Let us consider first a narrow section of a parabolic mirror whose plane is at the distance l from the focus of the paraboloid, F (Fig. 1). Rays parallel to the axis are concentrated by the mirror into a point at F. It can be shown that, on a first approximation, a parallel beam of rays, forming a small angle, α, with the axis, are concentrated on a circle in the focal plane whose center is at F and whose radius is $R = l\alpha$. Thus, a detector of radius R in the focal plane will record all rays striking the mirror and forming with the axis angles less than R/l.

In the actual design of the instrument it is necessary to consider two limitations: (1) for each wavelength, and for each material, the angle of the incident rays with the reflecting surface must be smaller than a certain value, θ, so that the reflection coefficient will be of the

Fig. 1. 'Image' formation by a small segment of a paraboloid. The incident rays are in the xy plane.

Wolter, 1952

Wolter's solution to the X-ray imaging

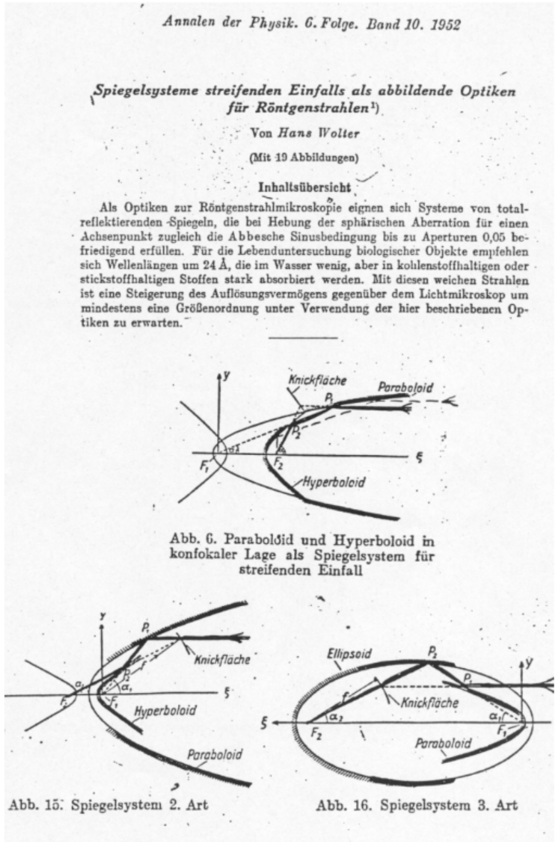

Annalen der Physik. 6. Folge. Band 10. 1952

***Spiegelsysteme streifenden Einfalls als abbildende Optiken für Röntgenstrahlen*[1])**

Von *Hans Wolter*

(Mit 19 Abbildungen)

Inhaltsübersicht

Als Optiken zur Röntgenstrahlmikroskopie eignen sich Systeme von totalreflektierenden Spiegeln, die bei Hebung der sphärischen Aberration für einen Achsenpunkt zugleich die Abbesche Sinusbedingung bis zu Aperturen 0,05 befriedigend erfüllen. Für die Lebenduntersuchung biologischer Objekte empfehlen sich Wellenlängen um 24 Å, die im Wasser wenig, aber in kohlenstoffhaltigen oder stickstoffhaltigen Stoffen stark absorbiert werden. Mit diesen weichen Strahlen ist eine Steigerung des Auflösungsvermögens gegenüber dem Lichtmikroskop um mindestens eine Größenordnung unter Verwendung der hier beschriebenen Optiken zu erwarten.

Knickfläche
Paraboloid
Hyperboloid

Abb. 6. Paraboloid und Hyperboloid in konfokaler Lage als Spiegelsystem für streifenden Einfall

Knickfläche
Hyperboloid
Paraboloid

Abb. 15. Spiegelsystem 2. Art

Ellipsoid
Knickfläche
Paraboloid

Abb. 16. Spiegelsystem 3. Art

Fine for X-ray astronomy

Applied in solar X-ray telescopes

Not adopted

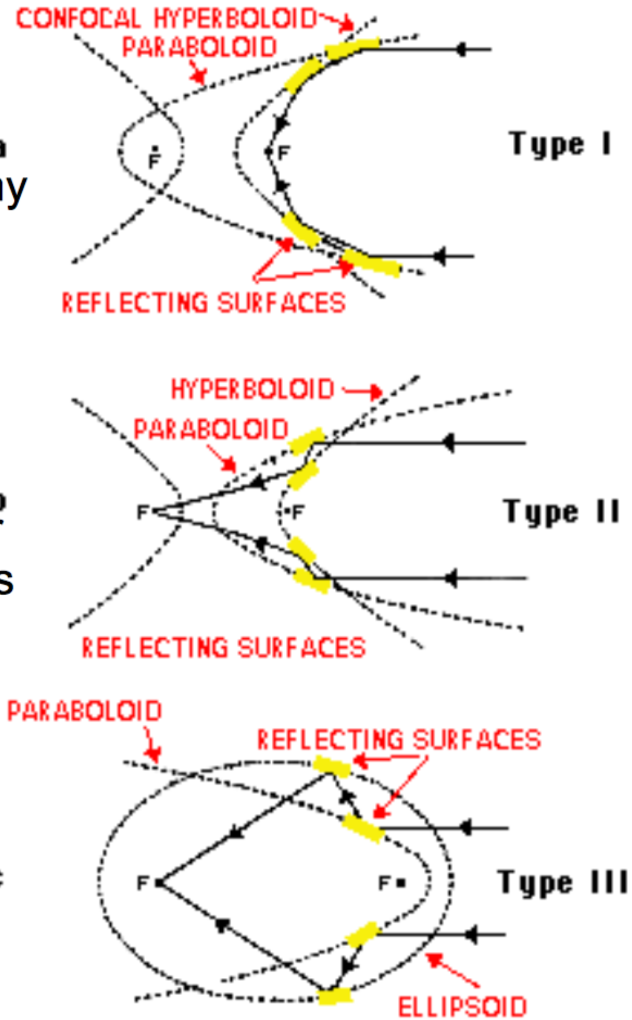

H. Wolter, Ann. Der Phys., NY10, 94 (1952)

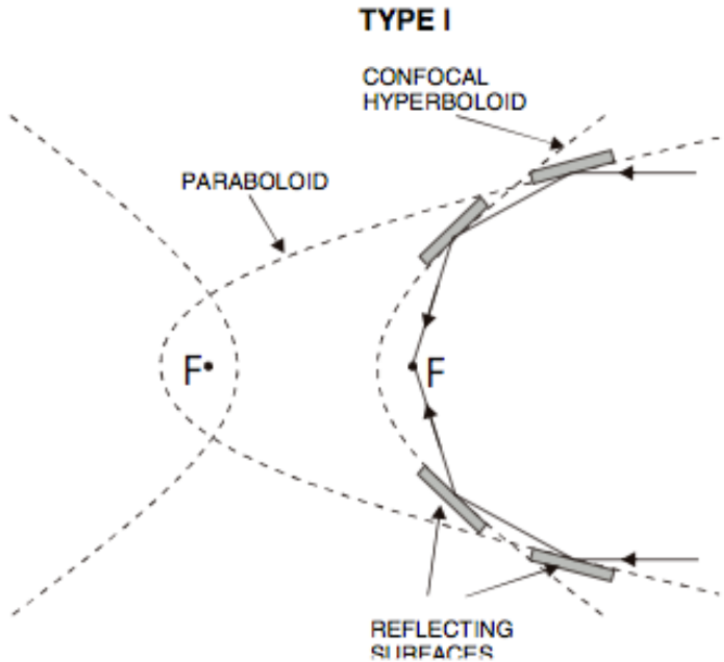

Wolter-I optics
Paraboloid ➔ Hyperboloid

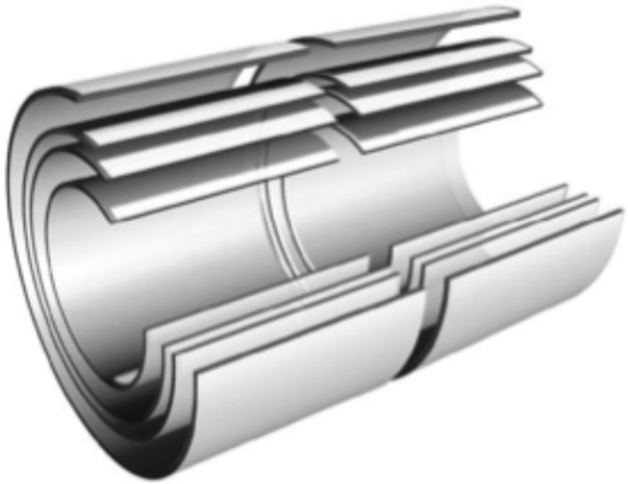

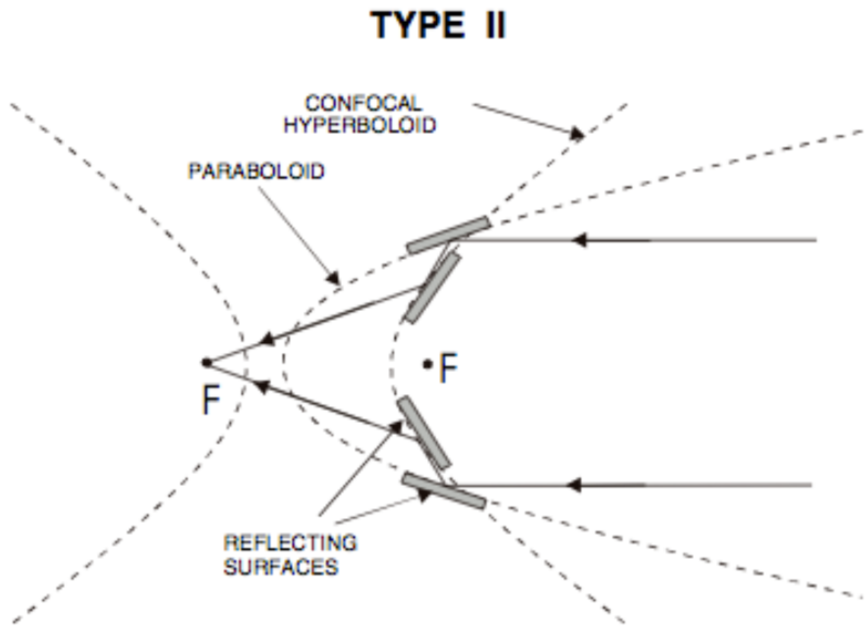

Wolter-II optics
Paraboloid ➔ Hyperboloid (ext. surface)

X-Ray Mirrors

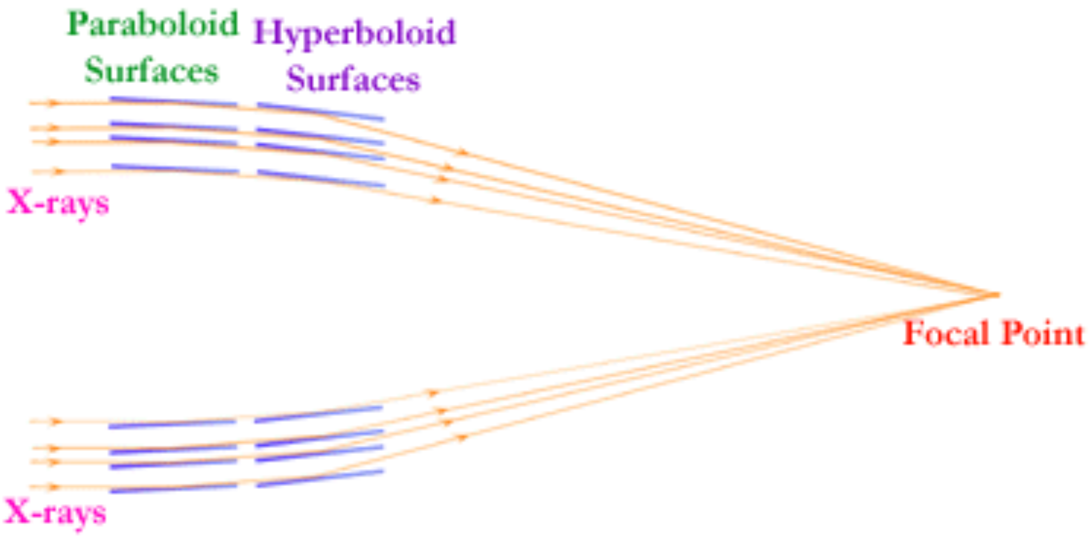

$$\cos\phi = 1 - \delta$$

$$\delta = 2.70 \times 10^{-6} \frac{Z_e}{A} \rho \lambda^2$$

Cf Aschembach et al. 1985

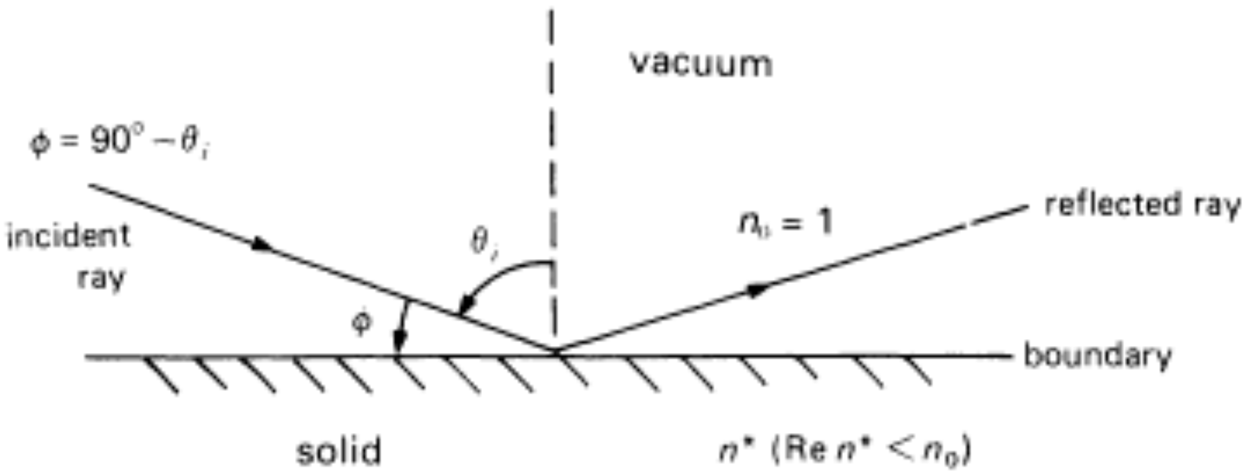

A_{geom} x Reflectivity

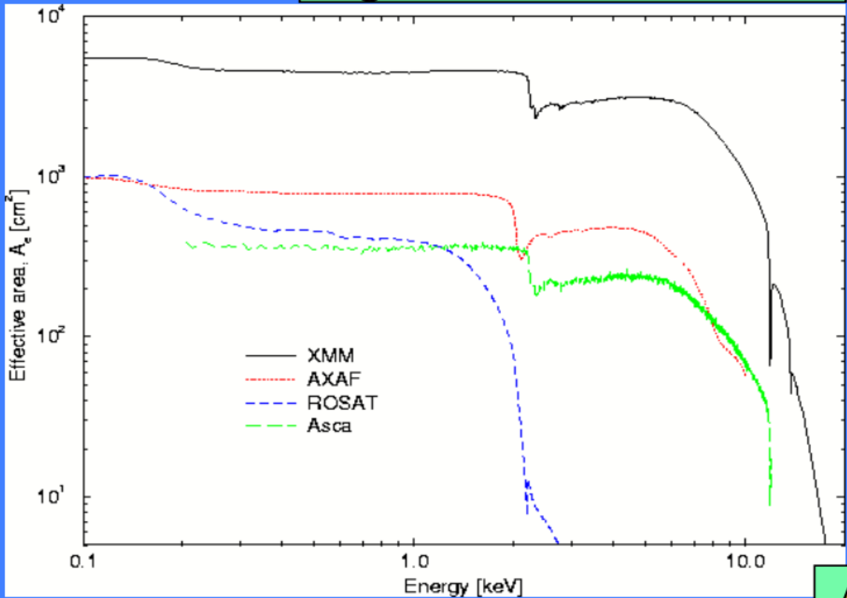

x

QE

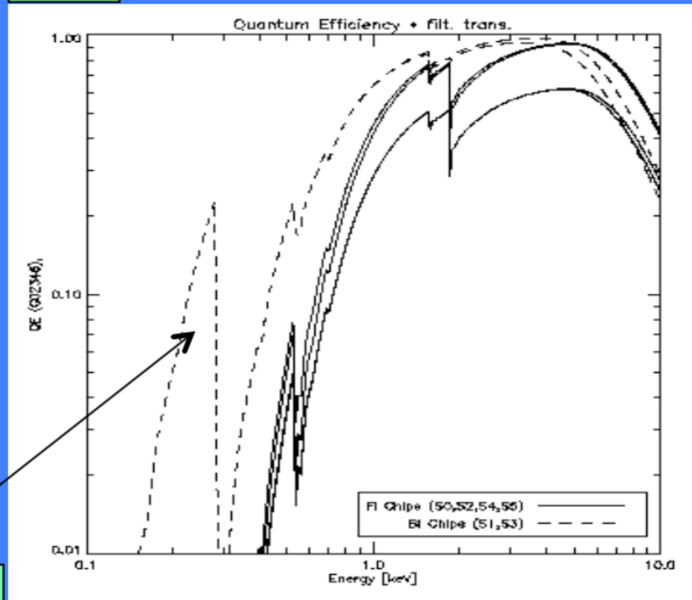

=

$A_{effective}$

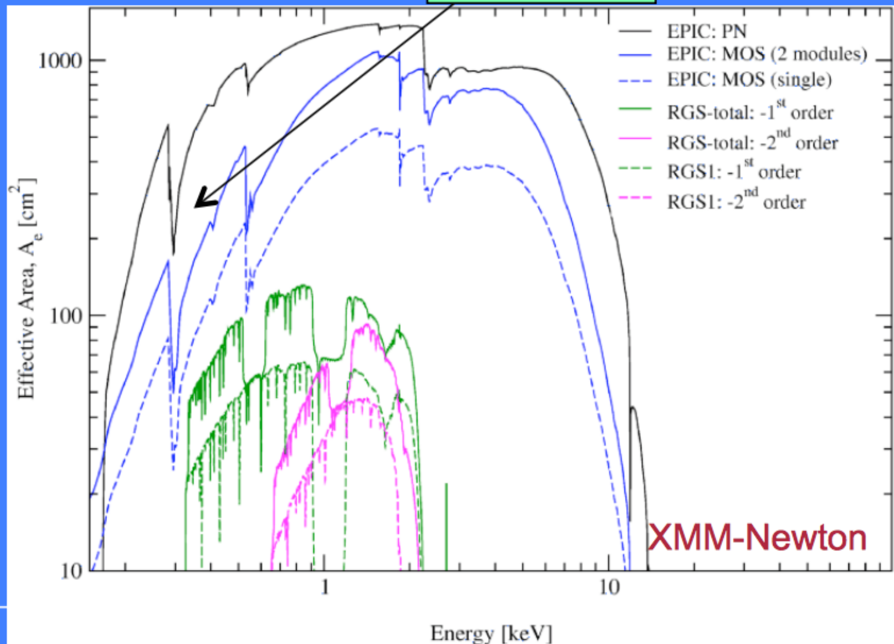

CCD

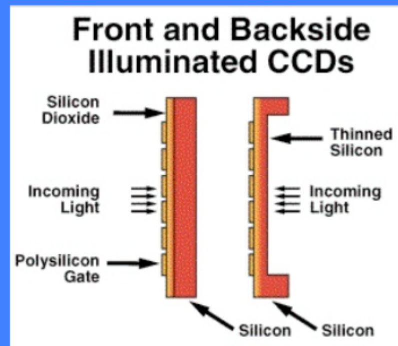

Focalizzazione vs collimazione

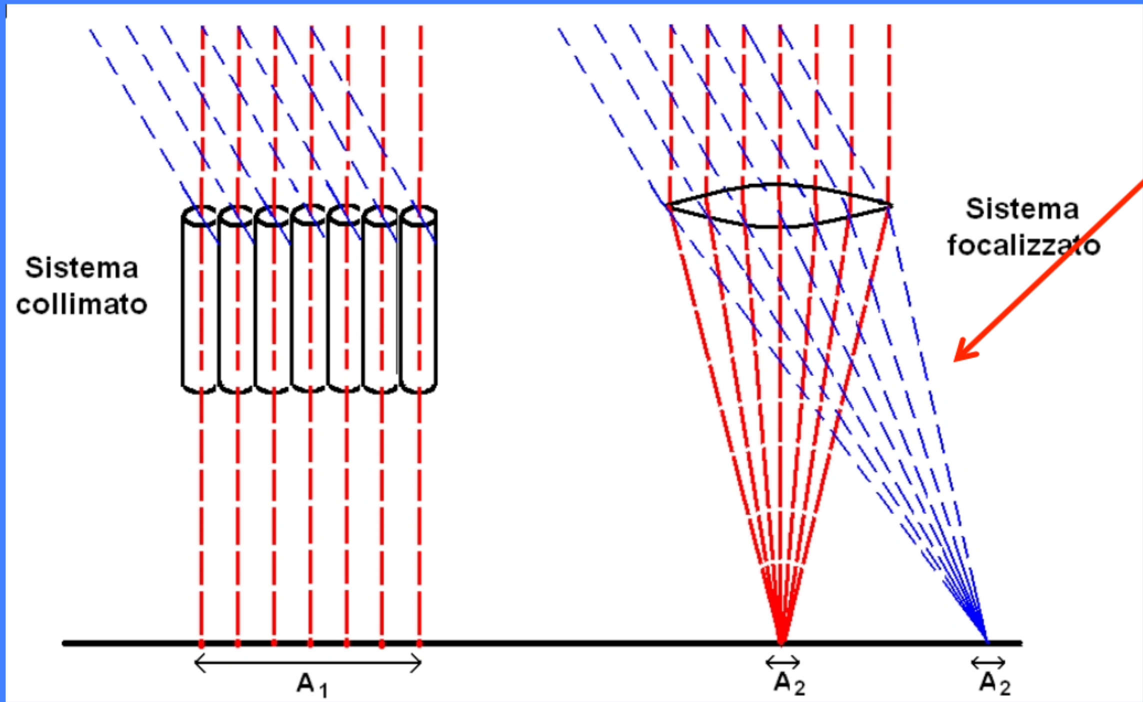

Proper imaging of X-rays below 20-40 keV

$$F_{\min} \approx n_\sigma \frac{\sqrt{2B}}{\sqrt{A_{\det} T_{\mathrm{int}} \Delta E}}$$

A_d= PSF projected on the focal plane

$$F_{\min} \approx n_\sigma \frac{\sqrt{B A_d}}{A_{eff} \sqrt{T_{\mathrm{int}} \Delta E}}$$

Sistema collimato: limita la regione di cielo da cui puo' provenire un segnale, (quindi limita il background), non incrementandone la "densita"

Sistema focalizzato: fa corrispondere ad ogni sorgente un punto nel piano focale, e "concentra" il segnale, producendo un'immagine

$$C_S = S_E\ A_e\ \Delta E\ \Delta t\ \eta_E$$

Detected signal

$$C_B = B\ \varepsilon\ A_d\ \Delta E\ \Delta t$$

Background signal (ε: region of the detector where B counts are focused)

$$S/N = n_\sigma = \frac{C_S}{\sqrt{C_S + 2C_B}} \approx \frac{S_E\ A_e\ \Delta E\ \Delta t\ \eta_E}{\sqrt{2B\ \varepsilon\ A_d\ \Delta E\ \Delta t}}$$

$$S_{E,\min} = \frac{n_\sigma}{\eta_E}\ \frac{1}{\mathrm{A_e}}\sqrt{\frac{2B\ \varepsilon\ A_d}{\Delta t\ \Delta E}}$$

Weak sources

Old slide but *Chandra* and XMM-*Newton* still working

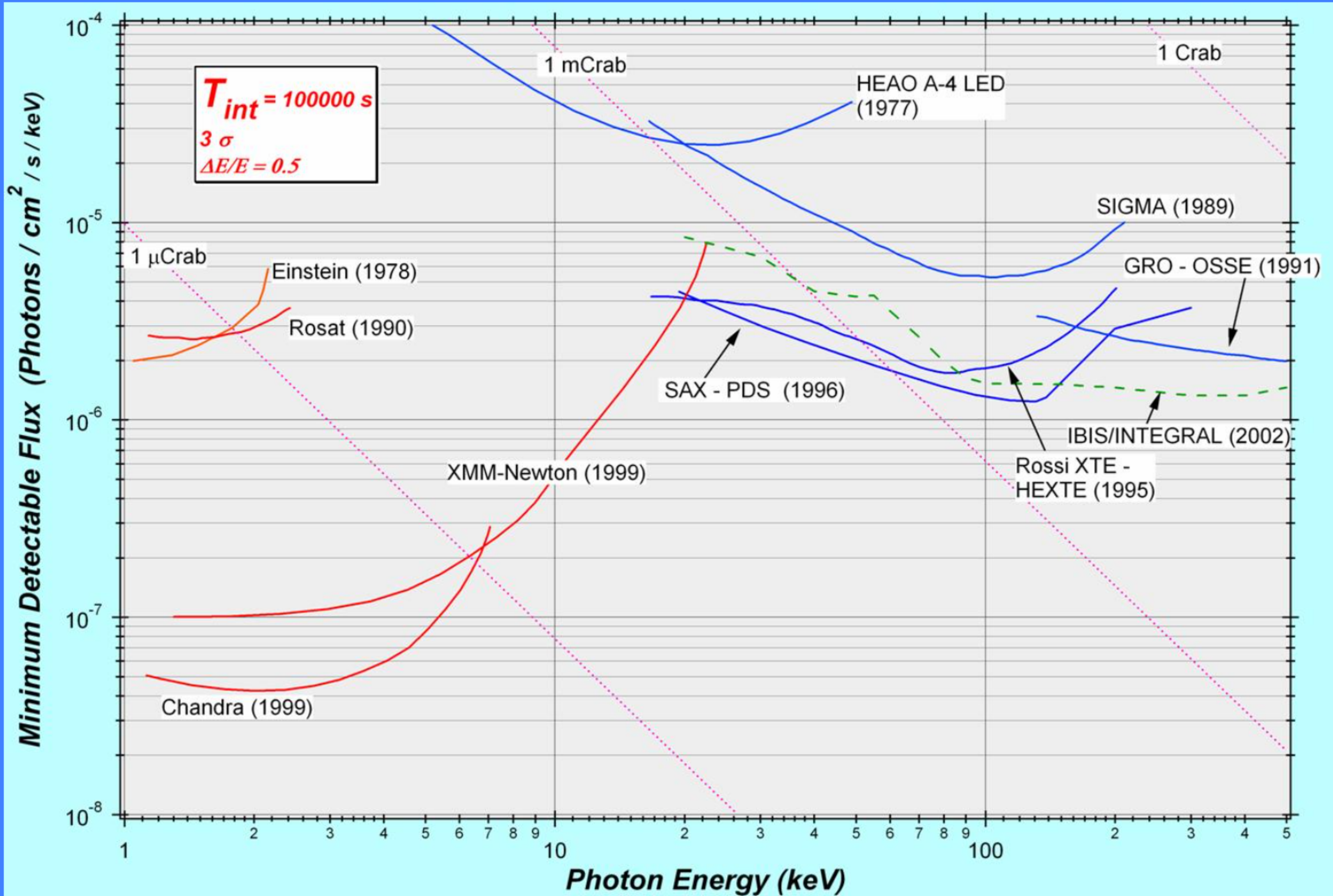

Single photon calorimeter

Individual X-ray photons are absorbed by a crystal which is maintained at a T very close to absolute zero (<0.1 K).
➔ 2-3 year lifetime

We measure the increase of T which is proportional to the energy of the X-ray photon

Energy resolution ~ 3 eV

High efficiency

The best spectral resolution of any non-dispersive (grating) spectrometer

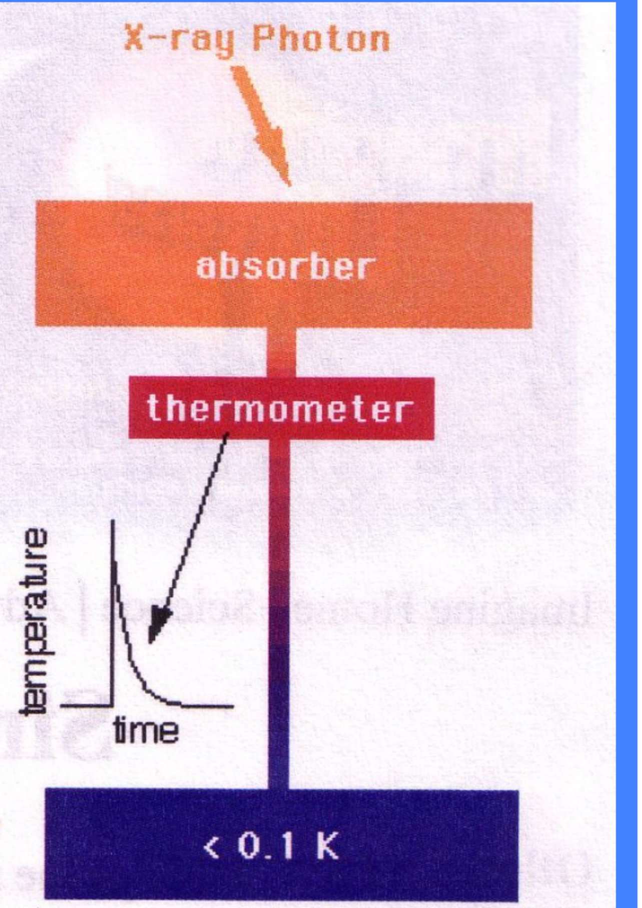

Diagram showing the essential elements of a calorimeter. Inset shows temperature response to an X-ray hit.

Onboard *Suzaku* – calibration source (^{55}Fe)

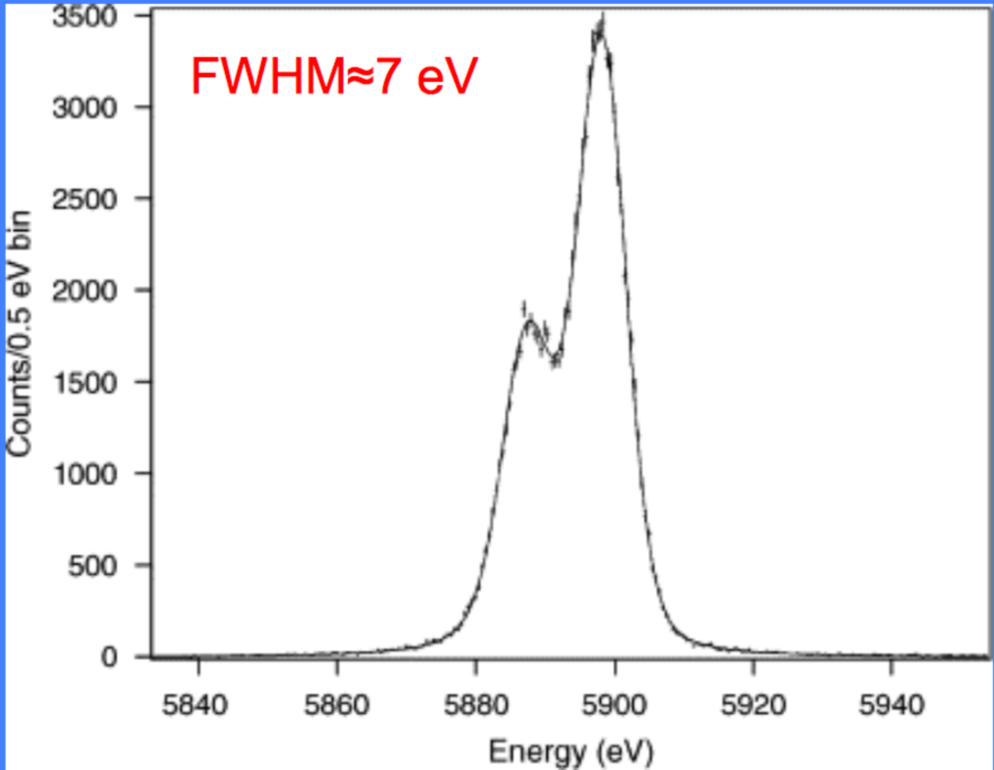

Expected spectral resolutions ≤2-3 eV in next-generation X-ray calorimeters (e.g., *Athena*)

Onboard of the Japanese mission ASTRO-H/*Hitomi* (Last year ☹)

X-ray spectroscopy

Telescopes and instruments

Dispersing elements – Bragg Crystal spectroscopy/1

(more details on dispersive spectrometers: Giacconi & Gursky, p. 81-90)

The reflection of X-rays from a crystal lattice follows the Bragg's law, and therefore the name Bragg spectrometer is usually given to the device with this kind of reflection grating.

Here the macroscopic shaping (grooves) of a metallic plate, which is used in longer wavelengths, is replaced by a material with regular lattice structure of atoms (crystal material). The reflection takes place by the same principle as from a macroscopic lattice, leading to a wavelength-dispersed output from a white light input.

The lattice of the crystal forms a 3-dimensional diffraction array which reflects X-rays of wavelength λ within a narrow range of wavelength satisfying the Bragg condition

$$n \lambda = 2d \sin\theta \quad , n = 1,2,3,\ldots \text{ (order of diffraction)}$$

where d is the crystal lattice spacing.

In practice, order n=1 is used.

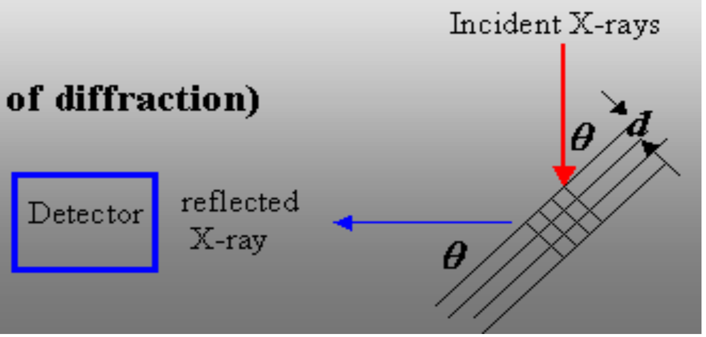

X-ray spectroscopy

Dispersing elements – Diffraction gratings/1

Ordinary diffraction gratings can also be used from from long wavelengths up to soft X-rays (< 1 keV, in practice).

The grating equation is

$$n\,\lambda = (1/N)\ (\sin\theta - \sin\theta_o),\ \ n = 1,2,3,\ldots \text{ (order of diffraction)}$$

where N is the grating constant (lines/cm), θ is the diffraction angle and θ_o is the angle of incidence. For X-rays this is usually rearranged in form valid for small angles

$$n\,\lambda\,N = \theta - \theta_o$$

There are two geometries usually applied in X-ray optics,

1. Conventional Johann mount geometry

2. Curved grating producing a line image

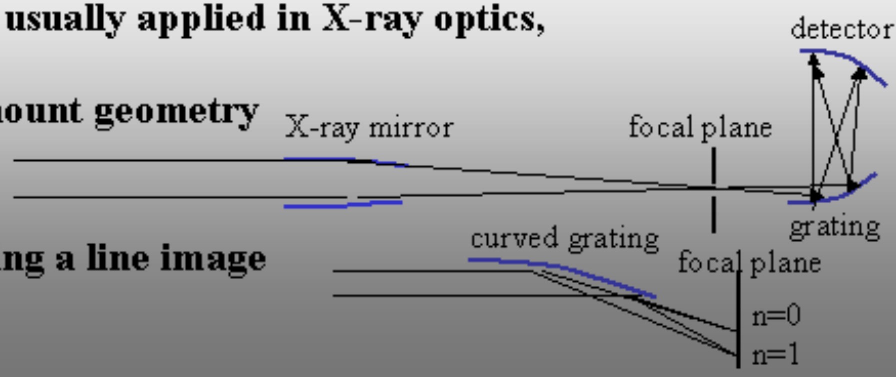

X-ray polarimetry

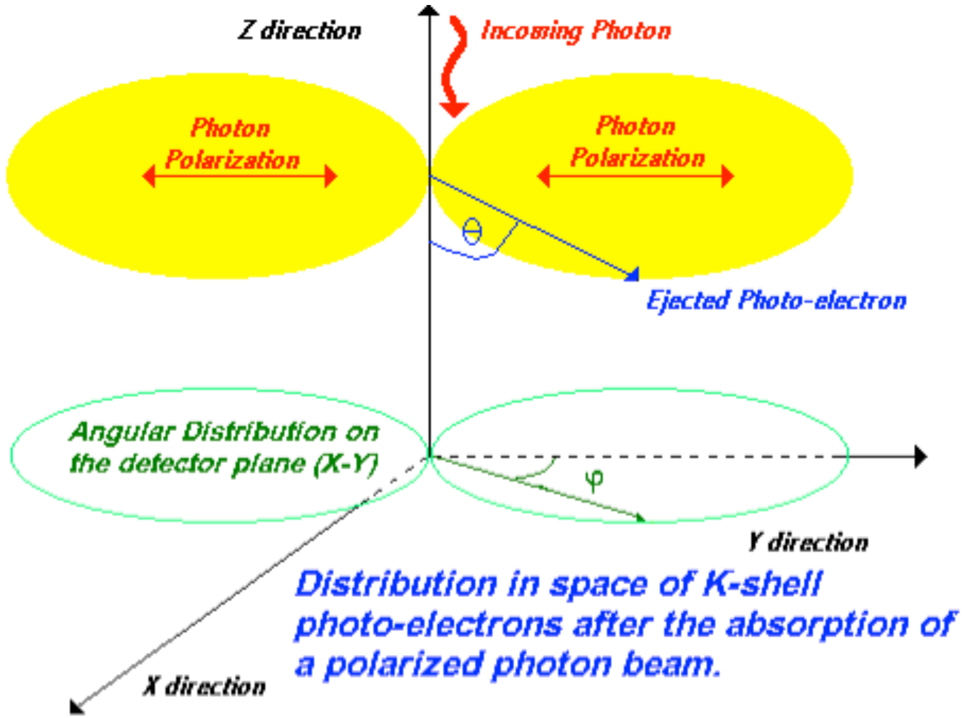

Costa et al. 2001

X-ray polarimetry